

Summer 8-15-2015

Escherichia coli Iron Acquisition Paradigms and Host Responses in the Human Urinary Milieu

Robin Reid Shields-Cutler
Washington University in St. Louis

Follow this and additional works at: https://openscholarship.wustl.edu/art_sci_etds

 Part of the [Biology Commons](#)

Recommended Citation

Shields-Cutler, Robin Reid, "Escherichia coli Iron Acquisition Paradigms and Host Responses in the Human Urinary Milieu" (2015). *Arts & Sciences Electronic Theses and Dissertations*. 582.
https://openscholarship.wustl.edu/art_sci_etds/582

This Dissertation is brought to you for free and open access by the Arts & Sciences at Washington University Open Scholarship. It has been accepted for inclusion in Arts & Sciences Electronic Theses and Dissertations by an authorized administrator of Washington University Open Scholarship. For more information, please contact digital@wumail.wustl.edu.

WASHINGTON UNIVERSITY IN ST. LOUIS

Division of Biology and Biomedical Sciences
Molecular Microbiology and Microbial Pathogenesis

Dissertation Examination Committee:

Jeffrey P. Henderson, Chair

Thomas J. Brett

Michael G. Caparon

Daniel E. Goldberg

Clay F. Semenkovich

Timothy A. Wencewicz

Escherichia coli Iron Acquisition Paradigms
and Host Responses in the Human Urinary Milieu

by

Robin R. Shields-Cutler

A dissertation presented to the
Graduate School of Arts & Sciences
of Washington University in
partial fulfillment of the
requirements for the degree
of Doctor of Philosophy

August 2015
St. Louis, Missouri

© 2015, Robin R. Shields-Cutler

Table of Contents

List of Figures.....	iii
List of Tables	v
Acknowledgements.....	vi
Abstract.....	viii
1. Introduction: Bacterial iron acquisition and the host’s response during UTI.....	1
1.1 Clinical challenges of urinary tract infections.....	2
1.2 Iron sequestration at the host-pathogen interface.....	3
1.3 Siderocalin’s Antimicrobial Activity	6
1.4 The SCN ligand dilemma.....	8
1.5 Questions and hypotheses	9
Chapter One: References.....	16
2. Human Urinary Composition Controls Antibacterial Activity of Siderocalin	30
Chapter Two: References	74
3. The innate immune protein siderocalin binds urinary metabolites to deprive bacteria of iron.....	83
Chapter Three: References	130
4. Conclusions, Implications, and Prospects.....	138
4.1 Summary of the Thesis.....	139
4.2 Therapeutic Implications and Prospects.....	140
4.3 Perspectives on E. coli Iron Acquisition in Human Urine	143
4.4 Methodology Developments and Applications	146
4.5 Closing Remarks	148
Chapter Four: References.....	154
Appendix: Detection and expression studies on uropathogenic <i>Escherichia coli</i> siderophores.....	163
Appendix: References	183
Curriculum Vitae	188

List of Figures

FIGURE	TITLE	PAGE
<u>CHAPTER ONE</u>		
1	Siderophore-based iron acquisition by pathogenic <i>E. coli</i>	12
2	UPEC produce several chemically distinct siderophores	13
3	Siderocalin's tertiary structure and binding site	14
<u>CHAPTER TWO</u>		
1	Urinary SCN concentrations are significantly elevated in women with uncomplicated <i>E. coli</i> cystitis	58
2	In human urine, SCN imposes an enterobactin biosynthesis requirement for <i>E. coli</i> growth	59
3	SCN inhibits wild type <i>E. coli</i> growth in restrictive urine at early time points	61
4	In human urine, the SCN calyx interferes with enterobactin-mediated iron acquisition by <i>E. coli</i>	62
5	An enterobactin biosynthesis inhibitor facilitates SCN activity against a panel of wild type UPEC isolates	63
6	Urinary pH distinguishes restrictive from permissive urine	64
7	Urinary metabolomes distinguish restrictive from permissive urine	66
8	Urinary aryl sulfometabolites distinguish restrictive from permissive urine	68
9	Urinary aryl metabolites increase SCN antimicrobial activity	69
10	Urinary pH and aryl sulfates are independently associated with restrictive urines	70
11	Proposed model of SCN antimicrobial activity in restrictive urine	72
<u>CHAPTER THREE</u>		
1	Differential scanning fluorimetry (DSF) detects SCN-ferric complexes	108
2	DSF screening reveals multiple iron-dependent SCN-binding fractions in human urine	109
3	Urinary aryl alcohols perturb SCN thermal stability	111
4	Direct measurement of SCN binding validates urinary ligands	112
5	Candidate ligands potentiate SCN's antimicrobial activity in defined growth media	113
6	Pyrogallol concentrations are significantly correlated with SCN's activity	115
7	SCN binds heterogeneous ligand complexes	116
S1	DSF screen identifies fractions with SCN-binding profiles	118
S2	A urinary metabolite that does not bind SCN also does not potentiate its antimicrobial activity in defined M63 media	121

S3	Equimolar pyrogallol synergizes with SCN to restrict uropathogen growth	122
S4	Rich media (LB) does not support SCN activity, with or without supplemented catechol	123
S5	Free urinary pyrogallol concentration is correlated with urinary sulfated pyrogallol	124
S6	Urinary ligand quantification	125
S7	Highly restrictive urines have improved correlation with urinary ligand concentrations	126
S8	Salicylic acid does not affect SCN melting in DSF	127
	<u>CHAPTER FOUR</u>	
1	Aryl alcohols make up the set of SCN ligands that contribute to its antimicrobial activity in urine	150
2	Diet-derived urinary metabolites promote SCN iron sequestration and antimicrobial activity	151
3	Among restrictive urine specimens, males exhibit higher SCN activity levels than females	152
	<u>APPENDIX</u>	
1	Negative mode LC-MS shows improved catecholate siderophore signal	176
2	Negative mode LC-MS-MRM detects cyclic enterobactin standards in urine	177
3	Enterobactin is sensitive to halogenation <i>in vitro</i>	178
4	Enterobactin is produced by UPEC during human UTI	179
5	Improved aerobactin detection sensitivity and specificity in negative ion MRM	180
6	Aerobactin expression varies among <i>iucD</i> ⁺ clinical isolates	182

List of Tables

TABLE	TITLE	PAGE
	<u>CHAPTER TWO</u>	
1	Aryl sulfate associations with restrictive urine	73
	<u>CHAPTER THREE</u>	
1	Characteristics and parameters of pooled restrictive and permissive urines	128
S1	GC-MS metabolomics identifies candidate ligands enriched in DSF-positive fractions	129
	<u>CHAPTER 4</u>	
1	Cranberry products may select for enterobactin-producing uropathogens in patients experiencing recurrent UTI	153
	<u>APPENDIX</u>	
1	MRM transitions for siderophore ions in positive and negative mode	168

Acknowledgements

This dissertation and all the scholarship, knowledge, and personal growth it represents would not have been possible without unwavering support from many individuals. Chief among these is my thesis mentor, Dr. Jeff Henderson. Joining Jeff's lab was the best decision of my graduate career. He encouraged me to pursue paradoxes, putting his faith in my work from the very beginning and giving me confidence to push forward. He has also become a personal mentor, by demonstrating a healthy and productive work-life balance and allowing me the flexibility to find that balance for myself. Our shared backgrounds, Minnesota roots, interests (including appreciation for/fascination with Sump Coffee), and enthusiasm have made Jeff a phenomenal mentor, and friend, for whom I am eternally grateful.

I have been lucky to work with many intelligent and kind people. Dr. Chia Hung and Dr. Kaveri Parker welcomed me into the lab (with a few laughs at my expense...) and quickly became mentors and friends, and time in the lab with these two will always remain some of my best memories of graduate school. I am thankful to Jan Crowley and Dr. Jonas Marschall for their enthusiasm, hard work, and kindness. I've been lucky to mentor Connelly Miller, an incredibly bright and motivated undergraduate student who constantly impresses me with his technical skill and maturity, and has contributed meaningfully to this dissertation. I would also like to acknowledge the support, wisdom, and expert guidance of my thesis committee, and their encouragement for my career in science.

The financial support I have received during my graduate career has also helped make this work possible. I received an NIH Training Grant (2T32GM007067-37), and a Monsanto Excellence Fund graduate fellowship by the Division of Biology and Biomedical Sciences. I am

grateful for these funding sources, not just for their monetary support, but for the opportunities for professional and personal growth they also provided.

Early career mentors often do not receive due credit, but in high school, Jeff Ranta and Andy Weaver opened my eyes to science as a possible career and life pursuit. In college, Dr. Tricia Humphreys, Dr. Mark Levandoski, and Dr. Shannon Hinsaleasure taught me how to ask questions and test hypotheses, and continue to be close mentors. I am grateful also to the friends I have made, who make life in school immeasurably better. I want to specifically thank Matt Hibberd, who has been a terrific friend from, quite literally, day one. His generosity and willingness to help has meant a lot to my family and me.

Last, but certainly not least, is the gratitude for my family. My parents have always encouraged me to be creative and responsible, and given me the love, support, and independence that have made me the person I am. But over the last five (or really 10) years, the most important person to me, and my greatest source of support, love, and friendship, is my partner, Nora Shields-Cutler. I cannot adequately describe how much joy she brings to my life, and how much her kindness and intelligence has meant throughout my schooling. I am a better and more complete individual as a result of her, and she amazes me everyday. Finally, this acknowledgment would not be complete without mention of my faithful hound, Gertrude. Whether taking a break to explore the park or keeping my feet warm when I'm up late studying, her companionship is invaluable and irreplaceable.

Robin R. Shields-Cutler

Washington University in St. Louis

June 2015

ABSTRACT OF THE DISSERTATION

Escherichia coli Iron Acquisition Paradigms

and Host Responses in the Human Urinary Milieu

by

Robin R. Shields-Cutler

Doctor of Philosophy in Biology and Biomedical Sciences

Molecular Microbiology and Microbial Pathogenesis

Washington University in St. Louis, 2015

Professor Jeffrey P. Henderson, Chair

Urinary tract infections (UTIs) are some of the most common bacterial infections worldwide and are increasingly complicated by high antibiotic resistance and recurrence rates. Explanations for the marked individual differences in UTI susceptibility remain incomplete. In this thesis we show that urinary colonization by uropathogenic *E. coli* (UPEC) is influenced by urine composition and the activity of an important innate immune protein, siderocalin (SCN; also called lipocalin 2 or neutrophil gelatinase-associated lipocalin/NGAL). During UTI, host factors limit the availability of iron, an essential nutrient for the invading pathogen. In response, UPEC modify the urinary environment with metal binding siderophores, some of which are bound by the soluble protein SCN. Interactions between these opposing factors during early UPEC colonization determine the pathogen's ability to successfully acquire iron and grow to a density sufficient to cause infection.

SCN has been described at length as an antimicrobial protein, exerting its effect by sequestering certain ferric siderophores. This has led to the hypothesis that a pathogen's additional, non-SCN-binding siderophores are adaptations to this host pressure; however, the role of individual siderophores has been shown in some models to depend greatly on the infection environment. Because human urine is chemically complex and distinct from other sites of infection, we first investigated SCN's effect on uropathogenic *E. coli* (UPEC) growth in human urine from a healthy reference population. Using genetic deletions, chemical inhibition, and chemical complementation, we observed enterobactin siderophore expression to be a key factor permitting UPEC growth in SCN-supplemented human urine from a subset of individuals. Because SCN neutralizes enterobactin in non-urinary experimental systems, this result suggests a determinative role for urine-specific components in manipulating antimicrobial paradigms.

Our initial inquiry showed dramatic variability in SCN's antimicrobial activity between individuals' urine specimens. We next used these individual differences as an independent variable, defining groups of high and low activity, in order to investigate the urinary factors controlling SCN activity. Chemical and demographic comparisons yielded a significant positive correlation between SCN activity and elevated urine pH. To determine whether further individual differences arose from differences in urinary small molecule composition (the urinary metabolome), we compared individuals using a mass spectrometry-based metabolomic approach. This approach identified aryl alcohols as significant correlates with SCN activity. These results support a model in which the urinary environment is able to influence urinary tract colonization by pathogens.

To further understand how these urinary metabolites may contribute to SCN antimicrobial activity, we sought to identify key metabolite cofactors present in restrictive urine specimens that actively participate in SCN's antimicrobial mechanism as observed above. We developed a robust biophysical screen that allowed us to look for urine fractions containing iron-dependent SCN ligands. A biophysical validation process identified several elevated aryl alcohols that bound SCN and were able to reconstitute SCN's antimicrobial activity in simple, defined media with limited iron. Demonstrating that urinary metabolites confer elevated SCN activity in a defined media provides mechanistic validation for our proposed urinary model, and further supports a dietary component to preventative UTI therapies. The human metabolome may thus represent an underappreciated contributor to disease susceptibility and pathogen evolution, and a potential target for future therapeutic interventions.

Collectively, the work presented in this thesis describes an emerging host-pathogen axis, where urinary composition plays a pivotal role in the efficacy of an innate immune response, and suggests targeted avenues for improved clinical control of UTI.

CHAPTER ONE

Introduction: Bacterial iron acquisition and the host's response during UTI

1.1 Clinical challenges of urinary tract infections

Urinary tract infections (UTIs) are one of the world's most common infectious diseases. Approximately half of all women will have experienced at least one UTI episode by their mid-30s (1, 2). Young children and the elderly also experience UTI with higher frequency, as do hospital inpatients with indwelling urinary catheters (1, 3). The typical pathogenic course for UTI begins when periurethral bacteria—most commonly *Escherichia coli*—colonize the bladder and then invade the epithelial cells and replicate, eventually leading to the inflammation responsible for UTI's major symptoms (2, 4, 5). Serious infections occur when bacteria ascend the ureters and access the kidney, causing an infection called pyelonephritis (3). From the kidney, bacteria may then infect the bloodstream, causing urinary-source bacteremia, a potentially life-threatening disease (3). Historically, UTI has been treated empirically with standard antibiotics but uropathogens are increasingly resistant to these drugs, creating therapeutic challenges that place a significant physical and financial burden on the healthcare system, and notably decrease patients' quality of life (1, 2, 6, 7).

In addition to the challenges of resistant infections, roughly one quarter of women with uncomplicated UTIs will go on to experience a recurrent infection within six months (8). These recurrent infections, often caused by the same strain, may happen as frequently as 5-10 episodes per year, which causes considerable morbidity and discomfort, and present unique challenges to developing preventative therapies (9). One challenge faced in treating UTI is heterogeneity in disease progression, where some individuals experience a single self-resolving cystitis episode, while others progress to highly recurrent or even life-threatening systemic infections (2, 10–12). Patient stratification could improve antibiotic stewardship and explorations into alternative

therapy, but individuals' wide-ranging susceptibilities to infection and recurrence are poorly understood.

As precision medicine becomes common in other fields, it is important to consider that host differences may also play determinative roles in infectious disease susceptibility and in responses to particular therapies (13–15). Currently, prophylactic antibiotics are commonly prescribed to limit recurrences, but this carries significant side effects and disadvantages, including selective pressure on pathogens and commensals for antibiotic resistance (2, 16). Therefore, reducing the reliance on traditional antibiotics has myriad advantages, including avoiding collateral damage to the host's commensal microbiota and slowing the emergence and spread of antibiotic resistant pathogens (16–18). Non-antibiotic therapies to prevent recurrent UTI have been explored but are largely inconsistent and poorly studied (2, 6, 19). Additional research on pathogen mechanism- and virulence-targeted therapies may provide novel avenues for effective treatments.

1.2 Iron sequestration at the host-pathogen interface

One of the most fundamental host responses to bacterial infection is micronutrient restriction (20, 21). When a bacterial infection is recognized, transcriptional responses rapidly produce, among many other effectors, proteins charged with limiting available concentrations of essential nutrients such as transition metals (22–24). The conflict over nutrient iron, in particular, is a major feature of both host and pathogen behavior during infection (25–27). During an infection, upregulation of host iron transport and storage factors drives the free iron concentration in the serum to an astonishing $\sim 10^{-24}$ M (28–30). This nutritional response is a key aspect of innate

immunity, and deficiencies or abnormalities in iron regulation are linked with a number of pathologies including susceptibility to infectious diseases (21, 31–33).

Iron restriction creates an environment where pathogenic bacteria require active processes to acquire iron in order to replicate. While the infection milieu may contain $\sim 10^{-24}$ M iron, bacterial cells demand on the order of 10^{-6} M iron for basic physiology and metabolism (34). To overcome this vast discrepancy, pathogens have evolved multiple virulence factors dedicated to acquiring iron from host proteins such as transferrin or ferritin, or iron-containing cofactors such as heme (30). The importance of this process is emphasized by the diversity and redundancy present in Gram-negative bacterial iron acquisition, and underscores their potential as targets for anti-virulence approaches (35, 36).

In order to compete with the host factors upregulated during infection, Gram-negative pathogens like *E. coli* have evolved small molecule (< 1.5 kDa), high-affinity iron chelators, called siderophores (Fig. 1a). Diverse organisms produce an equally diverse collection of siderophores (36), while this thesis specifically investigates the virulence-associated subset of siderophores expressed by uropathogenic *E. coli* (UPEC). Multiple genetic and phenotypic screens confirm that UPEC produce up to four siderophores (Fig. 2): the conserved catecholate siderophore enterobactin; the glucosylated enterobactins or salmochelins; the mixed hydroxamate-phenolate, yersiniabactin; and the citrate-hydroxamate, aerobactin (37–39). Each siderophore possesses unique physiochemical properties and genotypic frequencies, suggesting specialized roles for pathogenesis (36, 40).

Siderophores successfully circumvent host iron sequestration due to their incredible iron affinity (Fig. 1b), with pH-dependent stability constants of up to 10^{49} for enterobactin (41). Transferrin, on the other hand, binds two molecules of iron with stability constants of $\sim 10^{22}$ at pH 7.4 (28). Numerous studies have demonstrated these siderophores' ability to capture iron from transferrin, lactoferrin, and ferritin, though the process is often kinetically slow and pH-dependent (42–45). During UTI, iron limitation in the tissue and urine relieves transcriptional repression by the Fur regulator, leading to upregulated expression of siderophore operons (36, 46, 47). These secondary metabolites are synthesized from common metabolic precursors such as chorismate and amino acids, and are assembled by non-ribosomal peptide and/or polyketide synthases (36). This process consumes valuable biosynthetic precursors and can make a measurable impact on the pathogen's metabolism (48). Producing multiple factors at a notable cost to accomplish the same goal—iron acquisition from the host—suggests that the chemical diversity in siderophore structures provides fitness benefits in varying host environments. This has been demonstrated in lung models of *Klebsiella pneumoniae* infection (49), and in the copper-binding and superoxide dismutase activity of yersiniabactin during UTI (50, 51). In addition, expressing multiple siderophores has been hypothesized as a means of evading the host immune response, namely sequestration by the protein siderocalin (or lipocalin 2, neutrophil gelatinase-associated lipocalin/NGAL, 24p3) (52–54). This thesis further examines this hypothesis, investigating the roles of UPEC siderophores in acquiring iron from the human urinary environment in the presence of the innate immune protein siderocalin.

1.3 Siderocalin's Antimicrobial Activity

Siderocalin (SCN), also commonly called lipocalin 2 or neutrophil gelatinase-associated lipocalin (NGAL), is a member of the lipocalin protein family (55, 56). An 8-stranded β -barrel fold defines these soluble proteins, and also shapes the proteins' binding sites (Fig. 3a,b); typical ligands for these sites are small hydrophobic molecules. SCN was discovered by Kjeldsen and colleagues when it was co-purified with gelatinase from human neutrophils (57–59), but its function and ligand(s) would remain unknown for nearly a decade. In 2002, Goetz and colleagues published a seminal paper presenting SCN's crystal structure, showing that when purified from certain *E. coli* strains, the binding site (or calyx) was occupied with an iron atom chelated by a small molecule (60). They showed that the ligand was in fact ferric enterobactin, the common *E. coli* siderophore (29, 37, 60). When coordinated with Fe(III), enterobactin carries a delocalized net -3 charge. The SCN calyx is shaped by Lys125, Lys134, and Arg81, creating a positively-charged pocket that stabilizes the ferric enterobactin complex with sub-nanomolar affinity at physiologic pH (Fig 3c,d) (60, 61). This serendipitous discovery led to the hypothesis that SCN's role is to sequester ferric siderophores during infection (Fig. 1b), a proposal consistent with its abundance in neutrophil granules and upregulation in response to a number of infectious challenges (58, 60, 62, 63). In accordance with other lipocalin protein names, which are derived from their ligand, NGAL was re-named *siderocalin* (60).

Subsequent work by multiple laboratories has supported SCN's role in preventing bacterial iron acquisition. SCN has been implicated in the pathogenesis of *E. coli*, *K. pneumoniae*, *Mycobacterium tuberculosis*, *Vibrio cholerae*, *Streptococcus pneumoniae*, *Chlamydia pneumoniae*, *Salmonella enterica*, and *Pseudomonas aeruginosa*, for example (62, 64–67). For

most of these successful human pathogens, evading iron sequestration by SCN appears to be a factor driving virulence factor adaptation. Work in *Salmonella* first suggested that the salmochelins, or glucosylated enterobactins, produced by the *iroA* gene cluster were virulence-associated adaptations to overcome SCN (53, 68). Adding glucose moieties to linearized enterobactin's catecholate groups increases the siderophore's solubility and the bulky additions block binding in SCN's calyx, thus preventing SCN from sequestering the ferric salmochelin siderophore (40, 53). Similar stories describing “stealth” or “escape” siderophore behavior have since emerged for other pathogens including *E. coli*, *K. pneumoniae*, and *M. tuberculosis* (54, 65, 69). In these examples, pathogens maintain and express both SCN-sensitive and SCN-insensitive siderophores. As a result of these characterizations, SCN evasion has become a common explanation for encoding multiple iron-chelating secondary metabolites, despite the metabolic cost (36, 52, 70). This parallels the evidence that UPEC siderophore biosynthesis is highly upregulated and important for UTI pathogenesis (38, 39, 71–74).

Previous murine studies indicate that SCN is highly upregulated in UPEC-infected bladder tissue (71). Recently, several studies including one presented in this thesis showed that SCN is found at elevated levels in the urine of women with UTI, and another study proposed its use as a biomarker for pediatric UTI (72, 75–77). The high local SCN concentration during UTI—up to 10 μM in unfractionated urine (72)—likely derives from the characteristic neutrophil recruitment and inflammation in the bladder, neutrophils present in the urine, and epithelial cell secretion (78, 79). Specific cell types in the kidney are also implicated in SCN secretion (72). These data all point to SCN's involvement in the host response to *E. coli* UTI, however its role and efficacy as an iron-sequestering antimicrobial protein in this environment has been unclear, and is the

focus of this thesis. This question is particularly interesting, as UPEC isolates express an assortment of siderophores, possessing anywhere from one to four distinct siderophore pathways (37). Whether this diversity is driven by SCN or whether it has any relevant implications at all was unknown.

1.4 The SCN ligand dilemma

A careful reading of the SCN antimicrobial literature suggests that there is more to its story than “stealth” siderophores. Interestingly, a *K. pneumoniae* mutant lacking enterobactin biosynthesis (but capable of yersiniabactin biosynthesis) was inhibited by SCN in pooled urine, but not in RPMI media (65). This effect was noted only because some of the clinical isolates were obtained from urine; since the paper studied virulence factors in respiratory infection, this curious paradox was left untested and unaddressed. However, when this enterobactin-deficient strain was used to infect SCN-deficient transgenic mice, the animals tended to fare worse than their wild type, SCN^{+/+} counterparts. In both these subtle examples, SCN displayed a protective effect despite the absence of any known bacterial siderophore ligand. Separately, some studies have suggested that Gram-negative bacteria can access iron bound by small aromatic metabolites of the host (80–85), due to their chemical similarity to siderophores and intermediates. Combined, these findings raised the question of whether SCN could participate in iron sequestration independent from bacterial ligands such as enterobactin.

Bao and colleagues presented an important perspective on this question by testing human metabolites’ ability to bind SCN as ferric complexes (86). They established that SCN could indeed interact with ferric complexes other than bacterial siderophores and identified several

common catecholates as potential endogenous ferric ligands of SCN. These metabolites are structurally similar to the prototypic ligand, enterobactin, and chelate iron in the same hexadentate coordination, thus mimicking ferric enterobactin's shape and overall negative charge arrangement. This enables high-affinity binding in the SCN calyx, and stabilization by the same cation- π and electrostatic interactions as enterobactin (60, 87, 88). Furthermore, it appears that while these free ferric-catecholate complexes are transient and labile in solution, the SCN calyx provides a molecular template that drives formation of stable ferric complexes within the binding site (86). The authors then showed that the SCN-catecholate complex is stable when injected into mice, and proposed that this serves as yet another means of iron regulation and trafficking within mammalian host serum and tissues. Since they tested a limited number of pure metabolites from a commercial pool, there are likely additional potential ligands present in various host microenvironments with important physiochemical properties. Furthermore, although the biophysical details were thoroughly investigated, it was unclear whether these metabolite interactions truly contribute to SCN's role in any specific disease or metabolic process.

1.5 Questions and hypotheses

Curiously, while SCN's discovery and subsequent biochemical characterizations have focused on its antimicrobial roles, the SCN literature has been largely populated by studies unrelated to bacterial pathogenesis. As of this thesis' submission, a PubMed search for SCN (including its common aliases) yields nearly 2,000 articles; adding "bacteria" to the search term reduces this to just 61 publications. Since SCN is upregulated in response to general inflammatory stimuli, is found at relatively high levels in biofluids, and is relatively stable, it has been proposed as a biomarker for ailments ranging from acute kidney injury to late-life depression (89–91).

Correlative studies have also suggested its involvement in diseases such as breast cancer and diabetes (92–94). Mechanistic evidence in these associations is notably absent, however, and the question remains in what endogenous interactions and activities SCN might engage, in the absence of a bacterial ligand.

Together, early observations about SCN's interactions with endogenous metabolites and its perceived involvement in myriad host processes suggest functional consequences for this protein that have been previously unappreciated. Because SCN is upregulated during UTI (71, 77) and diet-derived host catecholates are known components of urine (95), we hypothesized that interactions between these components would affect SCN's anti-UPEC activity in urine, and could be relevant to UTI pathogenesis. Since all previous literature on SCN's activity, the consequences of interactions with host molecules, and the relationship between SCN and multiple bacterial siderophores had been carried out in non-urinary contexts, the specific and unique effect of urinary composition on SCN's activity is a compelling but unaddressed question, prior to the work presented in this thesis. We hypothesized that by sequestering iron in host-derived complexes SCN can limit bacterial growth, regardless of siderophore compatibility, by preventing access to the urine's bioavailable iron.

This thesis therefore investigates whether SCN's interactions with urinary cofactors can control UPEC growth, and whether certain siderophores are necessary to overcome this inhibition. Our investigations are guided by the following basic questions:

1. Does SCN restrict UPEC growth in human urine?
2. Do particular UPEC siderophores provide competitive advantages in the presence of SCN?

3. Do unique features of human urine play deterministic roles in SCN's antimicrobial activity?
4. If SCN does exhibit anti-UPEC activity, can human urine be manipulated to potentiate this effect?

These questions span the fields of basic biology, biophysical chemistry, and clinical medicine. To reconcile wide-ranging hypotheses, this thesis combines basic microbiology with biochemical observations made from individual human specimens. By recognizing patterns in SCN activity, we developed sensitive chemical analyses to identify host and microbial correlates to explain the differences between individual responses to UPEC infection (77). Biochemical and biophysical methods were also used to define the chemical players that ultimately determine SCN's activity. The findings of this thesis have important clinical implications for UTI patients, particularly those with susceptibility to frequent UTI.

CHAPTER ONE: FIGURES

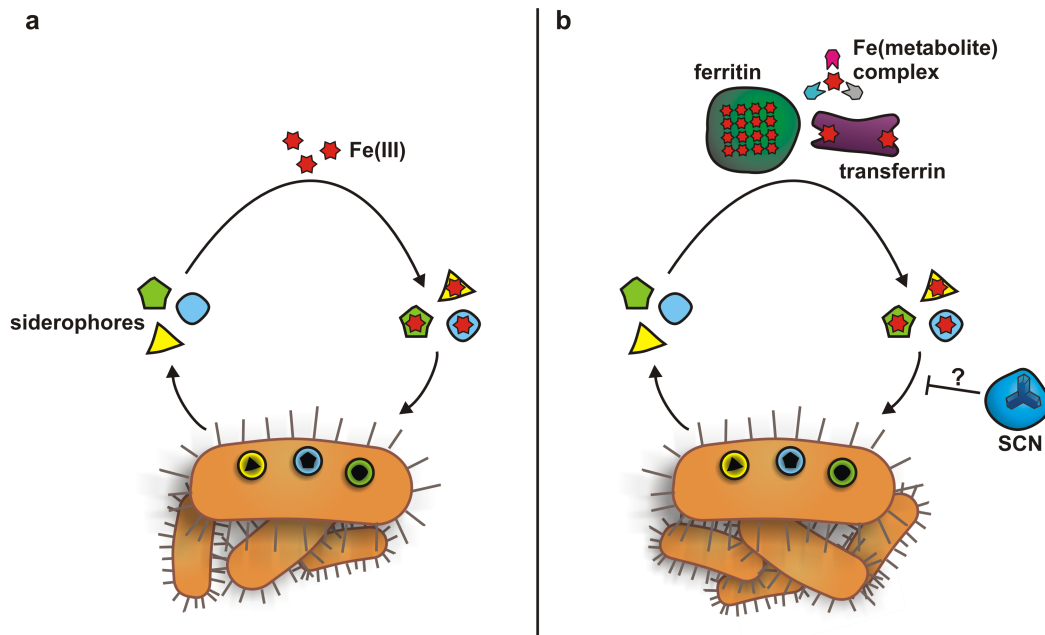


Figure 1. Siderophore-based iron acquisition by pathogenic *E. coli*. (a) *E. coli* bacteria (in brown) secrete siderophores (blue, yellow, and green shapes) to chelate ferric iron (red hexagons) from the environment. These small molecule chelators are then imported by specific receptors on the bacterial outer membrane (matching shapes on bacterial surface). To obtain essential iron in the context of a mammalian host (b), pathogenic *E. coli* secrete siderophores that effectively compete with host iron binding factors such as ferritin (in green), transferrin (in purple), and host metabolites (shown as a 3:1 ferric complex). The innate immune protein siderocalin (SCN, in blue) can counteract this process by sequestering some ferric-bound siderophores in its binding site. The extent to which SCN can inhibit bacterial iron uptake may be determined by the siderophores' chemical structures as well as the infection microenvironment.

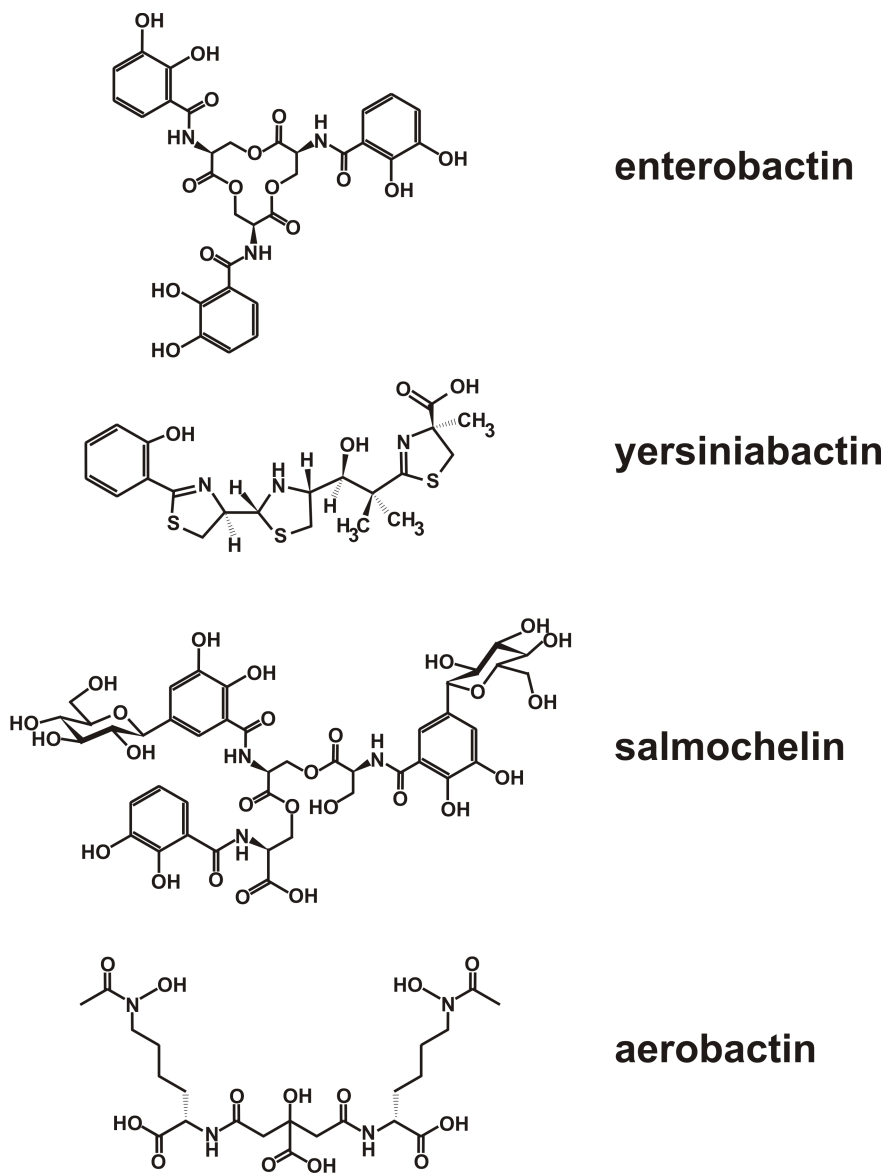


Figure 2. UPEC produce several chemically distinct siderophores. UPEC isolates possess biosynthetic machinery to make varying combinations of the four siderophores depicted above, with the exception of enterobactin, which is ubiquitously expressed by UPEC.

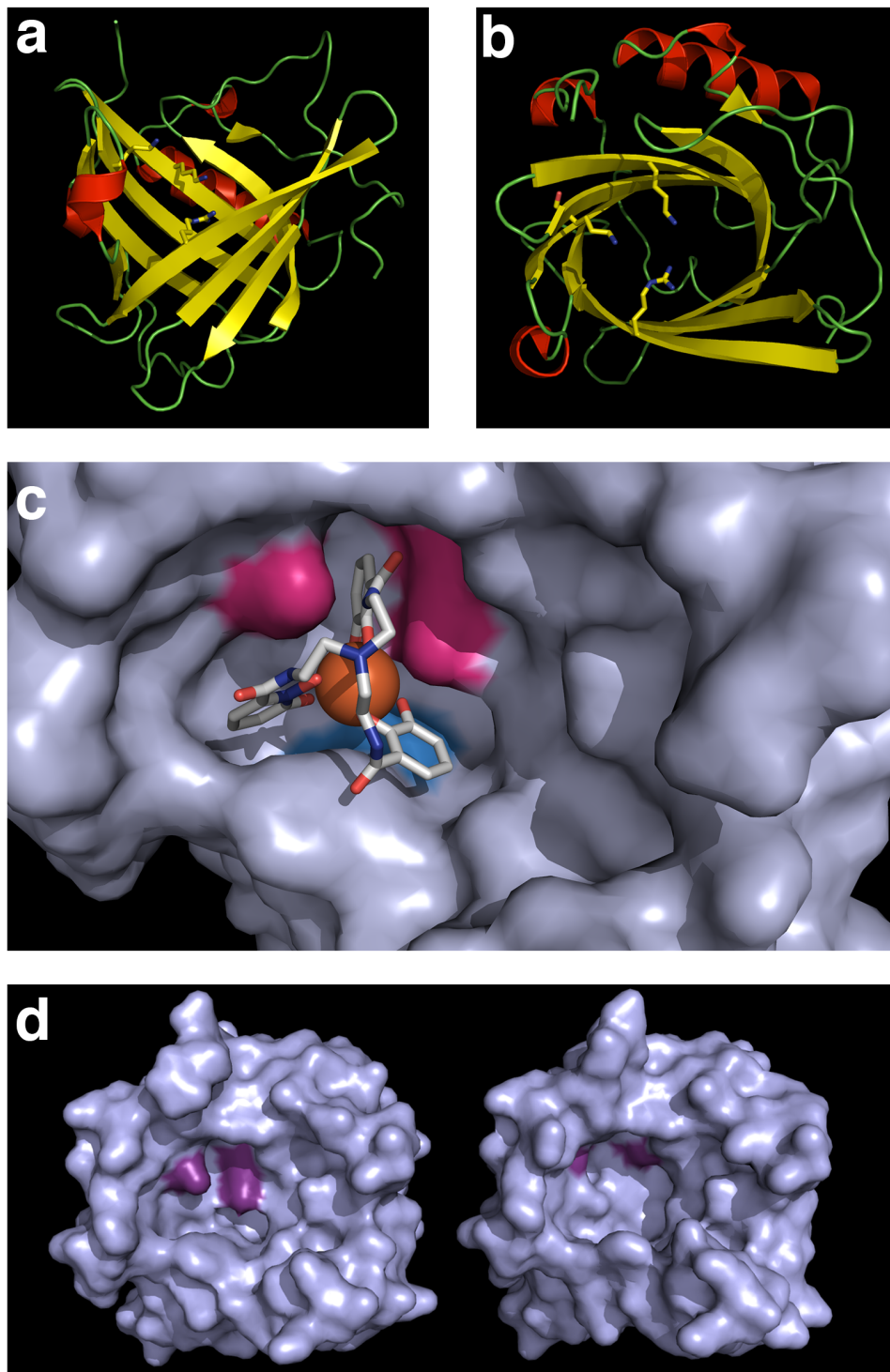


Figure 3. Siderocalin's tertiary structure and binding site. (a) Siderocalin displays the typical 8-stranded β -barrel lipocalin fold; the antiparallel sheets form the binding site viewed from the

top in **(b)**. Residues Lys125, Lys134, and Arg81 give the binding site its critical positive charge, and are indicated as sticks in **(a)** and **(b)**. The interaction between SCN and enterobactin is modeled in **(c)** using a non-hydrolyzable enterobactin analog, Fe(TrenCam). **(d)** On left, the wild-type SCN calyx is shown with calyx lysine residues in purple; on right, the K125A/K134A mutant calyx is shown with the substituted alanine residues in purple. Wild-type SCN PDB ID: 3HWF. Mutant SCN PDB ID: 3HWD.

CHAPTER ONE: REFERENCES

1. Foxman, B. (2010) The epidemiology of urinary tract infection. *Nat. Rev. Urol.* **7**, 653–660
2. Hooton, T. M. (2012) Uncomplicated Urinary Tract Infection. *N. Engl. J. Med.* **366**, 1028–1037
3. Lichtenberger, P., and Hooton, T. M. (2008) Complicated urinary tract infections. *Curr. Infect. Dis. Rep.* **10**, 499–504
4. Hannan, T. J., Mysorekar, I. U., Hung, C. S., Isaacson-Schmid, M. L., and Hultgren, S. J. (2010) Early Severe Inflammatory Responses to Uropathogenic *E. coli* Predispose to Chronic and Recurrent Urinary Tract Infection. *PLoS Pathog.* **6**, e1001042
5. Flores-Mireles, A. L., Walker, J. N., Caparon, M., and Hultgren, S. J. (2015) Urinary tract infections: epidemiology, mechanisms of infection and treatment options. *Nat. Rev. Microbiol.* **13**, 269–284
6. Foxman, B., and Buxton, M. (2013) Alternative approaches to conventional treatment of acute uncomplicated urinary tract infection in women. *Curr. Infect. Dis. Rep.* **15**, 124–129
7. Gupta, K., Hooton, T. M., and Stamm, W. E. (2001) Increasing antimicrobial resistance and the management of uncomplicated community-acquired urinary tract infections. *Ann. Intern. Med.* **135**, 41–50
8. Foxman, B. (2002) Epidemiology of urinary tract infections: incidence, morbidity, and economic costs. *Am. J. Med.* **113 Suppl 1A**, 5S–13S
9. Chen, S. L., Wu, M., Henderson, J. P., Hooton, T. M., Hibbing, M. E., Hultgren, S. J., and Gordon, J. I. (2013) Genomic diversity and fitness of *E. coli* strains recovered from the

- intestinal and urinary tracts of women with recurrent urinary tract infection. *Sci. Transl. Med.* **5**, 184ra60
10. Marschall, J., Zhang, L., Foxman, B., Warren, D. K., Henderson, J. P., and CDC Prevention Epicenters Program (2012) Both host and pathogen factors predispose to *Escherichia coli* urinary-source bacteremia in hospitalized patients. *Clin. Infect. Dis.* **54**, 1692–1698
 11. Marschall, J., Piccirillo, M. L., Foxman, B., Zhang, L., Warren, D. K., Henderson, J. P., and CDC Prevention Epicenters Program (2013) Patient characteristics but not virulence factors discriminate between asymptomatic and symptomatic *E. coli* bacteriuria in the hospital. *BMC Infect. Dis.* **13**, 213
 12. Scholes, D., Hooton, T. M., Roberts, P. L., Stapleton, A. E., Gupta, K., and Stamm, W. E. (2000) Risk factors for recurrent urinary tract infection in young women. *J. Infect. Dis.* **182**, 1177–1182
 13. Wilson, I. D. (2009) Drugs, bugs, and personalized medicine: Pharmacometabonomics enters the ring. *Proc. Natl. Acad. Sci.* **106**, 14187–14188
 14. Langley, R. J., Tsalik, E. L., Velkinburgh, J. C. van, Glickman, S. W., Rice, B. J., Wang, C., Chen, B., Carin, L., Suarez, A., Mohny, R. P., Freeman, D. H., Wang, M., You, J., Wulff, J., Thompson, J. W., Moseley, M. A., Reisinger, S., Edmonds, B. T., Grinnell, B., Nelson, D. R., Dinwiddie, D. L., Miller, N. A., Saunders, C. J., Soden, S. S., Rogers, A. J., Gazourian, L., Fredenburgh, L. E., Massaro, A. F., Baron, R. M., Choi, A. M. K., Corey, G. R., Ginsburg, G. S., Cairns, C. B., Otero, R. M., Fowler, V. G., Rivers, E. P., Woods, C.

- W., and Kingsmore, S. F. (2013) An Integrated Clinico-Metabolomic Model Improves Prediction of Death in Sepsis. *Sci. Transl. Med.* **5**, 195ra95–195ra95
15. Church, G. M. (2015) Precision Chemistry for Precision Medicine. *ACS Cent. Sci.* **1**, 11–13
 16. Sommer, M. O. A., and Dantas, G. (2011) Antibiotics and the resistant microbiome. *Curr. Opin. Microbiol.* **14**, 556–563
 17. Dethlefsen, L., Huse, S., Sogin, M. L., and Relman, D. A. (2008) The Pervasive Effects of an Antibiotic on the Human Gut Microbiota, as Revealed by Deep 16S rRNA Sequencing. *PLoS Biol.* **6**, e280
 18. Jernberg, C., Löfmark, S., Edlund, C., and Jansson, J. K. (2010) Long-term impacts of antibiotic exposure on the human intestinal microbiota. *Microbiology.* **156**, 3216–3223
 19. Vasileiou, I., Katsargyris, A., Theocharis, S., and Giaginis, C. (2013) Current clinical status on the preventive effects of cranberry consumption against urinary tract infections. *Nutr. Res. N. Y. N.* **33**, 595–607
 20. Diaz-Ochoa, V. E., Jellbauer, S., Klaus, S., and Raffatellu, M. (2014) Transition metal ions at the crossroads of mucosal immunity and microbial pathogenesis. *Front. Cell. Infect. Microbiol.* **4**, 2
 21. Hood, M. I., and Skaar, E. P. (2012) Nutritional immunity: transition metals at the pathogen-host interface. *Nat. Rev. Microbiol.* **10**, 525–537
 22. Song, J., and Abraham, S. N. (2008) TLR-mediated immune responses in the urinary tract. *Curr. Opin. Microbiol.* **11**, 66–73
 23. Kim, S., Becker, J., Bechheim, M., Kaiser, V., Noursadeghi, M., Fricker, N., Beier, E., Klaschik, S., Boor, P., Hess, T., Hofmann, A., Holdenrieder, S., Wendland, J. R., Fröhlich,

- H., Hartmann, G., Nöthen, M. M., Müller-Myhsok, B., Pütz, B., Hornung, V., and Schumacher, J. (2014) Characterizing the genetic basis of innate immune response in TLR4-activated human monocytes. *Nat. Commun.* 10.1038/ncomms6236
24. Godaly, G., Ambite, I., and Svanborg, C. (2015) Innate immunity and genetic determinants of urinary tract infection susceptibility. *Curr. Opin. Infect. Dis.* **28**, 88–96
25. Cassat, J. E., and Skaar, E. P. (2013) Iron in Infection and Immunity. *Cell Host Microbe.* **13**, 509–519
26. Cherayil, B. J. (2011) The role of iron in the immune response to bacterial infection. *Immunol. Res.* **50**, 1–9
27. Brown, J. S., and Holden, D. W. (2002) Iron acquisition by Gram-positive bacterial pathogens. *Microbes Infect. Inst. Pasteur.* **4**, 1149–1156
28. Martin, R. B., Savory, J., Brown, S., Bertholf, R. L., and Wills, M. R. (1987) Transferrin binding of Al³⁺ and Fe³⁺. *Clin. Chem.* **33**, 405–407
29. Raymond, K. N., Dertz, E. A., and Kim, S. S. (2003) Enterobactin: an archetype for microbial iron transport. *Proc. Natl. Acad. Sci. U. S. A.* **100**, 3584–3588
30. Becker, K. W., and Skaar, E. P. (2014) Metal limitation and toxicity at the interface between host and pathogen. *FEMS Microbiol. Rev.* **38**, 1235–1249
31. Melby, K., Slørdahl, S., Gutteberg, T. J., and Nordbø, S. A. (1982) Septicaemia due to *Yersinia enterocolitica* after oral overdoses of iron. *Br. Med. J. Clin. Res. Ed.* **285**, 467–468
32. Griffiths, E. (1991) Iron and bacterial virulence--a brief overview. *Biol. Met.* **4**, 7–13

33. Becroft, D. M., Dix, M. R., and Farmer, K. (1977) Intramuscular iron-dextran and susceptibility of neonates to bacterial infections. In vitro studies. *Arch. Dis. Child.* **52**, 778–781
34. Braun, V., and Killmann, H. (1999) Bacterial solutions to the iron-supply problem. *Trends Biochem. Sci.* **24**, 104–109
35. Cegelski, L., Marshall, G. R., Eldridge, G. R., and Hultgren, S. J. (2008) The biology and future prospects of antivirulence therapies. *Nat. Rev. Microbiol.* **6**, 17–27
36. Miethke, M., and Marahiel, M. A. (2007) Siderophore-based iron acquisition and pathogen control. *Microbiol. Mol. Biol. Rev.* **71**, 413–451
37. Henderson, J. P., Crowley, J. R., Pinkner, J. S., Walker, J. N., Tsukayama, P., Stamm, W. E., Hooton, T. M., and Hultgren, S. J. (2009) Quantitative metabolomics reveals an epigenetic blueprint for iron acquisition in uropathogenic *Escherichia coli*. *PLoS Pathog.* **5**, e1000305
38. Garcia, E. C., Brumbaugh, A. R., and Mobley, H. L. T. (2011) Redundancy and specificity of *Escherichia coli* iron acquisition systems during urinary tract infection. *Infect. Immun.* **79**, 1225–1235
39. Chen, S. L., Hung, C. S., Xu, J., Reigstad, C. S., Magrini, V., Sabo, A., Blasiar, D., Bieri, T., Meyer, R. R., and Ozersky, P. (2006) Identification of genes subject to positive selection in uropathogenic strains of *Escherichia coli*: a comparative genomics approach. *Proc. Natl. Acad. Sci.* **103**, 5977–5982

40. Luo, M., Lin, H., Fischbach, M. A., Liu, D. R., Walsh, C. T., and Groves, J. T. (2006) Enzymatic Tailoring of Enterobactin Alters Membrane Partitioning and Iron Acquisition. *ACS Chem. Biol.* **1**, 29–32
41. Loomis, L. D., and Raymond, K. N. (1991) Solution equilibria of enterobactin and metal-enterobactin complexes. *Inorg. Chem.* **30**, 906–911
42. Freestone, P. P. E., Haigh, R. D., Williams, P. H., and Lyte, M. (2003) Involvement of enterobactin in norepinephrine-mediated iron supply from transferrin to enterohaemorrhagic *Escherichia coli*. *FEMS Microbiol. Lett.* **222**, 39–43
43. Konopka, K., and Neilands, J. B. (1984) Effect of serum albumin on siderophore-mediated utilization of transferrin iron. *Biochemistry (Mosc.)*. **23**, 2122–2127
44. Brock, J. H., Williams, P. H., Licéaga, J., and Wooldridge, K. G. (1991) Relative availability of transferrin-bound iron and cell-derived iron to aerobactin-producing and enterochelin-producing strains of *Escherichia coli* and to other microorganisms. *Infect. Immun.* **59**, 3185–3190
45. Gobin, J., and Horwitz, M. A. (1996) Exochelins of *Mycobacterium tuberculosis* remove iron from human iron-binding proteins and donate iron to mycobactins in the M. tuberculosis cell wall. *J. Exp. Med.* **183**, 1527–1532
46. Braun, V., and Braun, M. (2002) Iron transport and signaling in *Escherichia coli*. *FEBS Lett.* **529**, 78–85
47. Troxell, B., and Hassan, H. M. (2013) Transcriptional regulation by Ferric Uptake Regulator (Fur) in pathogenic bacteria. *Front. Cell. Infect. Microbiol.* **3**, 59

48. Lv, H., Hung, C. S., and Henderson, J. P. (2014) Metabolomic analysis of siderophore cheater mutants reveals metabolic costs of expression in uropathogenic *Escherichia coli*. *J. Proteome Res.* **13**, 1397–1404
49. Bachman, M. A., Lenio, S., Schmidt, L., Oyler, J. E., and Weiser, J. N. (2012) Interaction of lipocalin 2, transferrin, and siderophores determines the replicative niche of *Klebsiella pneumoniae* during pneumonia. *mBio*. 10.1128/mBio.00224-11
50. Chaturvedi, K. S., Hung, C. S., Crowley, J. R., Stapleton, A. E., and Henderson, J. P. (2012) The siderophore yersiniabactin binds copper to protect pathogens during infection. *Nat. Chem. Biol.* **8**, 731–736
51. Chaturvedi, K. S., Hung, C. S., Giblin, D. E., Urushidani, S., Austin, A. M., Dinauer, M. C., and Henderson, J. P. (2014) Cupric yersiniabactin is a virulence-associated superoxide dismutase mimic. *ACS Chem. Biol.* **9**, 551–561
52. Clifton, M. C., Corrent, C., and Strong, R. K. (2009) Siderocalins: siderophore-binding proteins of the innate immune system. *Biometals Int. J. Role Met. Ions Biol. Biochem. Med.* **22**, 557–564
53. Fischbach, M. A., Lin, H., Zhou, L., Yu, Y., Abergel, R. J., Liu, D. R., Raymond, K. N., Wanner, B. L., Strong, R. K., Walsh, C. T., Aderem, A., and Smith, K. D. (2006) The pathogen-associated *iroA* gene cluster mediates bacterial evasion of lipocalin 2. *Proc. Natl. Acad. Sci. U. S. A.* **103**, 16502–16507
54. Abergel, R. J., Wilson, M. K., Arceneaux, J. E. L., Hoette, T. M., Strong, R. K., Byers, B. R., and Raymond, K. N. (2006) Anthrax pathogen evades the mammalian immune system through stealth siderophore production. *Proc. Natl. Acad. Sci. U. S. A.* **103**, 18499–18503

55. Breustedt, D. A., Schönfeld, D. L., and Skerra, A. (2006) Comparative ligand-binding analysis of ten human lipocalins. *Biochim. Biophys. Acta.* **1764**, 161–173
56. Flower, D. R., North, A. C., and Sansom, C. E. (2000) The lipocalin protein family: structural and sequence overview. *Biochim. Biophys. Acta.* **1482**, 9–24
57. Kjeldsen, L., Johnsen, A. H., Sengeløv, H., and Borregaard, N. (1993) Isolation and primary structure of NGAL, a novel protein associated with human neutrophil gelatinase. *J. Biol. Chem.* **268**, 10425–10432
58. Kjeldsen, L., Bainton, D. F., Sengeløv, H., and Borregaard, N. (1994) Identification of neutrophil gelatinase-associated lipocalin as a novel matrix protein of specific granules in human neutrophils. *Blood.* **83**, 799–807
59. Bundgaard, J. R., Sengeløv, H., Borregaard, N., and Kjeldsen, L. (1994) Molecular cloning and expression of a cDNA encoding NGAL: a lipocalin expressed in human neutrophils. *Biochem. Biophys. Res. Commun.* **202**, 1468–1475
60. Goetz, D. H., Holmes, M. A., Borregaard, N., Bluhm, M. E., Raymond, K. N., and Strong, R. K. (2002) The neutrophil lipocalin NGAL is a bacteriostatic agent that interferes with siderophore-mediated iron acquisition. *Mol. Cell.* **10**, 1033–1043
61. Goetz, D. H., Willie, S. T., Armen, R. S., Bratt, T., Borregaard, N., and Strong, R. K. (2000) Ligand preference inferred from the structure of neutrophil gelatinase associated lipocalin. *Biochemistry (Mosc.)*. **39**, 1935–1941
62. Flo, T. H., Smith, K. D., Sato, S., Rodriguez, D. J., Holmes, M. A., Strong, R. K., Akira, S., and Aderem, A. (2004) Lipocalin 2 mediates an innate immune response to bacterial infection by sequestering iron. *Nature.* **432**, 917–921

63. Holmes, M. A., Paulsene, W., Jide, X., Ratledge, C., and Strong, R. K. (2005) Siderocalin (Lcn 2) also binds carboxymycobactins, potentially defending against mycobacterial infections through iron sequestration. *Structure*. **13**, 29–41
64. Raffatellu, M., George, M. D., Akiyama, Y., Hornsby, M. J., Nuccio, S.-P., Paixao, T. A., Butler, B. P., Chu, H., Santos, R. L., Berger, T., Mak, T. W., Tsolis, R. M., Bevins, C. L., Solnick, J. V., Dandekar, S., and Bäumlér, A. J. (2009) Lipocalin-2 resistance confers an advantage to *Salmonella enterica* serotype Typhimurium for growth and survival in the inflamed intestine. *Cell Host Microbe*. **5**, 476–486
65. Bachman, M. A., Oyler, J. E., Burns, S. H., Caza, M., Lépine, F., Dozois, C. M., and Weiser, J. N. (2011) *Klebsiella pneumoniae* yersiniabactin promotes respiratory tract infection through evasion of lipocalin 2. *Infect. Immun.* **79**, 3309–3316
66. Johnson, E. E., Srikanth, C. V., Sandgren, A., Harrington, L., Trebicka, E., Wang, L., Borregaard, N., Murray, M., and Cherayil, B. J. (2010) Siderocalin inhibits the intracellular replication of *Mycobacterium tuberculosis* in macrophages. *FEMS Immunol. Med. Microbiol.* **58**, 138–145
67. Allred, B. E., Correnti, C., Clifton, M. C., Strong, R. K., and Raymond, K. N. (2013) Siderocalin Outwits the Coordination Chemistry of Vibriobactin, a Siderophore of *Vibrio cholerae*. *ACS Chem. Biol.* 10.1021/cb4002552
68. Abergel, R. J., Moore, E. G., Strong, R. K., and Raymond, K. N. (2006) Microbial evasion of the immune system: structural modifications of enterobactin impair siderocalin recognition. *J. Am. Chem. Soc.* **128**, 10998–10999

69. Hoette, T. M., Clifton, M. C., Zawadzka, A. M., Holmes, M. A., Strong, R. K., and Raymond, K. N. (2011) Immune interference in *Mycobacterium tuberculosis* intracellular iron acquisition through siderocalin recognition of carboxymycobactins. *ACS Chem. Biol.* **6**, 1327–1331
70. Sia, A. K., Allred, B. E., and Raymond, K. N. (2013) Siderocalins: Siderophore binding proteins evolved for primary pathogen host defense. *Curr. Opin. Chem. Biol.* **17**, 150–157
71. Reigstad, C. S., Hultgren, S. J., and Gordon, J. I. (2007) Functional genomic studies of uropathogenic *Escherichia coli* and host urothelial cells when intracellular bacterial communities are assembled. *J. Biol. Chem.* **282**, 21259–21267
72. Paragas, N., Kulkarni, R., Werth, M., Schmidt-Ott, K. M., Forster, C., Deng, R., Zhang, Q., Singer, E., Klose, A. D., Shen, T. H., Francis, K. P., Ray, S., Vijayakumar, S., Seward, S., Bovino, M. E., Xu, K., Takabe, Y., Amaral, F. E., Mohan, S., Wax, R., Corbin, K., Sanna-Cherchi, S., Mori, K., Johnson, L., Nickolas, T., D’Agati, V., Lin, C.-S., Qiu, A., Al-Awqati, Q., Ratner, A. J., and Barasch, J. (2014) α -Intercalated cells defend the urinary system from bacterial infection. *J. Clin. Invest.* **124**, 2963–2976
73. Snyder, J. A., Haugen, B. J., Buckles, E. L., Lockatell, C. V., Johnson, D. E., Donnenberg, M. S., Welch, R. A., and Mobley, H. L. T. (2004) Transcriptome of uropathogenic *Escherichia coli* during urinary tract infection. *Infect. Immun.* **72**, 6373–6381
74. Brumbaugh, A. R., Smith, S. N., Subashchandrabose, S., Himpsl, S. D., Hazen, T. H., Rasko, D. A., and Mobley, H. L. T. (2015) Blocking yersiniabactin import attenuates extraintestinal pathogenic *Escherichia coli* in cystitis and pyelonephritis and represents a novel target to prevent urinary tract infection. *Infect. Immun.* **83**, 1443–1450

75. Steigedal, M., Marstad, A., Haug, M., Damås, J. K., Strong, R. K., Roberts, P. L., Himpl, S. D., Stapleton, A., Hooton, T. M., Mobley, H. L. T., Hawn, T. R., and Flo, T. H. (2014) Lipocalin 2 imparts selective pressure on bacterial growth in the bladder and is elevated in women with urinary tract infection. *J. Immunol. Baltim. Md 1950.* **193**, 6081–6089
76. Yilmaz, A., Sevketoglu, E., Gedikbasi, A., Karyagar, S., Kiyak, A., Mulazimoglu, M., Aydogan, G., Ozpacaci, T., and Hatipoglu, S. (2009) Early prediction of urinary tract infection with urinary neutrophil gelatinase associated lipocalin. *Pediatr. Nephrol.* **24**, 2387–2392
77. Shields-Cutler, R. R., Crowley, J. R., Hung, C. S., Stapleton, A. E., Aldrich, C. C., Marschall, J., and Henderson, J. P. (2015) Human Urinary Composition Controls Siderocalin's Antibacterial Activity. *J. Biol. Chem.* 10.1074/jbc.M115.645812
78. Friedl, A., Stoesz, S. P., Buckley, P., and Gould, M. N. (1999) Neutrophil gelatinase-associated lipocalin in normal and neoplastic human tissues. Cell type-specific pattern of expression. *Histochem. J.* **31**, 433–441
79. Klausen, P., Niemann, C. U., Cowland, J. B., Krabbe, K., and Borregaard, N. (2005) On mouse and man: neutrophil gelatinase associated lipocalin is not involved in apoptosis or acute response. *Eur. J. Haematol.* **75**, 332–340
80. Freestone, P. P. E., Lyte, M., Neal, C. P., Maggs, A. F., Haigh, R. D., and Williams, P. H. (2000) The Mammalian Neuroendocrine Hormone Norepinephrine Supplies Iron for Bacterial Growth in the Presence of Transferrin or Lactoferrin. *J. Bacteriol.* **182**, 6091 – 6098

81. Burton, C. L., Chhabra, S. R., Swift, S., Baldwin, T. J., Withers, H., Hill, S. J., and Williams, P. (2002) The growth response of *Escherichia coli* to neurotransmitters and related catecholamine drugs requires a functional enterobactin biosynthesis and uptake system. *Infect. Immun.* **70**, 5913–5923
82. Rogers, H. J. (1973) Iron-binding catechols and virulence in *Escherichia coli*. *Infect. Immun.* **7**, 445–456
83. Kingsley, R., Rabsch, W., Roberts, M., Reissbrodt, R., and Williams, P. H. (1996) TonB-dependent iron supply in Salmonella by alpha-ketoacids and alpha-hydroxyacids. *FEMS Microbiol. Lett.* **140**, 65–70
84. Methner, U., Rabsch, W., Reissbrodt, R., and Williams, P. H. (2008) Effect of norepinephrine on colonisation and systemic spread of Salmonella enterica in infected animals: role of catecholate siderophore precursors and degradation products. *Int. J. Med. Microbiol. IJMM.* **298**, 429–439
85. Williams, P. H., Rabsch, W., Methner, U., Voigt, W., Tschäpe, H., and Reissbrodt, R. (2006) Catecholate receptor proteins in Salmonella enterica: role in virulence and implications for vaccine development. *Vaccine.* **24**, 3840–3844
86. Bao, G., Clifton, M., Hoette, T. M., Mori, K., Deng, S.-X., Qiu, A., Viltard, M., Williams, D., Paragas, N., Leete, T., Kulkarni, R., Li, X., Lee, B., Kalandadze, A., Ratner, A. J., Pizarro, J. C., Schmidt-Ott, K. M., Landry, D. W., Raymond, K. N., Strong, R. K., and Barasch, J. (2010) Iron traffics in circulation bound to a siderocalin (Ngal)-catechol complex. *Nat. Chem. Biol.* **6**, 602–609

87. Gallivan, J. P., and Dougherty, D. A. (2000) A Computational Study of Cation- π Interactions vs Salt Bridges in Aqueous Media: Implications for Protein Engineering. *J Am Chem Soc.* **122**, 870–874
88. Gómez-Casado, C., Roth-Walter, F., Jensen-Jarolim, E., Díaz-Perales, A., and Pacios, L. F. (2013) Modeling iron-catecholates binding to NGAL protein. *J. Mol. Graph. Model.* **45C**, 111–121
89. Nickolas, D. T. L., O'Rourke, M. M. J., Yang, D. J., Sise, M. M. E., Canetta, D. P. A., Barasch, M. N., Buchen, M. C., Khan, D. F., Mori, D. K., Giglio, D. J., Devarajan, D. P., and Barasch, D. J. (2008) Sensitivity and Specificity of a Single Emergency Department Measurement of Urinary Neutrophil Gelatinase-Associated Lipocalin for Diagnosing Acute Kidney Injury. *Ann. Intern. Med.* **148**, 810
90. Naudé, P. J. W., Eisel, U. L. M., Comijs, H. C., Groenewold, N. A., De Deyn, P. P., Bosker, F. J., Luiten, P. G. M., den Boer, J. A., and Oude Voshaar, R. C. (2013) Neutrophil gelatinase-associated lipocalin: a novel inflammatory marker associated with late-life depression. *J. Psychosom. Res.* **75**, 444–450
91. Li, C., and Chan, Y. R. (2011) Lipocalin 2 regulation and its complex role in inflammation and cancer. *Cytokine.* **56**, 435–441
92. Fried, S. K., and Greenberg, A. S. (2012) Lipocalin 2: a “sexy” adipokine that regulates 17β -estradiol and obesity. *Endocrinology.* **153**, 1582–1584
93. Yang, J., Bielenberg, D. R., Rodig, S. J., Doiron, R., Clifton, M. C., Kung, A. L., Strong, R. K., Zurakowski, D., and Moses, M. A. (2009) Lipocalin 2 promotes breast cancer progression. *Proc. Natl. Acad. Sci. U. S. A.* **106**, 3913–3918

94. Wu, G., Li, H., Zhou, M., Fang, Q., Bao, Y., Xu, A., and Jia, W. (2014) Mechanism and clinical evidence of lipocalin-2 and adipocyte fatty acid-binding protein linking obesity and atherosclerosis. *Diabetes Metab. Res. Rev.* **30**, 447–456
95. Bouatra, S., Aziat, F., Mandal, R., Guo, A. C., Wilson, M. R., Knox, C., Bjorndahl, T. C., Krishnamurthy, R., Saleem, F., Liu, P., Dame, Z. T., Poelzer, J., Huynh, J., Yallou, F. S., Psychogios, N., Dong, E., Bogumil, R., Roehring, C., and Wishart, D. S. (2013) The human urine metabolome. *PloS One.* **8**, e73076

CHAPTER TWO

Human Urinary Composition Controls Antibacterial Activity of Siderocalin

ABSTRACT

During *Escherichia coli* urinary tract infections, cells in the human urinary tract release the antimicrobial protein siderocalin (SCN; also known as lipocalin 2, neutrophil gelatinase-associated lipocalin/NGAL, or 24p3). SCN can interfere with *E. coli* iron acquisition by sequestering ferric iron complexes with enterobactin, the conserved *E. coli* siderophore. Here we find that human urinary constituents can reverse this relationship, instead making enterobactin critical for overcoming SCN-mediated growth restriction. Urinary control of SCN activity exhibits wide ranging individual differences. We used these differences to identify elevated urinary pH and aryl metabolites as key biochemical host factors controlling urinary SCN activity. These aryl metabolites are well-known products of intestinal microbial metabolism. Together, these results identify an innate antibacterial immune interaction that is critically dependent upon individualistic chemical features of human urine.

INTRODUCTION

Escherichia coli are the predominant cause of urinary tract infections (UTIs)⁵, one of the world's most common bacterial infections (1). Compared to familiar K12 strains, uropathogenic *E. coli* (UPEC) secrete an expanded repertoire of siderophores, low molecular weight metal ion chelators defined by their ability to scavenge Fe(III) for nutritional purposes (2, 3). Siderophore biosynthetic genes are dramatically upregulated during experimental UTI and a UPEC siderophore has been directly detected in urine from UTI patients using mass spectrometry (4–6). Genes encoding the enterobactin siderophore system are ubiquitous in *E. coli*, while the non-conserved yersiniabactin, salmochelin, and aerobactin systems exist in varying combinations (2). Expression of different siderophore types exacts varying metabolic costs that may affect each siderophore system's frequency within a population (7).

The evolutionary circumstances that have led UPEC to express multiple siderophore systems are incompletely understood. Differential susceptibility to sequestration by the innate immune defense protein siderocalin (SCN; also known as lipocalin 2/LCN2, neutrophil gelatinase-associated lipocalin/NGAL, or 24p3) has been proposed as a major selective pressure driving acquisition of chemically diverse, virulence-associated UPEC siderophores (8–10). SCN is introduced into the urinary tract by neutrophil granules and uroepithelial cells, which upregulate SCN >100-fold within 24 hours of bladder inoculation (4). SCN can restrict iron accessibility by binding Fe(III) complexes with high affinity within the protein's positively charged binding site, or calyx (11, 12). While enterobactin is the prototypical ferric ligand in these complexes, other siderophore and non-siderophore ligands have been described and substantiated in detailed

binding and crystallographic studies (12, 13).

Here, we used genetic and chemical approaches to determine how UPEC siderophores and SCN interact in the chemically distinctive urinary environment associated with human UTIs. We found that human urinary constituents make enterobactin critically important for resisting SCN, in contrast to its role as a SCN target in non-urinary environments (8, 14, 15). Individual differences in urinary properties allowed us to chemically dissect urinary composition, revealing pH and aryl alcohol metabolites as critical SCN antibacterial activity correlates. These results point to the existence of a urinary tract-specific host-pathogen interaction system involving siderocalin, host metabolites, and bacterial enterobactin biosynthesis. These findings suggest non-antibiotic chemical therapeutic strategies that potentiate innate antibacterial defenses against urinary pathogens.

EXPERIMENTAL PROCEDURES

Bacterial strains and media. We used the well-characterized *E. coli* uncomplicated UTI isolate UTI89 as the model uropathogenic *E. coli* strain in our studies. Cultures were grown from single colonies in Difco Luria-Bertani (LB; BD, Franklin Lakes, NJ) broth for 4-6 hours at 37°C. Isogenic siderophore biosynthesis mutants were constructed as in-frame deletions in UTI89 using the lambda Red recombinase method as previously described (2, 16, 17).

Human urine collection. Healthy donor urine was obtained from adult volunteers as approved by the Institutional Review Board of Washington University School of Medicine. Participants provided written informed consent for collection of up to two specimens, at least one week apart, for subsequent discovery and validation analyses. Exclusion criteria included recent UTI, antibiotic therapy, pregnancy, or any urogenital disease. To avoid donors with asymptomatic bacteriuria, urines were tested for growth on MacConkey II agar and TrypticaseTM soy agar with 5% sheep blood (BD). Urines were filter sterilized and stored at -80°C until use. For experiments on pooled urine, equal volumes of individuals' urines were mixed. One specimen was excluded because it did not support *E. coli* growth *in vitro*.

Cystitis urine collection. Urine specimens from subjects with *E. coli* cystitis were chosen from among samples collected in a prospective cohort study of immunological and other pathogenic factors in recurrent UTI conducted between 2008 and 2012 among 326 pre-menopausal women presenting with acute, uncomplicated cystitis at the University of Washington Hall Health Primary Care Center. Women were eligible if they were aged 18-49 years, in good general

health, and had fewer than 7 days of typical symptoms of acute cystitis per standard clinical definitions (dysuria, frequency, and/or urgency) (18). Exclusion criteria included signs or symptoms of pyelonephritis, chronic illness requiring medical supervision, known anatomic or functional abnormalities of the urinary tract, urinary catheterization, UTI within the preceding month, current or planned pregnancy within 3 months or non-use of contraceptives. The urine specimens examined here (n = 19) were obtained from subjects' initial visits with the diagnosis of *E. coli* acute uncomplicated cystitis with $\geq 10^5$ CFU/mL of a beta hemolytic isolate. The Human Subjects Review Committee of the University of Washington approved the study, and all subjects gave written informed consent. One-tenth volume of Sigma FAST protease inhibitor solution (Sigma) was added to freshly voided urines before clinical centrifugation to remove cellular material, and the supernatant was frozen at -80 °C until use in the study.

Protein production. SCN constructs (human SCN, the kind gift of Dr. Roland Strong; mouse SCN, the kind gift of Dr. Jonathan Barasch) were expressed in the BL21 *E. coli* strain, essentially as described (11, 13). Briefly, GST-tagged SCN protein was expressed on a pGEX4T vector (GE Healthcare, Fairfield, CT); we used Pierce glutathione agarose (Thermo Fisher Scientific, Rockford, IL) to affinity purify GST-SCN, digested on-column with thrombin (Sigma, St. Louis, MO) to liberate free SCN, and removed thrombin with *p*-aminobenzamidine agarose (Sigma). Mutant K125A/K134A human SCN (the kind gift of Dr. Roland Strong) was expressed periplasmically on a pET22b vector with a 6His-tag, purified on TALON cobalt affinity resin (Clontech, Mountain View, CA), and eluted with 200 mM imizadole (Sigma). SCN protein products were extensively desalted or dialyzed to 1X PBS and concentrated on 10 kDa cut-off

Centricon filters (EMD Millipore, Billerica, MA); protein purity was monitored and confirmed by SDS-PAGE, UV-Vis spectroscopy, and mass spectrometry. Similar conformation and folding between wild type and mutant SCN proteins was confirmed by identical circular dichroism spectra (Jasco J-810 spectropolarimeter, Easton, MD) and thermal denaturation profiles.

Urinary chemical characterization. Urine specific gravity was measured by urine refractometer (ATAGO, Bellevue, WA), pH was determined by pH probe (Denver Instruments, Bohemia, NY), and we used DiaScreen urinalysis dipstrips (Arkray, Edina, MN) for detection of ketones, urobilinogen, bilirubin, protein, glucose, nitrite, leukocytes, and blood. Urine metal content was determined by inductively coupled plasma-optical emission spectroscopy (ICP-OES) on a Perkin Elmer Optima 7300DV instrument, by the Nano Research Facility at Washington University in St. Louis, Department of Energy, Environmental and Chemical Engineering. Quantification was achieved using calibration standards at 5, 10, 20, and 100 µg/L iron; and 1, 5, 10, 50, and 100 µg/L for other metals. Urine samples were diluted 1:10 in trace-metal grade nitric acid (Fisher Scientific, Fairlawn, NJ) with a final acid concentration of 2% HNO₃ and analyzed in triplicate.

Urinary SCN ELISA. Urine SCN concentration was determined by commercial ELISA (BioPorto, Thermo Fisher Scientific). Cystitis and healthy control urines were processed and diluted according to the manufacturer's instructions, and the calibration curve was fit and interpolated using Prism v. 6.0d (GraphPad, San Diego, CA).

SCN growth assay. UPEC urinary growth and SCN activity were measured essentially as described (14). Urine samples were supplemented with either 1.5 μ M SCN or equivalent volume PBS. Urines were inoculated in triplicate with UTI89 or isogenic siderophore mutants in 96-well microtiter plates at 10^3 CFU/mL and incubated on a platform shaker at 37°C for 20 hours, at which point each well was serially diluted in PBS and plated on LB agar for CFU enumeration. For defined media controls, serum-free RPMI 1640 (Gibco, Thermo Fisher Scientific) was inoculated and growth measured identically as described above. As controls, enterobactin and iron were added to restrictive urine samples. Iron-free enterobactin was HPLC-purified from UTI89 Δ *iroA*/ Δ *ybtS*-conditioned M63 minimal media supernatant, quantified by UV-Vis spectroscopy ($\epsilon_{319} = 11,200$) (19), and added to urine to 15 μ M. Ferric chloride (Sigma) was prepared in millipore-grade H₂O, filter sterilized, and used to supplement urine by 0.08 μ g/mL. Urine pH was experimentally manipulated using sterile sodium bicarbonate (Sigma) or hydrochloric acid (Sigma).

Chemical enterobactin inhibition. To block enterobactin biosynthesis in wild-type UPEC, we used the drug ((2R,3S,4R,5R)-5-(6-amino-9H-purin-9-yl)-3,4-dihydroxytetrahydrofuran-2-yl)methyl (2,3-dihydroxybenzoyl)sulfamate, or 2,3-DHB-AMS, as described (20, 21). DMSO-solubilized 2,3-DHB-AMS was diluted in sterile millipore-grade H₂O before adding to urine samples at 100 μ M. UPEC growth assays were then carried out as described above.

Urine metabolomic analysis. Urinary LC-MS metabolomic profiles were generated as published (22, 23). Briefly, filtered urine samples were diluted 1:1 with HPLC-grade H₂O and analyzed.

Data was collected on a Shimadzu Prominence UFLC-coupled AB Sciex 4000 QTRAP mass spectrometer. Separation was carried out on a gradient of 0.1% formic acid (Fluka, Sigma) to 90% acetonitrile (EMD Millipore) + 0.1% formic acid, using an Ascentis Express phenyl-hexyl column (100 x 2.1 mm, 2.7 μ m; Supelco, Sigma). Samples were analyzed by negative electrospray ionization (ESI) over a mass range of m/z 50 to 1000. Each sample was analyzed in triplicate, and the entire run order randomized. A quality control (QC) sample, prepared by mixing an equal volume of each urine sample, was used to pre-condition the column and injected every ten samples as a measure of stability, confirmed by sample-centered clustering in PCA analysis (22, 23).

For neutral loss analysis, we selected for ions with an 80 a.m.u. neutral loss fragment to selectively monitor urinary sulfated aryl alcohols. Using a collision energy range of -20 to -60 V, we set Q1 to scan from m/z 100 to 1200 while Q3 simultaneously scanned at 80 m/z units less than Q1. Peaks highlighted for predictive models were then analyzed by enhanced resolution mode over \sim 30 m/z windows to confirm the precursor ion mass, and by collision induced dissociation fragmentation to confirm presence of the prominent $[M-H-80]^-$ fragment.

MarkerView v1.2.0 was used for peak alignment, resulting in a data matrix of 600 analyte ion features. Averaged triplicate runs were Pareto scaled, and unsupervised and discriminate principal components analyses (PCA and PCA-DA, respectively) were performed with the same software. Candidate ions were highlighted by the PCA-DA loading plots and by t -tests

comparing the identified restrictive and permissive sample sets, and were visually verified in the mass spectra.

Metabolite identification. To identify urinary metabolites we extracted urine using ENVI-Chrom P SPE (Supelco, Sigma) and eluted with methanol. Further fractionation was achieved by UFLC chromatography on a Shimadzu Prominence UFLC with a gradient of 0.1% formic acid to 90% acetonitrile + 0.1% formic acid equipped with an Ascentis Express phenyl-hexyl column (100 x 4.6 mm, 2.7 μ m; Supelco, Sigma); then, candidate-containing fractions as determined by LC-MS/MS were further purified over a Kinetex C18 column (Phenomenex, Torrance, CA). These fractions were analyzed on an Agilent 6550 LC-QTOF mass spectrometer to determine molecular formula. Instrument software (MassHunter B.06.00) matched the spectrum and calculated isotope distribution to the molecular formula. MS/MS spectra were used to make preliminary identifications from among the list of isobaric molecules identified by HR-MS. Preliminary identifications were compared to published urinary profiles and metabolome database entries for further confirmation (24–28).

Arylsulfatase digestion and gas chromatography-mass spectrometry. Human urine samples were fractionated by ENVI-Chrom P SPE, reconstituted in water, and analyzed by LC-MS/MS. Arylsulfatase (Sigma) or buffer control was added at 100 U/mL urine and incubated at 37°C for 4 hours prior to MS analysis. For GC-MS, MSTFA-derivatized samples were analyzed on an Agilent 7890A gas chromatograph interfaced to an Agilent 5975C mass spectrometer operated in the electron ionization (EI) mode; the source temperature, electron energy and emission current

were 230°C, 70eV and 300µA, respectively. GC chromatography was performed with an HP-5MS column (30 m, 0.25mm i.d., 0.25µm film coating; P.J. Cobert, St. Louis, MO) with a linear temperature gradient of 80-300°C at 10°C per minute; the injector and transfer line temperatures were 250°C. Peaks of interest were matched to the NIST11 Mass Spectral Library for chemical identification.

Quantitative LC-MS. Relative concentrations of specific sulfated urinary metabolites were measured by comparing their 80 mass unit neutral loss LC-MS/MS peak areas to that of a 4-flourosalicylic acid (4FSA, Sigma; final concentration 5 µM) internal standard. Urines were combined 1:1 with 10 µM 4FSA prior to analysis. The 4FSA peak was detected using the MS/MS transition 155>111. Triplicate analyses were performed with samples in randomized run order. Peaks were normalized and retention time corrected relative to 4FSA in Markerview before averaging replicate data. Processed peak areas were then normalized to the overall urinary solute concentration by adjusting to specific gravity as established (29), yielding relative urinary concentration in arbitrary units. Molecular features distinguishing restrictive and permissive urines were highlighted by PCA-DA loadings plot and *t*-test comparison between the groups. Peaks were confirmed by visual inspection of primary data.

Statistical analysis. Data were tested for significance at $\alpha = 0.05$ using Prism v. 6.0d (GraphPad). We used *t*-test for parametric, and Mann-Whitney U test for non-parametric comparisons, and one-way ANOVA for multi-group comparisons. Wilcoxon matched pairs sign rank test was used for non-parametric paired comparisons. Holm-Šídák or Dunn's tests were used to correct for

multiple comparisons where appropriate. Logistic regression and receiver operating characteristic (ROC) analyses were performed in SigmaPlot v. 12.3 (Systat Software, San Jose, CA).

RESULTS

SCN markedly inhibits growth of enterobactin-deficient UPEC in pooled human urine. Urinary SCN concentrations are elevated during *E. coli* urinary tract infections (Fig. 1), consistent with several recent studies (30, 31). Even higher local concentrations of this cationic protein (pI ~9) are likely in the bladder surface's anionic glycosaminoglycan layer. To determine whether SCN inhibits UPEC growth, we compared growth of the model *E. coli* cystitis (bladder infection) strain UTI89 (10^3 CFU/mL inoculum) and its siderophore-deficient mutants (2) (Fig. 2a) with and without purified human SCN. In a chemically defined and iron-poor medium (RPMI 1640), SCN limited UTI89 growth as previously described (8, 11, 14), with the greatest inhibitory effect on the mutant UTI89 Δ *iroA*/ Δ *ybtS* ($P < 0.01$), which expresses enterobactin as its sole siderophore, and the smallest effect on UTI89 Δ *entB*, which expresses yersiniabactin as its sole siderophore (Fig. 2b). In contrast, when these strains were grown in filtered and pooled human urine, SCN significantly ($P < 0.001$) inhibited the enterobactin-deficient mutant (UTI89 Δ *entB*) but not the yersiniabactin or salmochelin and yersiniabactin-deficient mutants (UTI89 Δ *ybtE* and UTI89 Δ *iroA*/ Δ *ybtS*, respectively) when compared to wild type UTI89 (Fig. 2b). Similar results were obtained with purified mouse SCN (data not shown). These results show that the urinary growth condition substantially alters the previously described relationship between SCN and *E. coli* siderophore biosynthesis. A similar growth discrepancy was previously noted for an enterobactin-deficient *Klebsiella pneumoniae* mutant (14). While the RPMI growth results are consistent with SCN's previously demonstrated ability to bind ferric enterobactin and deny its availability to *E. coli*, the urinary growth results suggest that urinary constituents play additional, determinative roles in SCN-mediated antibacterial activity.

Individual differences control SCN antibacterial activity. Urine is a remarkably complex and variable biofluid whose chemical composition is shaped by multiple idiosyncratic sources including host metabolism and the intestinal microbiome (26, 32). It is notable that SCN activity against UTI89 Δ *entB* varied widely between pooled urine sets from different donor groups (larger error in Fig. 2b). To determine whether this variation originated from individual differences in urine composition, we compared urinary SCN inhibitory activity between 50 adult healthy donor specimens (52 percent female; average age 38, range 21 – 76). We inoculated each urine specimen with UTI89, UTI89 Δ *entB*, or UTI89 Δ *iroA*/ Δ *ybtS* and determined SCN's effect on growth (Fig. 2c). In aggregate, SCN significantly ($P < 0.0001$) inhibited growth of each strain; SCN inhibited UTI89 Δ *entB* substantially more than wild type or UTI89 Δ *iroA*/*ybtS* (Fig. 2c). These results again show that disrupting biosynthesis of enterobactin, but not salmochelin and yersiniabactin, greatly increases SCN's urinary antibacterial activity.

SCN-mediated growth restriction exhibited the greatest inter-individual variation with UTI89 Δ *entB*, spanning over eight orders of magnitude, with 42% of samples exhibiting 10-fold or greater inhibition. To facilitate further between-individual investigations, we classified individual urines by their *entB*-dependent SCN activity as in Equation 1 (Fig. 2d).

$$\text{SCN activity} = \log_{10} [\text{WT+SCN growth} / \Delta\textit{entB+SCN growth}] \quad (\text{Equation 1})$$

When SCN activity values are displayed for each urine specimen, the wide range of individual variation is readily apparent. Within this distribution, a threshold is evident where SCN inhibits UTI89 Δ *entB* 10-fold (SCN activity = 1) more than wild type UTI89. Urine specimens with SCN activity >1 we therefore defined as *restrictive* (SCN restricts growth in the absence of enterobactin) while those with SCN activity <1 are defined as *permissive* (no SCN-mediated growth restriction).

To determine whether the differences between restrictive and permissive urines are evident at earlier bacterial growth time points, we measured viable bacterial counts six hours after inoculation (Fig. 3). At this time point, restrictive urines (Fig. 3a) exhibited significant SCN activity against both wild type UTI89 and UTI89 Δ *entB* (Fig. 3b-d), while permissive urines again exhibited little or no SCN activity (Fig. 3e-g). SCN activity against wild type UTI89 may reflect insufficient enterobactin accumulation to overcome SCN at this early time point. This suggests that restrictive urine may inhibit wild type uropathogen growth *in vivo* at low cell density.

Purified enterobactin or iron diminishes SCN antibacterial activity. To determine whether the Δ *entB* mutant phenotype in restrictive urine derives from deficient enterobactin-mediated iron import, we chemically complemented UTI89 Δ *entB* urinary cultures with exogenous *apo*-enterobactin or ferric chloride. In three representative restrictive specimens, enterobactin addition (15 μ M final concentration) restored growth to wild-type levels (Fig. 4a). Ferric chloride addition (0.08 μ g/mL) similarly restored growth (Fig. 4b). These results are consistent

with an important role for classic enterobactin-mediated iron acquisition in SCN-supplemented, restrictive urines.

SCN antibacterial activity requires an intact calyx. SCN binds ferric complexes with high affinity through electrostatic and cation- π interactions in its positively charged binding site, or calyx (11–13). Two lysine residues (K125, K134) and one arginine (R81) contribute local positive charges that facilitate ferric complex binding. To confirm that SCN's inhibitory activity is attributable to calyx binding, we compared urinary growth inhibitory activity between wild type SCN and a calyx mutant in which the two lysine residues have been mutated to alanines (SCN K125A/K134A), disrupting the binding site's shape and positive charge (12). Unlike the wild type protein, the K125A/K134A mutant failed to restrict bacterial growth in restrictive urines (Fig. 4b). These results demonstrate that an intact SCN calyx is necessary for SCN-mediated urinary growth inhibition.

An enterobactin biosynthesis inhibitor increases SCN antimicrobial activity in urine. To further discern the enterobactin biosynthetic pathway's contribution to SCN resistance, we used the EntE inhibitor 2,3-DHB-AMS as a chemical probe to inhibit enterobactin biosynthesis (20) (Fig. 6a). Compared to SCN or 2,3-DHB-AMS alone, the SCN + 2,3-DHB-AMS combination markedly inhibited ($P < 0.001$) UTI89 growth in restrictive urine (Fig. 5b). SCN + 2,3-DHB-AMS similarly inhibited growth ($P < 0.001$) of the genetically distinct pyelonephritis strains CFT073 and USB64 (33–35) (Fig. 5b). These data are consistent with a role for enterobactin biosynthesis in resisting SCN-mediated growth inhibition in urine.

SCN antibacterial activity is associated with urinary pH. To determine whether donor demographics or basic measures of urine composition are related to SCN activity, we compared their values in restrictive and permissive subgroups (Fig. 6a). We hypothesized that urine osmolarity, pH, endogenous SCN, and variations in total metal content could be possible restrictive correlates (36, 37). Neither age (Fig. 6a) nor individual gender ($P = 0.39$, Fisher's exact test) was significantly associated with restrictive or permissive designation. Among the chemical analyses, only urine pH, but not endogenous SCN, specific gravity, or metal content (determined by ICP-OES), distinguished the subgroups. Specifically, higher pH was significantly ($P < 0.0001$) associated with restrictive urines (Fig. 6a) and correlated with higher SCN activity ($P = 0.0005$; Fig. 6b). Within the urinary pH range, this trend mirrors the greater ferric complex binding affinity to SCN and the greater ferric ion binding affinity to enterobactin and other catecholate ligands observed with increasing pH (12, 38).

We further evaluated the relationship between urinary pH and restrictive urine by constructing a receiver operating characteristic (ROC) curve using the 50-specimen dataset (Fig. 6c). Urinary pH emerges as a sensitive and specific marker of the restrictive phenotype, with an area under the curve (AUC) of 0.86 ($P < 0.0001$). This relationship was confirmed (AUC of 0.87, $P < 0.001$) in a set of 37 new specimens from our healthy cohort. Using the pH 6.45 cutoff value from the initial ROC curve, high urinary pH predicted high SCN activity in this validation set, with a specificity of 92 percent and sensitivity of 80 percent ($P < 0.0001$, two-tailed Fisher's exact test). This relationship was not absolute, however; we observed urine samples with high

pH and low SCN activity or low pH and high activity (bottom-right and top-left quadrants of Figure 5b, respectively), as well as wide-ranging activity variation between samples with similar pH suggesting that other urinary factors influence SCN activity in urine.

Urinary alkalinization sensitizes E. coli to SCN-mediated growth inhibition. To determine whether urinary pH plays a causative role in making urine restrictive or permissive, we experimentally measured SCN activity in urine specimens before and after adjusting pH with reagent sodium bicarbonate or HCl. Bicarbonate alkalinization within a physiologic range (mean pH 5.9 ± 0.4 to 7.2 ± 0.3 , Fig. 6d), converted all tested specimens to restrictive urines. One specimen completely inhibited both wild type UTI89 and UTI89 Δ entB growth after alkalinization, and therefore could not be plotted. Conversely, HCl acidification within a physiologic range (mean pH 6.8 ± 0.4 to 5.7 ± 0.3) decreased SCN activity (Fig. 6e). By experimentally adjusting pH in voided urine, this approach avoids the possible confounding impact of pH-related changes in renal excretion of acidic or basic metabolites. Overall, these results show that increasing urinary pH promotes SCN activity.

SCN antibacterial activity is associated with urinary metabolomic features. To seek urinary SCN activity correlates beyond pH, we used a previously described LC-MS profiling approach to compare individual urine specimens (22). Unsupervised principal components analysis of LC-MS profiling data (PCA, identifies major sources of variation in the data set) revealed extensive overlap between restrictive and permissive urines, suggesting that SCN activity is not associated with the dominant sources of urinary metabolomic variation. Supervised PCA-discriminate

analysis (PCA-DA, highlights major restrictive/permissive associations; Fig. 7a) identified nine molecular features that best distinguished restrictive and permissive individuals. After eliminating uncommon molecular features (present in <10 samples) we selected three (m/z 187, 217, and 528 in negative ion ESI; Fig. 7b) that discriminated restrictive and permissive urines.

We hypothesized that these three urinary metabolites would help identify metabolite classes associated with SCN activity. Tandem mass analysis (MS/MS) revealed the same prominent 80 a.m.u. neutral loss from all three metabolites (Fig. 7c), corresponding to the SO_3 neutral loss observed with MS/MS of sulfated aromatic alcohols and enols by Yi and colleagues (39). Accurate mass analysis of the most abundant HPLC-purified metabolite at m/z 187.00728 confirmed that it is a sulfur-containing empiric formula ($\text{C}_7\text{H}_7\text{SO}_4^-$), matching cresol sulfate, a sulfated aryl alcohol (Fig. 7d). Arylsulfatase treatment abolished the molecule's LC-MS peak while generating a new GC-MS peak matching that of a *para*-cresol standard (Fig. 7e,f), confirming that the aryl sulfate is *p*-cresol sulfate. Together, these data link urinary aryl sulfates to urinary SCN antimicrobial activity.

SCN antibacterial activity is associated with urinary aryl sulfates. To more specifically investigate the association between urinary aryl sulfates and SCN activity we configured the mass spectrometer to detect only molecules that undergo the aryl sulfate-specific 80 a.m.u. loss (Fig. 8a) during negative ion MS/MS fragmentation. This LC-constant neutral loss (LC-CNL) approach greatly improves sensitivity to aryl sulfates in the chemically complex human urinary background when compared to the LC-MS profiling approach used above (Fig. 8b). PCA-DA

analysis of LC-CNL data from 20 specimens resolved restrictive from permissive urines (Fig. 8c), and further, this analysis identified new aryl sulfate ions associated with restrictive or permissive urines for further study.

SCN antibacterial activity is associated with increased urinary aryl sulfate concentrations. To determine whether specific aryl sulfates are associated with high SCN antibacterial activity, we compared relative concentrations of 14 aryl sulfates identified in the above aryl sulfometabolome analyses. In restrictive (n = 21) versus permissive (n = 29) urine specimens (Table 1), five aryl sulfate concentrations (m/z 189, 202, 217, 269, and 415 in negative ion ESI) were significantly ($P < 0.05$) higher in restrictive urine, while none were significantly lower. ROC curve analysis of the three most significantly elevated (m/z 202, 269, 415; $P < 0.002$) supported their ability to predict the restrictive phenotype (AUC values of 0.72, 0.76, and 0.72 for m/z 202, 269, and 415, respectively, $P < 0.01$; Fig. 9a). Arylsulfatase treatment further supported identification of these three diagnostic molecules as aryl sulfates (Fig. 9b), and the relative urinary concentrations were also significantly correlated with SCN activity level ($P < 0.002$; Fig. 9c). These trends were confirmed in a set of 37 new urine specimens. Together, these data further support a positive association between urinary aryl sulfates and SCN activity.

Structural analyses of the 14 analytes supported their identification as sulfated aryl alcohols, 11 of which have been previously documented in human urine (Table 1) (24–28, 40). This urinary metabolite class derives from human sulfate conjugation of phenolic metabolites originating from human, dietary and/or intestinal microbial sources (28, 32, 40, 41). Catechol-containing

metabolites are notably prominent among these molecules, and their SCN activity associations are consistent with SCN calyx binding preferences for ferric-catechol complexes. While the sulfated forms of these aryl alcohols are unlikely to participate directly in iron sequestration (12), they may be readily detectable (in negative ion ESI-MS) markers of endogenous SCN ligands and the metabolic processes that produce them.

Aryl alcohol supplementation increases SCN antimicrobial activity. To determine whether unconjugated urinary catechols contribute to SCN activity in urine, we measured the effect of model catecholates on urinary SCN activity. We supplemented ten permissive urine specimens (urinary pH range 5.53 – 7.40) with physiologically achievable concentrations (15 μ M) (25, 42) of three urinary catechol metabolites found in urine that are also known to chelate iron within SCN complexes: catechol, pyrogallol, and 3-methylcatechol (12). Catechol supplementation significantly ($P = 0.0039$) increased urinary SCN activity in permissive urines (Fig. 9d), with typical individual variations in effect magnitudes. These results support a model in which elevated aryl alcohol concentrations in restrictive urine directly potentiate SCN's urinary antimicrobial activity.

Urinary pH and aryl sulfates are independently associated with SCN antibacterial activity. To determine whether the urinary aryl sulfometabolome and pH are independently associated with restrictive urines, we conducted a multivariate logistic analysis. Urinary aryl sulfates were expressed as the PCA-DA score derived from LC-MS/MS data of the 14 urinary aryl sulfates. Multiple logistic regression analysis of the complete 87-specimen dataset showed that both urine

pH ($P < 0.001$) and LC-MS/MS-derived aryl sulfometabolite DA score ($P = 0.002$) are independently and significantly correlated with SCN activity (odds ratio of 48.62 and 2.11, respectively; Fig. 10a).

Independent contributions of pH and aryl sulfometabolites to SCN activity are visually evident in a bubble plot of log DA score vs. pH (Fig. 10b) (43). Here, the bubble radius is defined by SCN activity, and clearly shows both the individual differences in these parameters and the strong associations between pH, aryl sulfates, and SCN activity. Notably, only a single urine specimen (1/37, 3%) with borderline low pH and low DA values is restrictive while nearly all (16/18, 89%) of those with high pH and high DA values are restrictive. A heat map in which urines are arranged by SCN activity (Fig. 10c) reveals that the highest DA scores ($>\log 3$) are observed in urines with the highest SCN activity; this is supported by logistic regression analysis, where the DA score odds ratio is higher, while the pH odds ratio is lower (Fig. 10a). These results show that urinary aryl sulfates are most highly associated with urines supporting the highest SCN antibacterial activity levels.

To experimentally determine whether combined pH and aryl alcohol treatment facilitates SCN activity, we monitored bacterial growth in SCN-treated permissive urines from ten individuals following combined *ex vivo* aryl alcohol (as in Figure 9d) and bicarbonate supplementation (as in Figure 6d, 5 mg/mL as sodium salt). SCN significantly inhibited growth of both wild type ($P < 0.001$, Fig. 10d) and enterobactin-deficient UTI89 ($P < 0.0001$, Fig. 10e) in the presence, but not

absence, of combined aryl alcohol and bicarbonate treatment. These results are consistent with a critical role for both pH and aryl alcohols upon SCN's urinary antimicrobial activity.

DISCUSSION

Together, these results describe a biochemical network in which siderocalin, urinary aryl metabolites, and enterobactin interact to control bacterial growth. Our conclusion that SCN uses a subset of urinary metabolites as cofactors to withhold iron from *E. coli* emerges from an experimental strategy that used individual human differences as an independent variable; this approach informed further analyses that identified urinary pH and aryl metabolite associations with SCN activity. Consistent with these associations are the known pH and catechol requirements for ferric ion binding by SCN (12). While enterobactin's role in resisting siderocalin-mediated growth inhibition in urine was unexpected, it is consistent with the concept that niche-specific roles drive siderophore diversity among bacterial pathogens (6, 44–47). Therefore, while enterobactin may be particularly consequential in the urinary environment examined here, SCN evasion by non-enterobactin “stealth siderophores” may dominate in non-urinary environments lacking urine's unique aryl metabolite composition.

SCN's documented ability to form a highly stable complex with ferric enterobactin led us to initially hypothesize that salmochelin and/or yersiniabactin biosynthesis would be necessary for growth. Our contrary observations in urine can be explained by the presence of one or more non-enterobactin urinary ligands within the SCN calyx that function as host-derived cofactors (12, 48). Previous work by Bao and colleagues demonstrated that endogenous urinary ligands, including aryl alcohols as described here, do form stable ferric complexes with SCN (12). Due to its insolubility in aqueous environments, “free” iron exists in a labile pool, for which aryl alcohols are well-suited ligands. Indeed, the higher pH associated with restrictive urine closely

parallels the trends in ferric complex stability and SCN binding observed for catecholate ligands (12, 38). Because ferric complexes can form from multiple aryl alcohol chelators (*e.g.*, three divalent catechol chelators per ferric ion) and multiple members of this class may be present in human urine, restrictive urines may arise from idiosyncratic combinations of these molecules. The sulfated aryl metabolites tracked here likely represent readily detectable markers of free aryl alcohols. Future studies will be necessary to identify which of these contribute to SCN activity.

A proposed model for SCN function in the urinary tract is shown in Figure 11. In this model, the host responds to UPEC by producing SCN, which (at $\text{pH} > 6.45$) stabilizes ferric complexes of appropriate urinary metabolites in its calyx (Fig. 11a,b). While SCN can bind enterobactin with high affinity, this interaction may be greatly impeded when urine-derived ferric complexes occupy the calyx. In this setting, enterobactin's remarkable ferric ion affinity may instead enable it to competitively liberate iron from SCN-bound cofactors (Fig. 11c), thus promoting bacterial growth. This ability suggests a basis for the ubiquitous expression of enterobactin observed to date in urinary *E. coli* isolates. While yersiniabactin can avoid SCN binding, it is also an avid Cu(II) ligand with lower ferric affinity than enterobactin and so may be less able to liberate iron from SCN as suggested in Figure 2b (3, 6, 49). Similarly, while loss of salmochelin production did not affect urinary growth (Fig. 2b), we cannot rule out its potential role in liberating SCN-bound iron. Further studies are necessary to determine how ferric enterobactin avoids binding to the SCN calyx following ferric ion removal, which may be attributable to competitive binding or slow release of aferric urinary ligands. This working model (Fig. 11) suggests important areas for

future investigation and opportunities for new virulence-targeting UTI therapeutic approaches distinct from broad-spectrum antibiotics.

The biochemical network described here raises the possibility that promoting restrictive urinary characteristics in patients may prevent or treat antibiotic-resistant *E. coli* UTI without incurring “collateral damage” on the vaginal or gut microbiome (1, 50). This strategy may benefit from an enterobactin biosynthesis inhibitor such as DHB-AMS. Urinary alkalinization is readily achieved through existing interventions such as oral bicarbonate therapy. Although favorable urinary aryl metabolite profiles are associated with the highest level of SCN activity, future studies will be required to determine how to therapeutically recapitulate this in susceptible patients. The urinary aryl sulfates identified here (Table 1) and in prior studies are known to originate from the combination of diet, gut microbial metabolism, and host liver metabolism. Individual differences in these metabolites may thus have multiple origins. Of note, urinary catechols are associated with consumption of polyphenol-rich foods such as tea, coffee, wine and cranberries (25, 32, 41, 51), suggesting that dietary strategies may be feasible.

Mass spectrometry-based metabolomic approaches have excellent potential to resolve individual differences relevant to many disease processes (22, 52, 53). While definitive metabolite identification using these methods is often a laborious process, we were aided here by a specific ion fragmentation process (neutral loss of 80 a.m.u.) characteristic of a urinary biochemical class linked by structure to candidate SCN ligands (12, 39). This “molecular bootstrapping” approach, in which a molecular lead derived from untargeted profiling is used to inform a second round of

class-specific profiling, may aid further metabolomic discovery work in UTI and other disease processes.

ACKNOWLEDGEMENTS

The authors would like to thank Bradley Ford and Kaveri Chaturvedi for helpful discussions; as well as Roland Strong and Jonathan Barasch for sharing siderocalin constructs. J.P.H. holds a Career Award for Medical Scientists from the Burroughs Wellcome Fund and acknowledges National Institute of Diabetes and Digestive and Kidney Diseases grants R01DK099534 and P50DK064540, the National Center for Advancing Translational Sciences UL1TR000448, and the Longer Life Foundation. Mass spectrometry was supported by United States Public Health Service grants P41-RR00954, P30-DK20579, and P30-DK56341. R.R.S.-C. acknowledges T32GM007067-37 and a Monsanto Excellence Fund Graduate Fellowship. C.C.A acknowledges support from grant AI070219 from the National Institutes of Health. J.M. acknowledges U54 CK000162, K12HD001459 and the Barnes-Jewish Hospital Patient Safety & Quality Fellowship Program.

CHAPTER TWO: FIGURES

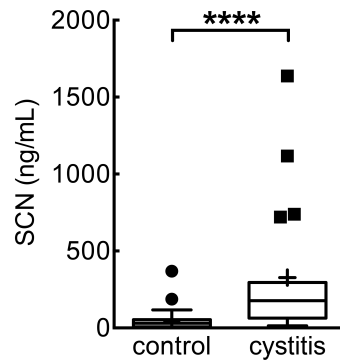


FIGURE 1. Urinary SCN concentrations are significantly elevated in women with uncomplicated *E. coli* cystitis. Female cystitis patients (cystitis, n = 19) exhibit significantly higher urinary SCN concentrations than asymptomatic controls (controls, n = 30). Data displayed as Tukey box plots, where the horizontal line shows the median and the mean is indicated by “+”. $P < 0.0001$, Mann-Whitney test.

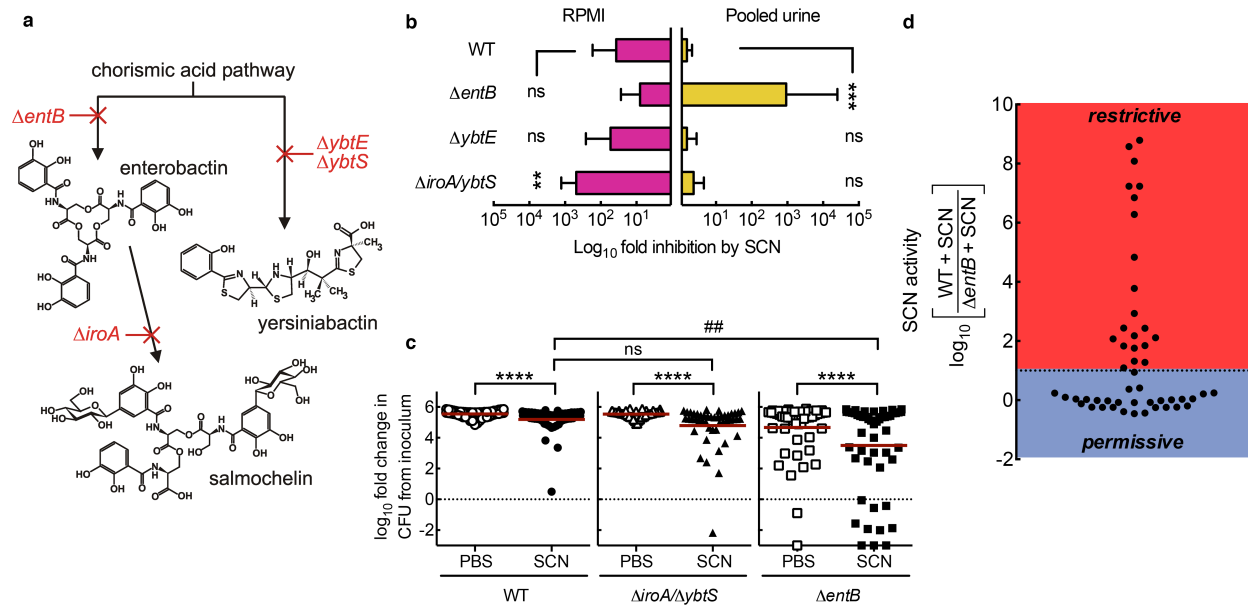


FIGURE 2. In human urine, SCN imposes an enterobactin biosynthesis requirement for *E. coli* growth. (a) The model UPEC strain UTI89 produces three siderophores derived from chorismic acid precursors. Isogenic mutants disrupting biosynthesis in each pathway are indicated in red. (b) In RPMI media, 1.5 μM SCN most effectively inhibits a mutant lacking non-enterobactin siderophores as previously described. In pooled human urine, 1.5 μM SCN conversely inhibits only the enterobactin-deficient strain. 20-hour growth was monitored by CFU in urine specimens following a 10^3 CFU/mL inoculation, and data are shown as mean \pm SD of at least three separate cultures; ns = not significant, ** $P < 0.01$, *** $P < 0.001$, one-way ANOVA compared to WT with multiple comparison correction. (c) Bacterial growth phenotypes exhibit substantial individual variation among unpooled urine specimens from 50 normal donors. Each data point represents triplicate measures of an individual urine sample, and a red line indicates the overall mean. Urine was supplemented with 1.5 μM SCN (filled symbols) or PBS control

(open symbols). **** $P < 0.0001$, Wilcoxon matched pairs sign rank test; ## $P < 0.01$, one-way ANOVA with multiple comparisons. **(d)** Individual urine specimens can be defined as “permissive” or “restrictive” based upon their ability to force an enterobactin biosynthesis requirement for growth in the presence of SCN.

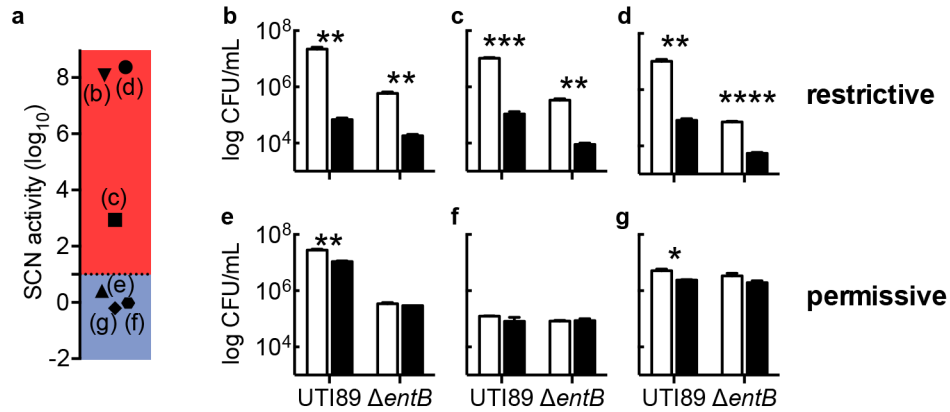


FIGURE 3. SCN inhibits wild type *E. coli* growth in restrictive urine at early time points.

Wild type strain UTI89 or its enterobactin-deficient mutant ($\Delta entB$) was inoculated into restrictive and permissive urine specimens (a) with PBS control (white bars) or 1.5 μ M SCN (black bars) at 10^3 CFU/mL and grown at 37°C for 6 hours (b-g). Notably, urines (b), (c), and (d) are restrictive while (e), (f), and (g) are permissive, as defined in Figure 2d; SCN activities based upon 20-hour growth are re-plotted in (a). These data (b-g) show that restrictive urine supports significant SCN-mediated antimicrobial activity against wild-type UPEC at this early time point. Data shown as mean \pm SD for three independent cultures. ** $P < 0.01$, *** $P < 0.001$, student's t -test.

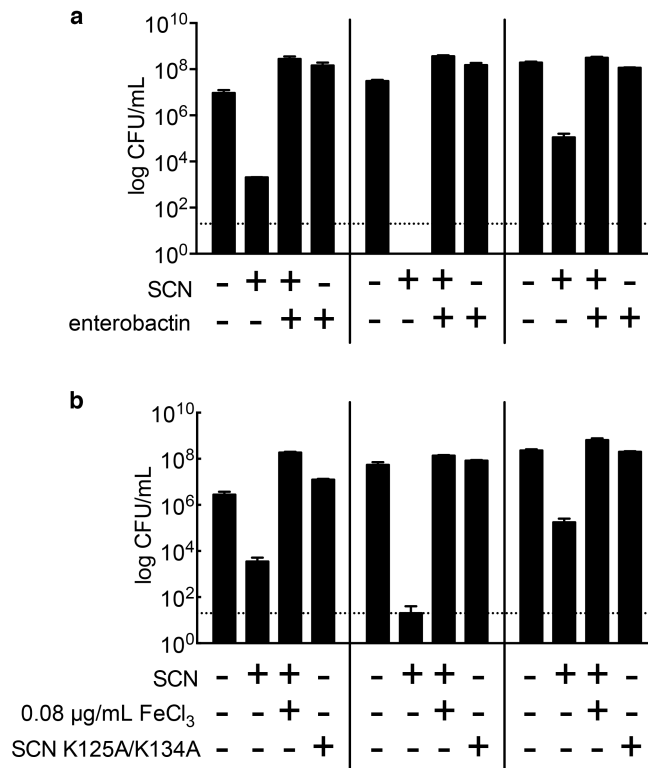


FIGURE 4. In human urine, the SCN calyx interferes with enterobactin-mediated iron acquisition by *E. coli*. (a) Purified enterobactin (15 μM) restores enterobactin biosynthesis mutant (UTI89Δ*entB*) growth in three representative SCN-supplemented restrictive urines. (b) Similarly, ferric iron (0.08 μg/mL FeCl₃) supplementation restores UTI89Δ*entB* growth in the presence of SCN (1.5 μM). A SCN calyx mutant (SCN K125A/K134A, 1.5 μM) does not inhibit urinary growth of UTI89Δ*entB*. Bars show means ± SD of three independent cultures.

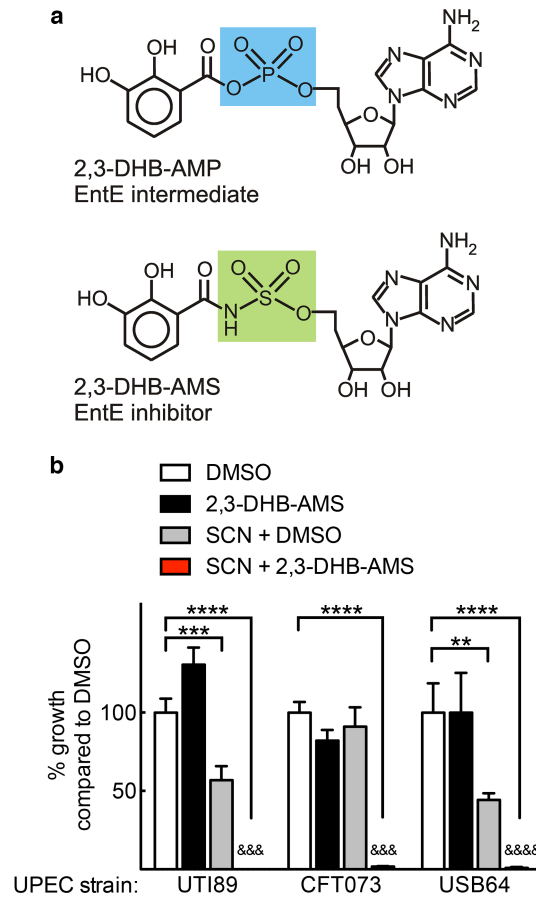


FIGURE 5. An enterobactin biosynthesis inhibitor facilitates SCN activity against a panel of wild type UPEC isolates. The compound 2,3-DHB-AMS, which inhibits EntE by mimicking the enterobactin biosynthetic intermediate 2,3-DHB-AMP (**a**), mimics the enterobactin-deficient ($\Delta entB$) phenotype in wild type UPEC strains UTI189, CFT073, and USB64. (**b**) Specifically, combined SCN (1.5 μ M) and 2,3-DHB-AMS (100 μ M) treatment significantly inhibits all wild type UPEC growth in restrictive urine. Bars show means \pm SD from three independent cultures. $**P < 0.01$, $***P < 0.001$, $****P < 0.0001$ by one-way ANOVA compared to DMSO. $***P < 0.001$, $****P < 0.0001$, SCN + 2,3-DHB-AMS compared to SCN + DMSO, t -test.

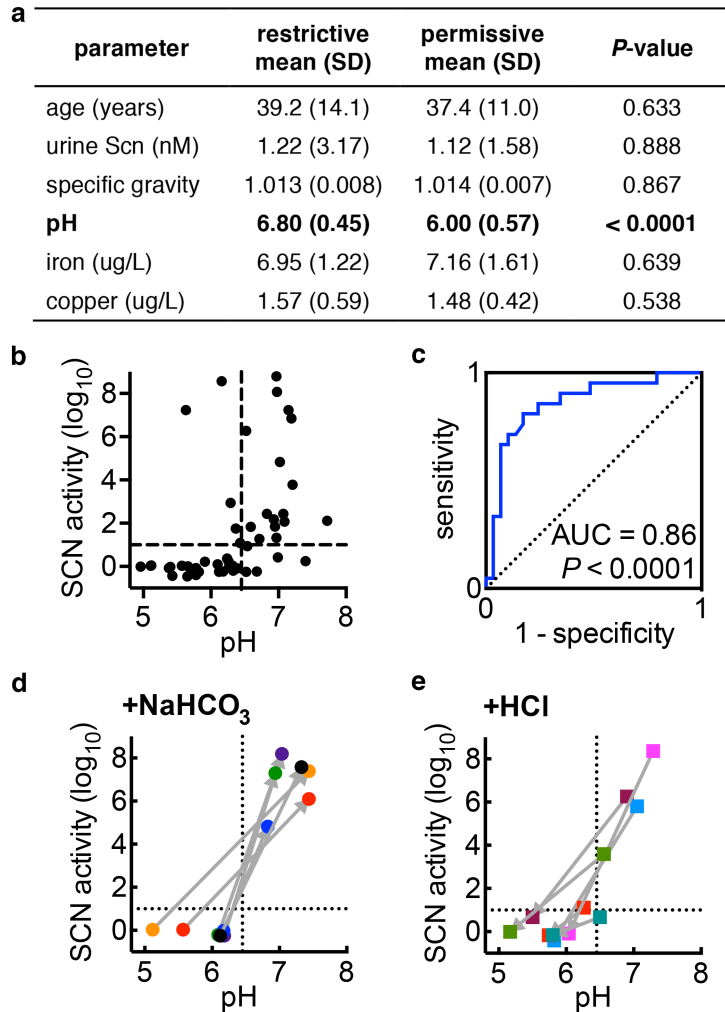


FIGURE 6. Urinary pH distinguishes restrictive from permissive urine. (a) Age and urine composition of restrictive and permissive urines from normal volunteers. (b) Urine pH is associated with SCN activity such that more restrictive urines exhibit higher pH values ($P = 0.0005$; Spearman correlation). The vertical dotted line in (b) indicates the pH 6.45 threshold for distinguishing restrictive urine identified by ROC curve analysis of 50 urinary pH values (c). The area under the curve (AUC) value of 0.86 is statistically significant from the null hypothesis of

0.5 (diagonal dotted line; $P < 0.0001$). **(d)** Permissive urine becomes restrictive following *ex vivo* bicarbonate (NaHCO_3) alkalization, consistent with a direct urinary pH effect upon SCN activity [converting from upper left to lower right quadrants in **(b)**]. **(e)** Conversely, restrictive urine becomes permissive following *ex vivo* HCl acidification, again consistent with a direct urinary pH effect upon SCN activity. For **(d)** and **(e)**, connected data points represent the means of triplicate cultures on a single donor specimen before and after pH manipulation, the order of which is indicated by the connecting arrow.

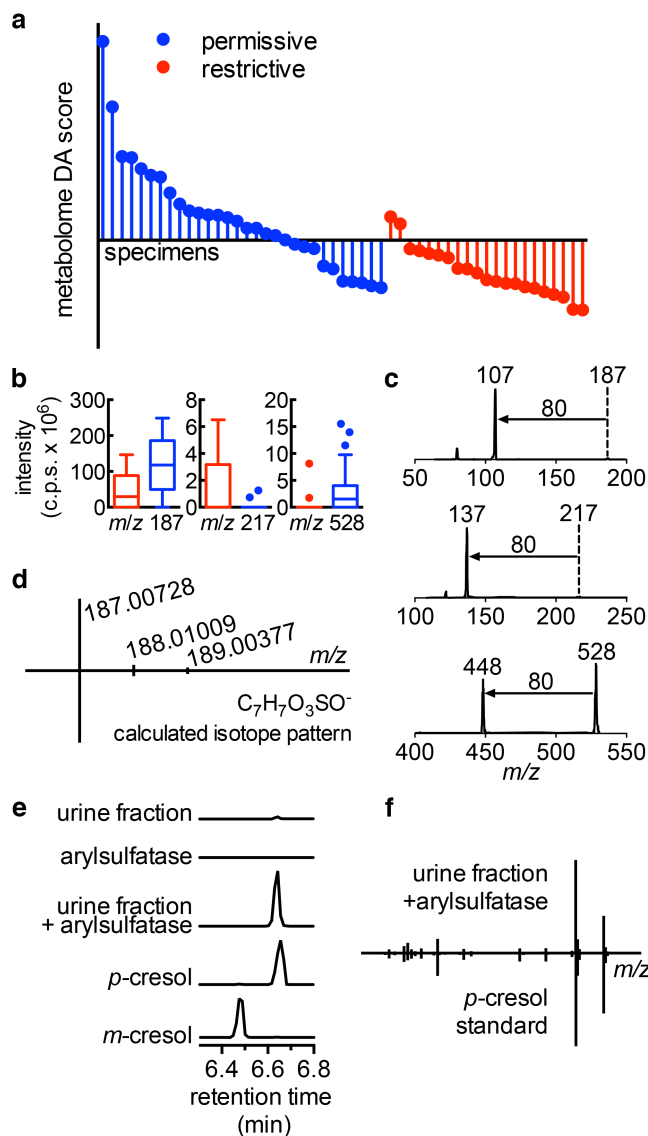


FIGURE 7. Urinary metabolomes distinguish restrictive from permissive urine. (a) Restrictive and permissive urine samples were analyzed in triplicate by negative ESI LC-MS for principal components-discriminant analysis (PCA-DA). The discriminant analysis (DA) score is the supervised principal component distinguishing restrictive and permissive groups in PCA-DA. **(b)** Tukey box plots of three metabolites (m/z 187, 217, and 528) that contribute to the DA score in restrictive (red) and permissive (blue) specimens. **(c)** MS/MS spectra of these three

metabolites are dominated by 80 a.m.u. neutral losses. **(d)** High resolution mass spectra of the abundant m/z 187 ion matches the exact mass and isotope pattern of cresol sulfate ($[M-H]^- = C_7H_7SO_4^-$). **(e-f)** Arylsulfatase digestion of this purified metabolite produces a new GC-MS peak matching that of *p*-cresol (but not *m*-cresol) by retention time **(e)** and EI mass spectrum **(f)**.

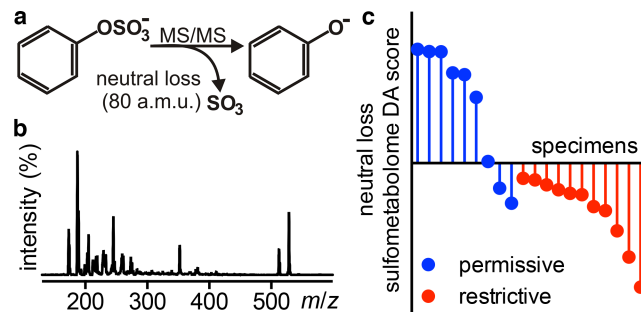


FIGURE 8. Urinary aryl sulfometabolites distinguish restrictive from permissive urine. (a) Different sulfated aryl alcohols fragment to lose a common 80 a.m.u. neutral loss in negative ion ESI MS/MS. **(b)** Scanning constant neutral loss (-80 a.m.u.) mass spectrum (LC-CNL, retention time 1-13 min) from a representative urine sample reveals a complex sulfometabolome profile. **(c)** Twenty randomly selected (constrained to 10 male, 10 female) urine specimens were re-analyzed by LC-CNL to compare urinary aryl sulfate content in restrictive vs. permissive urines by PCA-DA. The resulting neutral loss sulfometabolome DA score is the first supervised principal component distinguishing restrictive and permissive groups in PCA-DA.

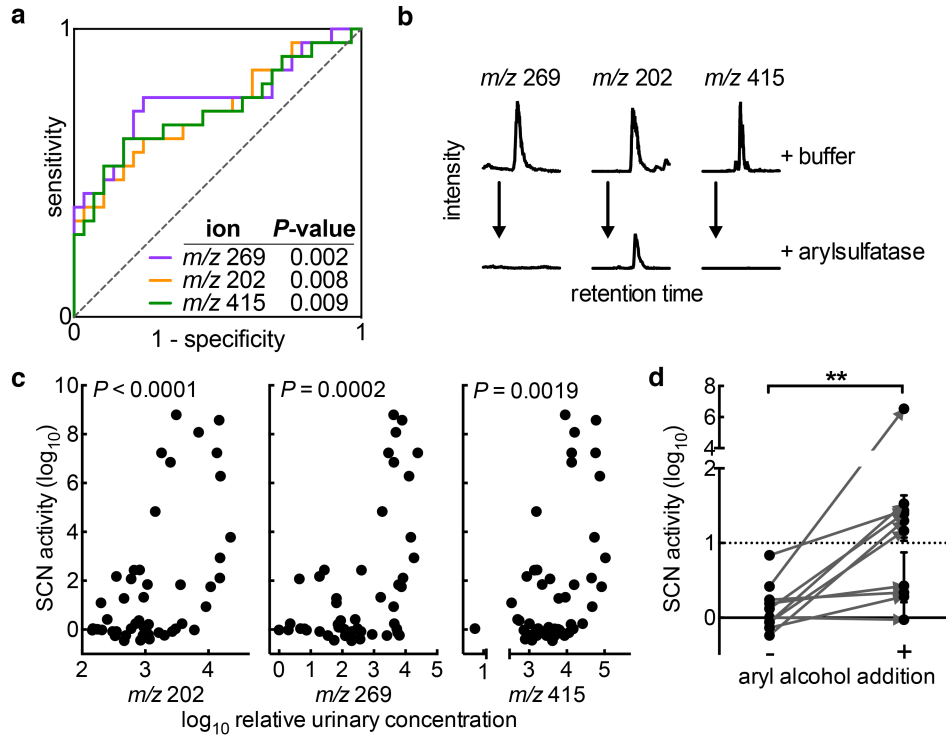


FIGURE 9. Urinary aryl metabolites increase SCN antimicrobial activity. (a) ROC curve analysis indicates the correlation and predictive capacity for the three most predictive aryl sulfate ions, measured quantitatively by LC-MS/MS. (b) Arylsulfatase addition reduces LC-MS/MS signal for each metabolite, further supporting the classification of these molecules as aryl sulfates. (c) Concentrations of these three metabolites are significantly correlated with SCN activity (Pearson correlation), and show particular association with high level UPEC growth restriction (SCN activity $>\log 3$ on y-axis). (d) *Ex vivo* aryl alcohol supplementation (catechol, pyrogallol, 3-methylcatechol; 15 μM each) to permissive urines significantly increases SCN activity. Supplemented (+) and unsupplemented (-) permissive urines (+) was tested for growth inhibition by 1.5 μM SCN, as before. Points represent experiments from three independent cultures. ** $P = 0.0039$, Wilcoxon signed rank test.

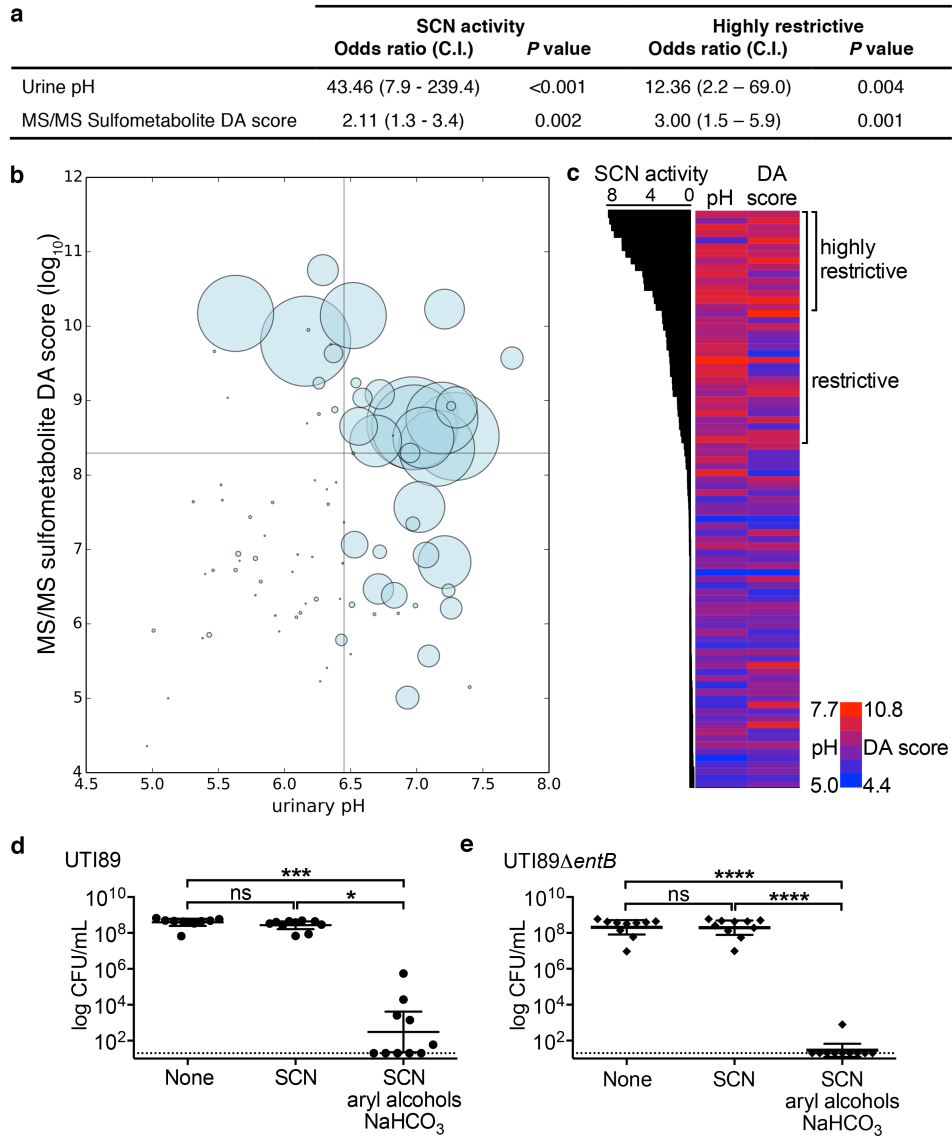


FIGURE 10. Urinary pH and aryl sulfates are independently associated with restrictive urines. (a) Multiple logistic regression analysis of SCN activity shows significant ($P < 0.005$), independent associations between SCN activity and pH or sulfometabolite composition. (b) Bubble plot of all 87 urine specimens tested in this study as a function of pH and aryl sulfometabolite DA score, where the radius of the bubble equals the SCN activity of the

specimen. ROC curve-derived cutoffs are indicated by lines. All but one urine specimen with low pH and LC-MS/MS sulfometabolite DA score are permissive, and the lone exception possesses a borderline pH value (pH 6.43). (c) Heat map of pH and LC-MS/MS sulfometabolite DA score ordered by urinary SCN activity level. SCN activity is plotted as bars on the left for each specimen. Urine pH for each specimen is plotted in heat map from dark blue (lowest value) to red (highest value; see scale). The rightmost column displays the log LC-MS/MS sulfometabolite DA score; coloring is the same as for urine pH. The association between highly restrictive urine ($>\log 3$ SCN activity, “highly restrictive”) and high sulfometabolite DA score is visually apparent (c) and supported by logistic regression using this elevated activity threshold (a). Urinary alkalinization combined with aryl alcohol supplementation significantly potentiates SCN antimicrobial activity against wild type UTI89 (d) and enterobactin-deficient UTI89 Δ *entB* (e). Ten permissive urines were supplemented as in Figure 9d and alkalinized with 5 mg/mL sodium bicarbonate, then tested for growth in the presence of 1.5 μ M SCN as before. Points represent experiments on single donor urines from three independent cultures; a horizontal line indicates the geometric mean \pm 95% C.I. ns = not significant, * $P < 0.05$, *** $P < 0.001$, **** $P < 0.0001$; paired, nonparametric Friedman test with multiple comparisons.

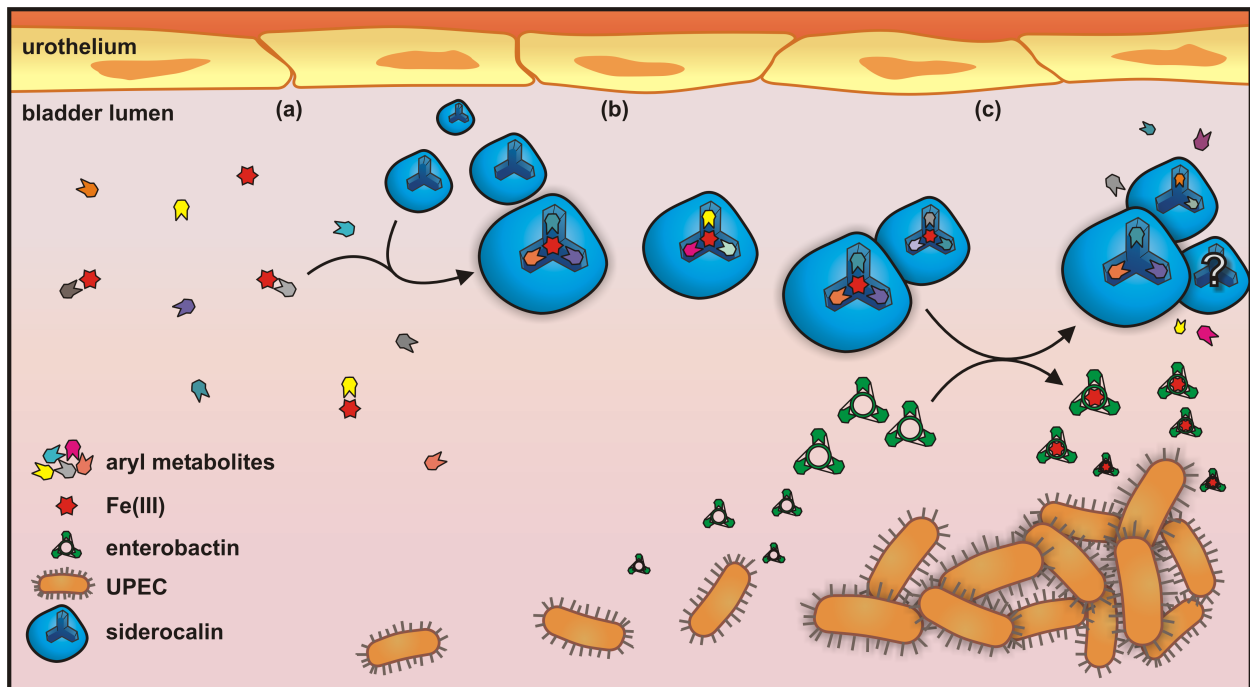


FIGURE 11. Proposed model of SCN antimicrobial activity in restrictive urine. (a) Human urine contains a complex and variable mixture of metabolites, including aryl metabolites such as catecholates. Iron is limiting, and exists as a labile pool of low-affinity complexes with numerous ligands. (b) When UPEC enters the bladder, SCN is upregulated and secreted into the bladder lumen. Elevated pH facilitates host-derived ferric-aryl complex assembly in the SCN calyx, starving UPEC of iron. (c) In this context, the siderophore enterobactin is able to outcompete the SCN-bound complexes for iron, making it bioavailable to UPEC.

CHAPTER TWO: TABLES

TABLE 1. Aryl sulfate associations with restrictive urine.

<i>m/z</i> feature	fold higher in restrictive ^a	<i>P</i> -value	exact mass [M-H] ⁻	atomic formula [M-H] ⁻	preliminary identification ^b	ref.
187	0.93	0.7899	187.0073	[C ₇ H ₇ O ₄ S] ⁻	<i>p</i> -cresol sulfate	(24)
189	1.96	0.0176	188.9867	[C ₆ H ₅ O ₅ S] ⁻	catechol sulfate	(26)
202	4.30	0.0009	202.0185	[C ₇ H ₈ NO ₄ S] ⁻	amino cresol sulfate	(40)
203	0.86	0.7170	203.0036	[C ₇ H ₇ O ₅ S] ⁻	methylcatechol sulfate	(25)
205	1.51	0.3515	204.9827	[C ₆ H ₅ O ₆ S] ⁻	trihydroxybenzene sulfate	(25)
212	0.67	0.2840	212.0038	[C ₈ H ₆ NO ₄ S] ⁻	indoxy sulfate	(26)
216	2.13	0.1559	216.0342	[C ₈ H ₁₀ NO ₄ S] ⁻	tyramine sulfate	(26)
217	2.66	0.0182	217.0181	[C ₈ H ₉ O ₅ S] ⁻	ethylcatechol sulfate	(25)
219	1.75	0.1393	218.9986	[C ₇ H ₇ O ₆ S] ⁻	O-methyl pyrogallol sulfate	(27)
232	1.05	0.7966	232.0298	[C ₈ H ₁₀ NO ₅ S] ⁻	dopamine sulfate	(26)
269	5.46	0.0004	269.0139	[C ₁₁ H ₉ O ₆ S] ⁻	--	
274	0.98	0.9647	274.0046	[C ₉ H ₈ NO ₇ S] ⁻	--	
415	4.25	0.0018	415.0372	[C ₁₆ H ₁₅ O ₁₁ S] ⁻	CQAL sulfate ^d	(28)
528	1.43	0.3033	528.2649	-- ^c	--	

^a Urinary aryl sulfates were selectively quantified by LC-MS/MS and compared between restrictive and permissive urines. Five metabolites were significantly ($P < 0.02$) elevated in restrictive urines. Fold difference presented as restrictive vs. permissive concentration. *P*-values determined by student's *t*-test.

^b Preliminary identifications were determined by considering exact mass and atomic formulae, MS/MS spectra, and reference to published urinary metabolites. Dashes indicate features that could not be identified with sufficient confidence due to degeneracy of the atomic formula results or inconclusive MS/MS spectra.

^c Atomic formula could not be determined with sufficient confidence from the exact mass.

^d CQAL = caffeoylquinic acid lactone

CHAPTER TWO: REFERENCES

1. Foxman, B. (2010) The epidemiology of urinary tract infection. *Nat. Rev. Urol.* **7**, 653–660
2. Henderson, J. P., Crowley, J. R., Pinkner, J. S., Walker, J. N., Tsukayama, P., Stamm, W. E., Hooton, T. M., and Hultgren, S. J. (2009) Quantitative metabolomics reveals an epigenetic blueprint for iron acquisition in uropathogenic *Escherichia coli*. *PLoS Pathog.* 10.1371/journal.ppat.1000305
3. Miethke, M., and Marahiel, M. A. (2007) Siderophore-based iron acquisition and pathogen control. *Microbiol. Mol. Biol. Rev.* **71**, 413–451
4. Reigstad, C. S., Hultgren, S. J., and Gordon, J. I. (2007) Functional genomic studies of uropathogenic *Escherichia coli* and host urothelial cells when intracellular bacterial communities are assembled. *J. Biol. Chem.* **282**, 21259–21267
5. Snyder, J. A., Haugen, B. J., Buckles, E. L., Lockett, C. V., Johnson, D. E., Donnenberg, M. S., Welch, R. A., and Mobley, H. L. T. (2004) Transcriptome of uropathogenic *Escherichia coli* during urinary tract infection. *Infect. Immun.* **72**, 6373–6381
6. Chaturvedi, K. S., Hung, C. S., Crowley, J. R., Stapleton, A. E., and Henderson, J. P. (2012) The siderophore yersiniabactin binds copper to protect pathogens during infection. *Nat. Chem. Biol.* **8**, 731–736
7. Lv, H., Hung, C. S., and Henderson, J. P. (2014) Metabolomic analysis of siderophore cheater mutants reveals metabolic costs of expression in uropathogenic *Escherichia coli*. *J. Proteome Res.* **13**, 1397–1404

8. Fischbach, M. A., Lin, H., Zhou, L., Yu, Y., Abergel, R. J., Liu, D. R., Raymond, K. N., Wanner, B. L., Strong, R. K., Walsh, C. T., Aderem, A., and Smith, K. D. (2006) The pathogen-associated *iroA* gene cluster mediates bacterial evasion of lipocalin 2. *Proc. Natl. Acad. Sci.* **103**, 16502–16507
9. Hoette, T. M., Clifton, M. C., Zawadzka, A. M., Holmes, M. A., Strong, R. K., and Raymond, K. N. (2011) Immune interference in *Mycobacterium tuberculosis* intracellular iron acquisition through siderocalin recognition of carboxymycobactins. *ACS Chem. Biol.* **6**, 1327–1331
10. Abergel, R. J., Moore, E. G., Strong, R. K., and Raymond, K. N. (2006) Microbial evasion of the immune system: structural modifications of enterobactin impair siderocalin recognition. *J. Am. Chem. Soc.* **128**, 10998–10999
11. Goetz, D. H., Holmes, M. A., Borregaard, N., Bluhm, M. E., Raymond, K. N., and Strong, R. K. (2002) The neutrophil lipocalin NGAL is a bacteriostatic agent that interferes with siderophore-mediated iron acquisition. *Mol. Cell.* **10**, 1033–1043
12. Bao, G., Clifton, M., Hoette, T. M., Mori, K., Deng, S.-X., Qiu, A., Viltard, M., Williams, D., Paragas, N., Leete, T., Kulkarni, R., Li, X., Lee, B., Kalandadze, A., Ratner, A. J., Pizarro, J. C., Schmidt-Ott, K. M., Landry, D. W., Raymond, K. N., Strong, R. K., and Barasch, J. (2010) Iron traffics in circulation bound to a siderocalin (Ngal)-catechol complex. *Nat. Chem. Biol.* **6**, 602–609
13. Holmes, M. A., Paulsene, W., Jide, X., Ratledge, C., and Strong, R. K. (2005) Siderocalin (Lcn 2) also binds carboxymycobactins, potentially defending against mycobacterial infections through iron sequestration. *Structure.* **13**, 29–41

14. Bachman, M. A., Oyler, J. E., Burns, S. H., Caza, M., Lépine, F., Dozois, C. M., and Weiser, J. N. (2011) *Klebsiella pneumoniae* yersiniabactin promotes respiratory tract infection through evasion of lipocalin 2. *Infect. Immun.* **79**, 3309–3316
15. Raffatellu, M., George, M. D., Akiyama, Y., Hornsby, M. J., Nuccio, S.-P., Paixao, T. A., Butler, B. P., Chu, H., Santos, R. L., Berger, T., Mak, T. W., Tsolis, R. M., Bevins, C. L., Solnick, J. V., Dandekar, S., and Bäumlner, A. J. (2009) Lipocalin-2 resistance confers an advantage to *Salmonella enterica* serotype Typhimurium for growth and survival in the inflamed intestine. *Cell Host Microbe.* **5**, 476–486
16. Murphy, K. C., and Campellone, K. G. (2003) Lambda Red-mediated recombinogenic engineering of enterohemorrhagic and enteropathogenic *E. coli*. *BMC Mol. Biol.* **4**, 11
17. Datsenko, K. A., and Wanner, B. L. (2000) One-step inactivation of chromosomal genes in *Escherichia coli* K-12 using PCR products. *Proc. Natl. Acad. Sci.* **97**, 6640–6645
18. Hooton, T. M. (2012) Uncomplicated Urinary Tract Infection. *N. Engl. J. Med.* **366**, 1028–1037
19. Matzanke, B. F., Ecker, D. J., Yang, T. S., Huynh, B. H., Müller, G., and Raymond, K. N. (1986) *Escherichia coli* iron enterobactin uptake monitored by Mössbauer spectroscopy. *J. Bacteriol.* **167**, 674–680
20. Sikora, A. L., Wilson, D. J., Aldrich, C. C., and Blanchard, J. S. (2010) Kinetic and inhibition studies of dihydroxybenzoate-AMP ligase from *Escherichia coli*. *Biochemistry.* **49**, 3648–3657

21. Miethke, M., Bisseret, P., Beckering, C. L., Vignard, D., Eustache, J., and Marahiel, M. A. (2006) Inhibition of aryl acid adenylation domains involved in bacterial siderophore synthesis. *FEBS J.* **273**, 409–419
22. Lv, H., Hung, C. S., Chaturvedi, K. S., Hooton, T. M., and Henderson, J. P. (2011) Development of an integrated metabolomic profiling approach for infectious diseases research. *Analyst.* **136**, 4752–4763
23. Want, E. J., Wilson, I. D., Gika, H., Theodoridis, G., Plumb, R. S., Shockcor, J., Holmes, E., and Nicholson, J. K. (2010) Global metabolic profiling procedures for urine using UPLC–MS. *Nat. Protoc.* **5**, 1005–1018
24. Clayton, T. A., Baker, D., Lindon, J. C., Everett, J. R., and Nicholson, J. K. (2009) Pharmacometabonomic identification of a significant host-microbiome metabolic interaction affecting human drug metabolism. *Proc. Natl. Acad. Sci. U. S. A.* **106**, 14728–14733
25. Lang, R., Mueller, C., and Hofmann, T. (2006) Development of a stable isotope dilution analysis with liquid chromatography-tandem mass spectrometry detection for the quantitative analysis of di- and trihydroxybenzenes in foods and model systems. *J. Agric. Food Chem.* **54**, 5755–5762
26. Bouatra, S., Aziat, F., Mandal, R., Guo, A. C., Wilson, M. R., Knox, C., Bjorndahl, T. C., Krishnamurthy, R., Saleem, F., Liu, P., Dame, Z. T., Poelzer, J., Huynh, J., Yallou, F. S., Psychogios, N., Dong, E., Bogumil, R., Roehring, C., and Wishart, D. S. (2013) The human urine metabolome. *PloS One.* 10.1371/journal.pone.0073076

27. Booth, A. N., Masri, M. S., Robbins, D. J., Emerson, O. H., Jones, F. T., and De Eds, F. (1959) The metabolic fate of gallic acid and related compounds. *J. Biol. Chem.* **234**, 3014–3016
28. Stalmach, A., Mullen, W., Barron, D., Uchida, K., Yokota, T., Cavin, C., Steiling, H., Williamson, G., and Crozier, A. (2009) Metabolite profiling of hydroxycinnamate derivatives in plasma and urine after the ingestion of coffee by humans: identification of biomarkers of coffee consumption. *Drug Metab. Dispos.* **37**, 1749–1758
29. Miller, R. C., Brindle, E., Holman, D. J., Shofer, J., Klein, N. A., Soules, M. R., and O'Connor, K. A. (2004) Comparison of Specific Gravity and Creatinine for Normalizing Urinary Reproductive Hormone Concentrations. *Clin. Chem.* **50**, 924–932
30. Paragas, N., Kulkarni, R., Werth, M., Schmidt-Ott, K. M., Forster, C., Deng, R., Zhang, Q., Singer, E., Klose, A. D., Shen, T. H., Francis, K. P., Ray, S., Vijayakumar, S., Seward, S., Bovino, M. E., Xu, K., Takabe, Y., Amaral, F. E., Mohan, S., Wax, R., Corbin, K., Sanna-Cherchi, S., Mori, K., Johnson, L., Nickolas, T., D'Agati, V., Lin, C.-S., Qiu, A., Al-Awqati, Q., Ratner, A. J., and Barasch, J. (2014) α -Intercalated cells defend the urinary system from bacterial infection. *J. Clin. Invest.* **124**, 2963–2976
31. Steigedal, M., Marstad, A., Haug, M., Damås, J. K., Strong, R. K., Roberts, P. L., Himpsl, S. D., Stapleton, A., Hooton, T. M., Mobley, H. L. T., Hawn, T. R., and Flo, T. H. (2014) Lipocalin 2 Imparts Selective Pressure on Bacterial Growth in the Bladder and Is Elevated in Women with Urinary Tract Infection. *J. Immunol.* 10.4049/jimmunol.1401528

32. Van Duynhoven, J., Vaughan, E. E., Jacobs, D. M., Kemperman, R. A., van Velzen, E. J. J., Gross, G., Roger, L. C., Possemiers, S., Smilde, A. K., Doré, J., Westerhuis, J. A., and Van de Wiele, T. (2011) Metabolic fate of polyphenols in the human superorganism. *Proc. Natl. Acad. Sci.* **108 Suppl 1**, 4531–4538
33. Marschall, J., Zhang, L., Foxman, B., Warren, D. K., Henderson, J. P., and CDC Prevention Epicenters Program (2012) Both host and pathogen factors predispose to *Escherichia coli* urinary-source bacteremia in hospitalized patients. *Clin. Infect. Dis.* **54**, 1692–1698
34. Hung, C., Marschall, J., Burnham, C.-A. D., Byun, A. S., and Henderson, J. P. (2014) The Bacterial Amyloid Curli Is Associated with Urinary Source Bloodstream Infection. *PLoS ONE*. 10.1371/journal.pone.0086009
35. Mobley, H. L., Green, D. M., Trifillis, A. L., Johnson, D. E., Chippendale, G. R., Lockett, C. V., Jones, B. D., and Warren, J. W. (1990) Pyelonephritogenic *Escherichia coli* and killing of cultured human renal proximal tubular epithelial cells: role of hemolysin in some strains. *Infect. Immun.* **58**, 1281–1289
36. Simerville, J. A., Maxted, W. C., and Pahira, J. J. (2005) Urinalysis: a comprehensive review. *Am. Fam. Physician.* **71**, 1153–1162
37. Sieniawska, C. E., Jung, L. C., Olufadi, R., and Walker, V. (2012) Twenty-four-hour urinary trace element excretion: reference intervals and interpretive issues. *Ann. Clin. Biochem.* **49**, 341–351

38. Abergel, R. J., Warner, J. A., Shuh, D. K., and Raymond, K. N. (2006) Enterobactin Protonation and Iron Release: Structural Characterization of the Salicylate Coordination Shift in Ferric Enterobactin. *J. Am. Chem. Soc.* **128**, 8920–8931
39. Yi, L., Dratter, J., Wang, C., Tunge, J. A., and Desaire, H. (2006) Identification of sulfation sites of metabolites and prediction of the compounds' biological effects. *Anal. Bioanal. Chem.* **386**, 666–674
40. Wikoff, W. R., Nagle, M. A., Kouznetsova, V. L., Tsigelny, I. F., and Nigam, S. K. (2011) Untargeted metabolomics identifies enterobiome metabolites and putative uremic toxins as substrates of organic anion transporter 1 (Oat1). *J. Proteome Res.* **10**, 2842–2851
41. Gonthier, M.-P., Cheynier, V., Donovan, J. L., Manach, C., Morand, C., Mila, I., Lapiere, C., Rémésy, C., and Scalbert, A. (2003) Microbial Aromatic Acid Metabolites Formed in the Gut Account for a Major Fraction of the Polyphenols Excreted in Urine of Rats Fed Red Wine Polyphenols. *J. Nutr.* **133**, 461–467
42. Carmella, S. G., La Voie, E. J., and Hecht, S. S. (1982) Quantitative analysis of catechol and 4-methylcatechol in human urine. *Food Chem. Toxicol.* **20**, 587–590
43. Hunter, J. (2007) Matplotlib: A 2D graphics environment. *Comput. Sci. Eng.* **9**, 90–95
44. Chaturvedi, K. S., Hung, C. S., Giblin, D. E., Urushidani, S., Austin, A. M., Dinauer, M. C., and Henderson, J. P. (2014) Cupric yersiniabactin is a virulence-associated superoxide dismutase mimic. *ACS Chem. Biol.* **9**, 551–561

45. Bachman, M. A., Lenio, S., Schmidt, L., Oyler, J. E., and Weiser, J. N. (2012) Interaction of lipocalin 2, transferrin, and siderophores determines the replicative niche of *Klebsiella pneumoniae* during pneumonia. *mBio*. 10.1128/mBio.00224-11
46. Brock, J. H., Williams, P. H., Licéaga, J., and Wooldridge, K. G. (1991) Relative availability of transferrin-bound iron and cell-derived iron to aerobactin-producing and enterochelin-producing strains of *Escherichia coli* and to other microorganisms. *Infect. Immun.* **59**, 3185–3190
47. Luo, M., Lin, H., Fischbach, M. A., Liu, D. R., Walsh, C. T., and Groves, J. T. (2006) Enzymatic Tailoring of Enterobactin Alters Membrane Partitioning and Iron Acquisition. *ACS Chem. Biol.* **1**, 29–32
48. Correnti, C., and Strong, R. K. (2012) Mammalian siderophores, siderophore-binding lipocalins, and the labile iron pool. *J. Biol. Chem.* **287**, 13524–13531
49. Perry, R. D., Balbo, P. B., Jones, H. A., Fetherston, J. D., and DeMoll, E. (1999) Yersiniabactin from *Yersinia pestis*: biochemical characterization of the siderophore and its role in iron transport and regulation. *Microbiology.* **145**, 1181–1190
50. Barber, A. E., Norton, J. P., Spivak, A. M., and Mulvey, M. A. (2013) Urinary Tract Infections: Current and Emerging Management Strategies. *Clin. Infect. Dis.* **57**, 719–724
51. Pérez-Jiménez, J., Hubert, J., Hooper, L., Cassidy, A., Manach, C., Williamson, G., and Scalbert, A. (2010) Urinary Metabolites as Biomarkers of Polyphenol Intake in Humans: A Systematic Review. *Am. J. Clin. Nutr.* **92**, 801–809
52. Wang, J. H., Byun, J., and Pennathur, S. (2010) Analytical Approaches to Metabolomics and Applications to Systems Biology. *Semin. Nephrol.* **30**, 500–511

53. Vinayavekhin, N., Homan, E. A., and Saghatelian, A. (2010) Exploring Disease through Metabolomics. *ACS Chem. Biol.* **5**, 91–103

CHAPTER THREE

The innate immune protein siderocalin binds urinary metabolites to deprive bacteria of iron

ABSTRACT

During urinary tract infections (UTIs) uropathogenic *Escherichia coli* (UPEC), the bacterial pathogen associated with most UTIs, must acquire iron to grow in the micronutrient-limited bladder environment. Host cells secrete the innate immune protein siderocalin, which accumulates in the urine and further restricts UPEC iron access by binding ferric complexes. Recent evidence suggests that urinary composition plays an important role in determining SCN's efficacy. The association between SCN antimicrobial activity and small diet-derived aryl alcohols, some of which are proposed SCN ligands, strongly suggests that urinary ferric complex formation and sequestration by SCN contributes to its antimicrobial mechanism in urine. Here, we screened fractionated urine for SCN ligands using a multistep fractionation and validation assay. Biophysical interactions were validated for several small catecholate metabolites that were found to be elevated in urines supporting SCN antimicrobial activity. These ligands were then shown to promote SCN's antimicrobial activity in defined media conditions, demonstrating that they indeed are the urinary components that synergize with SCN to restrict UPEC growth. Lastly, we used native mass spectrometry to highlight the existence of heterogeneous ferric-ligand complexes within the SCN calyx. Together, these results illuminate how dietary factors interact with the innate immune protein SCN to fight infections in urine. These findings further describe how urinary compositional manipulations could aid in controlling UTI susceptibility and reduce dependencies on traditional antibiotics.

INTRODUCTION

Urinary tract infections (UTIs) are one of the most commonly experienced bacterial infections worldwide. Uncomplicated UTIs are most commonly associated with uropathogenic *Escherichia coli* (UPEC) colonization, and have historically been treated using common antibiotics (1, 2). However, rapid emergence and spread of antibiotic resistance in UPEC combined with a paucity of novel therapies necessitates exploring bacterial pathogenesis to identify new approaches to combat infection (1, 3). Recurrent infections further complicate treatment options for roughly 25 percent of UTI patients, with unexplained differences in individual susceptibilities (2, 4, 5). A better understanding of pathogenic mechanisms in the human urinary tract may inform individualized approaches that promote improved clinical outcomes and antibiotic stewardship (2, 6).

At the host-pathogen interface, one important mechanistic interaction involves the sequestration and acquisition of iron (7, 8). Iron is an essential micronutrient for nearly all organisms, and the human host has developed elaborate systems to restrict its availability and starve pathogens during infection (9). This innate immune barrier forces UPEC to carry specialized pathways in order to obtain iron. During UTI, UPEC respond to iron limitation by upregulating the biosynthetic machinery to make siderophores, or small iron-chelating secondary metabolites, which effectively compete with host iron binding proteins (10–16). Humans, in turn, express and secrete the siderophore binding protein siderocalin (SCN), which binds small molecule ferric complexes including some siderophores (17–20).

We recently investigated SCN's ability to restrict UPEC growth in human urine and found dramatic variability between individuals in the extent of antimicrobial activity. SCN's activity was iron dependent, and correlated with elevated pH and sulfated aryl metabolites in the urine. Because this class of sulfated metabolites contains catecholates and other potential ferric chelators and SCN ligands (20), we hypothesized that SCN's antimicrobial mechanism in urine involves sequestering host-derived ferric complexes. This activity could therefore precede bacterial siderophore accumulation and fend off infection at an early stage.

Here, we aimed to test this hypothesis, employing a biophysical and mass spectrometry-based screening methodology to discover physiologic SCN ligands directly from human urine that supported its antimicrobial activity. Through these analyses, we found that urine supporting greater SCN activity was indeed enriched for several catecholate metabolites that bound SCN in ferric complexes. These metabolites are of the chemical class identified by correlation previously, and derive largely from host and microbiome metabolism of plant-based dietary precursors (19, 21). These ferric cofactors were able to promote SCN's activity in defined, iron-limiting media, thus reconstituting the urinary mechanism in a simplified background. Finally, we suggest that the *in vivo* context and true SCN calyx occupancy may be overwhelmingly combinatorial, supporting heterogeneous assemblies of metabolites as preferred ligands. Together, these results describe the mechanism behind SCN's antimicrobial activity in human urine, and provide a blueprint for a urine composition refractory to UPEC colonization.

EXPERIMENTAL PROCEDURES

Protein purification. Human SCN protein (the kind gift of Roland Strong) was expressed on a pGEX4T vector in BL21 *E. coli* as previously described (17, 19). The human SCN calyx mutant K125A/K134A was expressed on a pET22b vector in BL21 *E. coli* and purified as described (19, 20). Protein purity was monitored by mass spectrometry and SDS-PAGE.

Media growth assay. Defined media used to test metabolite supplementation were M63 minimal salts media supplemented with 0.2% glycerol and 10 $\mu\text{g/mL}$ niacin, and serum-free RPMI (Gibco). SCN activity assays were performed essentially as described (19, 22). Briefly, media was inoculated with the uncomplicated cystitis isolate UTI89 or isogenic siderophore mutants (12) at 10^3 cfu/mL, from 4-6 hour cultures in LB broth. Cultures were grown with 1.5 μM SCN or an equivalent volume of PBS. After 20 hours, viable bacterial concentrations were determined by cfu enumeration. Where indicated, media was supplemented with candidate metabolites at 5 μM .

Urine fractionation. Healthy donor urines were collected as approved by the Washington University School of Medicine Institutional Review Board, and described previously (19). To fractionate and concentrate urinary small molecules, we used a multi-step chromatographic scheme. Four urines of either high or low SCN antimicrobial activity were pooled (2 mL each) and applied to Chrom P SPE cartridges (Supelco). The flow through, water wash, and elutions with 50% and then 100% HPLC-grade methanol (Sigma) were all collected and lyophilized to dryness. Each of the four preparations was then rehydrated in HPLC-grade water (Sigma) and

fractionated over a phenyl-hexyl Eternity column (250 x 4.6 mm, 5 μ m; Supelco) using a water:methanol gradient on a BioLogic DuoFlow chromatography system (Bio-Rad). All fractions (~290 total) were lyophilized to dryness and stored at -80°C until analysis.

Differential scanning fluorimetry. To screen for SCN binding in urinary fractions, we measured thermal denaturation through differential scanning fluorimetry (DSF), essentially as described (23). Lyophilized urinary HPLC fractions were reconstituted in 100 μ L HPLC-grade water thus yielding a roughly 80-fold concentration from the original bulk urine. Fractions (10 μ L) were added to a final concentration of 3 μ M SCN in PBS with a 5X concentration of SYPRO Orange dye (Sigma), and allowed to equilibrate for 20 minutes. Using a CFX96 real-time PCR machine (Bio Rad), reactions were then heated in 96-well quantitative PCR plates (Bio Rad) from 22°C to 98°C at 1°C per minute, with plate reading at each increment. Melt transitions were monitored on the HEX channel and displayed as the derivative of relative fluorescence units with respect to temperature (dRFU/dT). Fractions were also analyzed in the absence of protein as a negative control, and SCN was incubated with ferric catechol (30 μ M) as a positive control, and negative controls included protein plus iron and fractions without protein present. Interesting fractions were identified by a melting temperature (T_M) shift.

Preliminary compounds identified by GC-MS were also confirmed by DSF. These reactions were carried out as above, but with a ferric complex (FeL_3) concentration of 30 μ M. Chemicals were purchased from Sigma Aldrich and prepared with $FeCl_3$ or without (equal volume PBS) at a

1:3 ratio of iron to ligand (i.e. FeL₃). SCN melt curves were performed as above, and a positive DSF result was considered a T_M shift or loss of the melt signal.

Fluorescence quenching. We confirmed metabolite-SCN interactions by measuring binding of DSF-positive candidates by intrinsic tryptophan fluorescence quenching, essentially as described (17, 20). SCN protein (500 nM) was mixed with a dilution series of ligand in the presence and absence of iron in PBS with 2% DMSO in black 96-well fluorescence plates (Corning). After one-hour equilibration, tryptophan fluorescence was monitored at excitation and emission wavelengths of 281 nm and 340 nm, respectively, on a TECAN M200 plate reader at room temperature. Binding was monitored up to 48 hours later with no loss of signal or notable change in fluorescence quenching patterns (data not shown).

Gas chromatography-mass spectrometry. Fractions identified by DSF as containing SCN-binding character were profiled by gas chromatography-mass spectrometry (GC-MS). Briefly, MSTFA-derivatized samples were analyzed on an Agilent 7890A gas chromatograph interfaced to an Agilent 5975C mass spectrometer operated in the electron ionization (EI) mode; the source temperature, electron energy and emission current were 230°C, 70eV and 300µA, respectively. GC chromatography was performed with an HP-5MS column (30 m, 0.25mm i.d., 0.25µm film coating; P.J. Cobert, St. Louis, MO) with a linear temperature gradient of 80-300°C at 10°C per minute; the injector and transfer line temperatures were 250°C. Fraction spectra were matched to the NIST11 Mass Spectral Library for chemical identification using AMDIS, and metabolites

elevated in binding fractions compared to non-binding fractions were identified as potential ligand candidates and analyzed further by DSF and FQ.

To quantify SCN-binding metabolites by GC-MS, we produced calibration curves for each metabolite relative to the exometabolite 4-fluorosalicylic acid (4FSA) (19). Several metabolites could not be quantified because no standard was available, or the standard was not reliably detectable by GC-MS. Urine specimens (100 μ L) were spiked with 200 picomoles of 4FSA and treated with 2.4 units of urease (Sigma) for 40 minutes before quenching with 1 volume of methanol. The reaction was dried under nitrogen and derivatized as described above. GC-MS was performed in SIM mode based on the two fragment ions for each candidate that were used for standard curves. Both fragment ions were monitored to assure correct identification. Molar concentrations were determined using the standard curve slope to correct the integrated peak area ratio of 4FSA and the analytes of interest.

Native mass spectrometry. SCN protein (30 μ M) was prepared in 50 mM ammonium acetate (Sigma), pH 6.95. Where indicated, FeCl₃ (50 μ M) and ligand compounds (60 μ M for individual compounds; 100 μ M for mixed compounds) were added, equilibrated at room temperature for 2 hours, then stored at 4°C until analysis. A 10 μ L sample was loaded into a nanoES spray capillary (Thermo Scientific) for native electrospray ionization and mass spectra were acquired with a Bruker Solarix 12T FTICR mass spectrometer (Bruker Daltonics, Bremen, Germany). The capillary voltage was 0.9-1.3 kV. The drying gas temperature was 30°C; its flow was 1 L/min. The voltage for ISCID was set at 70 V to help desolvation. The ion-funnel RF amplitude was 300

V_{pp}, and the ion-funnel voltages were 200 V (funnel 1) and 18 V (funnel 2). RF frequencies used in all ion-transmission regions were the lowest available value: multipole 1 (2 MHz), quadrupole (1.4 MHz) and transfer line (1 MHz). The collision voltage for the collision cell varied from 0 to 50 V. Ions were accumulated for 500 ms in the RF-hexapole ion trap before being transmitted to the infinity ICR trap. The time-of-flight was 1.3 ms for the protein-ligand ions. The source region pressure was 2.3 mbar; the quadrupole region pressure was 4.4×10^{-6} mbar, and the trap-chamber pressure was 1.3×10^{-9} mbar. The typical ECD pulse length was 0.06 s, with ECD bias 0.6 V and ECD lens 10 V. The ECD hollow cathode heater current was 1.6 A. MS parameters were slightly modified in each individual sample to obtain an optimized signal. One to several hundred scans was averaged for each spectrum. External calibration was done by ESI of cesium perfluoroheptanoic acetate, up to m/z 8500.

Statistical analyses. Data were analyzed in Prism v. 6.0d (GraphPad). For parametric and non-parametric two-sample unpaired comparisons we used *t*-test and Mann-Whitney U test, respectively. To compare multiple groups versus control or each other, we used one-way ANOVA. Where appropriate, post-tests were used to correct for multiple comparisons.

RESULTS

SCN ligand detection using differential scanning fluorimetry. Our previous work suggested that urinary constituents control SCN's antimicrobial activity through interactions with its calyx. To test the hypothesis that SCN ligands present in urine are causative players in its antimicrobial activity, we screened restrictive and permissive human urine specimens for SCN binding. However, human urine is chemically complex and highly variable between individuals; furthermore, salt concentrations and buffer incompatibilities preclude using many biophysical binding assays for SCN ligand screening. We therefore exploited ligand effects on protein thermal stability to screen for binding by differential scanning fluorimetry (DSF). Compared to many common binding assays, this technique is highly tolerant to variable ligand concentrations and complex sample matrices, and is amenable to semi-high-throughput screening with low reagent consumption.

To confirm that DSF is an appropriate assay for SCN binding, we compared binding to between DSF and intrinsic tryptophan fluorescence quenching (FQ), which has been demonstrated extensively for this protein (17, 20). Enterobactin exhibited stoichiometric binding to SCN by FQ, as expected (Fig. 1a) (17). SCN quenching was also achieved by titration with ferric 2,3-dihydroxybenzoic acid (2,3-DHBA; Fig. 1b), but this quenching effect was lost in the SCN calyx mutant (SCN K125A/K134A; Fig. 1d) (20). A non-binding benzoic acid, 2,5-dihydroxybenzoic acid (2,5-DHBA, or gentisic acid) does not quench SCN fluorescence, as established (Fig. 1c) (24). These results are recapitulated in DSF as shown in Figures 1e-h. Ferric complex binding shifted and reduced the melting transition of *apo*-SCN, as shown for enterobactin and ferric 2,3-

DHBA (Fig. 1e,f), effects that were not seen with the negative control 2,5-DHBA (Fig. 1g), or with SCN K125A/K134A and ferric 2,3-DHBA (Fig. 1h). These results establish DSF as an effective screening tool for SCN ligand binding.

Urines supporting SCN antimicrobial activity possess SCN-binding chromatographic fractions.

We hypothesized that fractions of human urine would display SCN binding by DSF. To improve binding assay interpretation and downstream chemical comparisons, we aimed to reduce the chemical complexity of a single DSF reaction. To accomplish this, we devised a multi-step chromatographic fractionation protocol (Fig. 2a). We previously divided urine specimens into two categories based on their level of antimicrobial SCN activity (19). Urines where SCN was able to restrict growth of the enterobactin-deficient UTI89 Δ *entB* relative to wild type by at least 90% were termed *restrictive*; urines that supported no measurably SCN activity were called *permissive*. In order to compare restrictive and permissive compositions more generally here, we pooled four restrictive urines and four permissive urines (Table 1), then extracted metabolites over solid phase ENVI-Chrom-P resin (Fig. 2a). We collected flow-through, water wash, and elutions with 50% and 100% methanol (v/v). These preparations were each then fractionated further by HPLC, dried, and reconstituted in water. The reconstituted fractions represented a roughly 80-fold concentration over the initial urine matrix, assuming minimal loss due to chromatography or chemical instability.

All 290 reconstituted urine fractions were used in DSF reactions at a 1:4 dilution, in the presence and absence of 3.2 μ g/mL iron (Supplementary Fig. 1). SCN protein was melted and monitored

as above. Melt transitions were compared to identify fractions yielding a ΔT_M representing possible SCN ligand binding. As would be expected, ΔT_M transitions clustered into groups of several fractions, likely representing both the main area of chromatographic peaks (Supplementary Fig. 1). Particularly interesting were fractions that showed increased ΔT_M values in response to additional iron; these fractions are highlighted in Figure 2b,c. This response would be predicted with iron-dependent ligand complex formation in the SCN calyx (20). We detected these binding signatures in fractions from each SPE elution, suggesting the presence of multiple chemically distinct ligands. Despite no significant difference in the average specific gravity (Table 1), the restrictive fractions contained noticeably larger thermal shifts, particularly in the presence of iron, than the permissive samples (Fig. 2b vs. Fig. 2c). These data represent direct detection of iron-dependent urinary SCN binding activity from human urine. Our method yielded fractions with reduced chemical complexity, which enabled both binding assay sensitivity and the ability to proceed with mass spectrometry-based ligand identification directly from these same fractions without further purification.

Metabolomic analyses of SCN-binding urinary fractions. We next asked how the composition of these binding fractions differed from those without evident binding. We hypothesized that the responsible molecules would be small, aromatic metabolites based on the structure of the SCN calyx and existing work on potential urinary ligands of SCN (19, 20, 24). Furthermore, previous work from our laboratory identified markers of aryl alcohol metabolites as correlates of SCN antimicrobial activity in urine (19). Because of this, we used gas chromatography-mass spectrometry (GC-MS) to profile the urinary fractions and preliminarily identify candidates

enriched in binding relative to non-binding fractions. Supplementary Table 1 summarizes the results of these comparisons. Candidates shown were detected in binding fractions, and the summed peak heights across the binding fraction were compared between restrictive and permissive pools. This comparison highlights potential contributions to the observed antimicrobial activity in restrictive urines. Metabolites enriched in permissive urines are also of interest for the possibility that they act as decoy ligands that prevent antimicrobial activity.

Among the metabolites preliminarily identified as enriched in restrictive urines are previously proposed SCN ligands (e.g. pyrogallol and methylcatechol) (20), as well as other novel catecholates (propyl gallate, 3,4-dihydroxyhydrocinnamic acid, 4-hydroxyhippuric acid) and non-catecholates (ferulic acid, hydroxyphenylacetic acid) (Supplementary Table 1). Notable also is the presence of several methylated catecholate, or methoxy, benzoic acid derivatives, which may arrive from host catechol-O-methyltransferase activity on catecholate species (25, 26). Despite the reduced chemical complexity in these HPLC fractions, they are still complex mixtures of metabolites. To validate each candidate's contribution to the observed SCN thermal shift, we turned to a binding assay with purified components.

Urinary metabolites exhibit iron-dependent SCN binding. To determine which metabolites in the DSF-positive fractions truly contribute to SCN binding, we repeated our SCN DSF screen using pure compounds. In this assay, we included all GC-MS candidates that were commercially available, as well as the free aryl alcohols of several sulfated metabolites previously associated with SCN activity by an LC-MS metabolomics strategy (19, 27). Candidate metabolites were

measured in the presence and absence of iron at a 1:3 ratio to ligand (expressed as FeL_3), consistent with typical iron coordination by catecholates (20, 28). Ligand alone or ligand with iron was added to 3 μM SCN and melted as described above. Melting temperature shifts or ablation of the protein melt signature were considered positive results (Fig. 1d,e). In our analysis, 12 of 22 tested metabolites affected SCN melting measured by DSF (Fig. 3). Interestingly, all DSF-positive candidates contained a di- or tri-hydroxybenzene motif, consistent with Fe(III) chelation and SCN binding (20, 29).

The loss of a SCN melt transition in the presence of some ligands, including enterobactin (Fig. 1a), was intriguing. While this result could be explained by greatly enhanced stability of the protein complex, it is also possible the redox-sensitive catecholate ligands disrupted the behavior of the SYPRO dye. To more directly measure iron-dependent SCN binding, we followed up our DSF screen with SCN fluorescence quenching on DSF-positive ligands, which relies on SCN's intrinsic tryptophan fluorescence, as previously described (Fig. 1a-d) (17, 20). We measured SCN's ability to bind DSF-positive candidates using this method in the presence and absence of iron (Fig. 4). As shown above, the SCN calyx mutant K125A/K134A was unable to bind ferric complexes in this assay (Fig. 1d). Here, pyrogallol was uniquely capable at binding SCN in the absence of iron, while several other candidates including pyrogallol exhibited strong iron-dependent binding (Fig. 4a,b), consistent with the iron effect seen in our original DSF screen. Ferric complex binding divided these candidates into three categories (Fig. 4a,b): those with little or no quenching, such as 2-amino-4-methylphenol and *t*-ferulic acid (black lines); those with moderate quenching, such as caffeic acid and 4-methyl catechol (blue lines); and those with

nearly complete quenching at high concentrations, including catechol, pyrogallol, and 3-methoxycatechol (red lines). These data confirm both novel and previously proposed metabolites as SCN ferric ligands, and serve as an orthogonal validation strategy in our physiologic ligand screen.

Comparing chemical structures within each level of SCN binding (Fig. 4b) revealed intra-group structural preferences consistent with the calyx topography (20, 24, 29). The greatest binding signature was detected in small, di- and tri-hydroxybenzenes with aromatic substitutions located at 1, 2, and 3-carbon positions. Consistent with previous findings, substitutions at the 4-position were less sterically favorable and indeed, di- and tri-hydroxybenzene metabolites with this structure produce only moderate quenching (24, 30). Finally, metabolites without di- or tri-hydroxy moieties and 3,4-dihydroxybenzoic acid derivatives were unable to bind and quench SCN fluorescence (Fig. 4b). Together, these results used an unbiased binding screen to detect and validate physiologic SCN ligands from human urine that were enriched in samples supporting greater antimicrobial activity.

SCN's ligands potentiate its antibacterial activity. We next sought to recapitulate the urinary antimicrobial mechanism in a defined system, hypothesizing that if these urinary ligands directly participate in potentiating SCN's antimicrobial activity, supplementing a minimal, defined chemical media with these metabolites could mimic the antimicrobial activity seen in urine. To test this, we used two defined conditions: the minimal salts media M63, and serum-free RPMI. While both are iron limiting, RPMI is more chemically rich. We then supplemented these media

with physiologically relevant concentrations of caffeic acid, catechol, or pyrogallol (5 μM) and measured 20-hour bacterial growth in the presence and absence of SCN (1.5 μM) (19). In M63, SCN restricted wild-type UTI89 and the enterobactin-deficient mutant, UTI89 ΔentB growth only when supplemented with ligands (Fig. 5a). In contrast, a non-binding metabolite, *t*-ferulic acid, did not synergize with SCN to restrict growth in M63 (Supplementary Fig. 2). This effect was also evident with lower ligand concentrations, as 1.5 μM pyrogallol significantly ($p < 0.05$) restricted UTI89 ΔentB growth in combination with 1.5 μM SCN (Supplementary Fig. 3).

In non-supplemented RPMI, SCN restricted wild-type UTI89 growth, but not UTI89 ΔentB , consistent with enterobactin sequestration as demonstrated previously (Fig. 5b) (19, 22, 31). When supplemented with candidate ligands however, SCN significantly restricted only the *entB* mutant (Fig. 5b). A slight growth increase was observed in UTI89 with catechol and pyrogallol, which may be an effect of improved iron solubility or excess exogenous SCN ligands that allowed enterobactin to function unperturbed. Overall, distinct SCN effects in M63 and RPMI are further evidence that growth environment, whether human-derived or chemically-defined, can have a determinative role when measuring antimicrobial activity. Catecholate supplementation in rich media (LB), for example, did not potentiate SCN activity against wild type or enterobactin-deficient UTI89 (Supplementary Fig. 4).

In both media conditions, the ligands' potentiating effects were most significant against UTI89 ΔentB , where the bacteria lack endogenous enterobactin production (Fig. 5). This is consistent with our hypothesis from studies on human urine that enterobactin is especially suited

to liberating iron from SCN-bound ferric complexes (19). Overall, these results demonstrate that urinary SCN ligands associated with restrictive specimens are sufficient to reconstitute SCN activity in a simple, defined chemical system.

Urinary ligand concentrations are correlated with antimicrobial activity. To more accurately correlate SCN ligands' presence with antimicrobial status, we wanted to determine their absolute concentrations in human urine specimens. To accomplish this, we developed GC-MS standard curves relative to an exometabolite standard, 4-fluorosalicyclic acid (4FSA). Urine samples were urease treated and derivatized for GC-MS analysis without any further extraction or manipulation. Some metabolites of interest could not be quantified by this method due to low abundance or poor ionization and detection in GC-MS. We successfully measured absolute concentrations of 5 ligands in human urines (n = 28) for which the SCN activity was previously tested (19). Pyrogallol, one of the best candidate ligands in our screen and fluorescence assay, was significantly ($p = 0.0007$) elevated in the restrictive relative to permissive urines (Fig. 6a). More specifically, pyrogallol concentrations were significantly ($p < 0.0001$) correlated with increasing SCN activity as measured previously (Fig. 6b) (19). Furthermore, free pyrogallol concentrations measured here were highly correlated ($p < 0.0001$) with the relative abundance of its sulfate conjugate, pyrogallol sulfate (m/z 205 in negative ion ESI), identified in our previous study (Supplementary Fig. 5). This finding supports our previous hypothesis that the aryl sulfate signatures represent their free aryl alcohols (19).

While the other metabolites quantified in the urine set showed a consistent tendency toward higher molar concentrations in restrictive urines, these did not reach statistical significance at this sample size (Supplementary Fig. 6). However, our previous study showed that the aryl metabolite contribution was particularly correlated with high SCN activity ($> \log 3$) samples (19). When we examined the ligand concentrations among highly restrictive urines in this dataset ($n = 7$) versus permissive urines ($n = 9$), the association with restrictive urines improved for pyrogallol ($p = 0.0006$), catechol ($p = 0.09$), and caffeic acid ($p = 0.02$; Supplementary Fig. 7).

SCN binds heteromeric ligand complexes. The SCN calyx contains three similar, but not identical, pockets that each bind one of enterobactin's catecholate rings (17, 32). These sites are also responsible for binding other ferric catecholate and non-catecholate siderophores and small molecule ligands, demonstrating the SCN calyx's versatility and ligand degeneracy (20, 32–34). Because the urinary ligands and enterobactin fragments exist mostly as single catecholate rings, we hypothesized that SCN may bind mixtures of these ligands as a single ferric complex; due to the calyx asymmetry, some mixtures may even be more avid ligands than a single homogeneous complex. Previous ligand studies using predominantly crystallography and biophysical assays could not resolve heterogeneous complexes, as the data interpretation relies on population averages (17, 20, 32). Indeed, our DSF screens may reflect ligand combinations, but those species are not identifiable by melting or fluorescence. In order to resolve whether SCN can bind heterogeneous mixtures, we used non-denaturing, or native, mass spectrometry. This technique uses “soft” ionization coupled with high-resolution mass spectrometry to detect intact non-

covalent complexes (35–38). Because each *holo*-SCN complex has a unique mass, mixed calyx occupants can be differentiated by their distinct m/z shift from the *apo* protein.

To determine whether SCN can stably bind mixed complexes, we analyzed SCN by native MS in the presence of iron and several aryl alcohols. Using FTICR mass spectrometry, *apo*-SCN appeared as a sharp peak at m/z 2298.2, matching the $[\text{SCN}+9\text{H}]^{9+}$ charge state ion with an observed mass of 20,674.8 Da (calculated mass from sequence = 20,675 Da; Fig. 7a). Equilibrating SCN with Fe(III) and ligand compounds resulted in new peaks corresponding to ferric pyrogallol and caffeic acid dimers but did not show complex formation with salicylic acid, consistent with biophysical binding data (Supplementary Fig. 8) (24). Interestingly, when pyrogallol, caffeic acid, and catechol were mixed together with SCN, a single new peak was evident. This peak had a 356 Da mass shift, closely matching that for a mixed $[\text{Fe}(\text{pyrogallol})(\text{caffeic acid})]^{1-}$ complex.

We then analyzed SCN complexes by nano-electrospray ionization coupled qTOF mass spectrometry. This native MS platform detected the $[\text{SCN}+8\text{H}]^{8+}$ charge state with an observed deconvoluted mass of 20673.5 ± 3.1 Da, as well as a +60 adduct species (Fig. 7b). SCN was then equilibrated with the urinary ligand catechol and 2,3-dihydroxybenzoic acid (2,3-DHB), the catecholate biosynthetic building block of enterobactin (39). Here, nearly all *apo*-SCN was converted to mass-shifted complex species (Fig. 7b). We detected a smaller peak that closely corresponds to $[\text{Fe}(\text{DHB})(\text{catechol})]^{1-}$, and prominent peaks that match the expected shift for $[\text{Fe}(\text{DHB})(\text{catechol})_2]^{3-}$ and $[\text{Fe}(\text{DHB})_2(\text{catechol})]^{3-}$.

Together, these results underline SCN's degenerate binding capacity and highlight the strength of mass spectrometry in identifying small molecule-protein complexes from samples with potential mixed species. To our knowledge, this is the first demonstration that SCN binds heterogeneous ligand complexes.

DISCUSSION

Together, these results show how human urinary metabolites govern the antimicrobial mechanism of an important innate immune protein, siderocalin. By starting with human specimens and developing a sequential fractionation scheme, we were able to reduce the chemical complexity and employ direct biophysical measurements on physiologically relevant mixtures. Coupling binding assays with mass spectrometry allowed us to identify multiple SCN ligands present in human urine, that were correlated with SCN's previously demonstrated urinary antimicrobial activity (19, 22). Supplementing defined media with these ligands at relevant concentrations potentiated SCN activity, thus supporting the mechanistic link between endogenous SCN ligands and its ability to control UPEC iron acquisition and growth in human urine.

We hypothesized that aryl alcohol metabolites present in urine might act as key SCN cofactors in restricting bacterial iron uptake. This chemical class was previously highlighted as putative *in vivo* SCN cofactors, first by a crystallographic screen using pure compounds (20), and recently in a targeted metabolomic study correlating sulfated aryl alcohols and elevated pH with SCN activity in human urine (19). Our findings presented here are consistent with these reports, and demonstrate the mechanistic role for aryl metabolites in SCN antimicrobial activity. Several of the catecholate metabolites, such as pyrogallol, methylcatechol, and catechol, have now been identified by multiple distinct approaches as relevant SCN cofactors. These ligands are also known to chelate iron in a pH-sensitive manner that closely marks the elevated pH correlation with SCN activity (19).

These SCN-ligand interactions may have applications beyond urinary tract pathogenesis. The metabolites identified here, along with similar metabolites, are not exclusively found in urine, but present in tissue and serum as well, where metabolic diversity is increasingly gaining recognition for its impact on human health (40–42). Since its discovery, SCN has been implicated in metabolic diseases, cancer, endogenous iron homeostasis, and other non-urinary infectious diseases (43–49), however its role or mechanism of action in these conditions has largely remained a mystery. The ligand interactions described here could occur in other host environments, providing SCN a means of transporting iron, as proposed previously (20), and also sequestering iron from pathogens that do not rely on siderophores bound by SCN. These interactions could, for example, help explain SCN's protective effect against *Klebsiella pneumoniae* respiratory infection models, even when the pathogen encodes multiple SCN-evading siderophores (22). Further studies including metabolomic manipulations as a mechanistic variable in inflammatory models will be necessary to determine SCN's action in these contexts.

The ligands' ability to promote SCN's antimicrobial activity in defined media, as shown here, also supports the previously proposed role of enterobactin. We previously showed that in urines with restrictive composition, UPEC required the siderophore enterobactin to acquire iron in the presence of SCN (19). In both supplemented media conditions, the enterobactin-deficient mutant UTI89 Δ *entB* was especially susceptible to cofactor-mediated SCN growth restriction. Enterobactin faces similar pH dependencies as the catecholate ligands, and its superior iron

affinity may contribute to its protective effect here (20, 50). Ultimately, the fate of SCN following this confrontation is unclear; it may retain de-ferrated aryl ligands or bind a subset of the ferric enterobactin pool, and likely exists in some dynamic mixture of these states *in vivo*, reflecting constant changes in urine composition, volume, and bacterial presence. Our biophysical measurements suggest that as pure complexes, these metabolites do not bind with as high an affinity as enterobactin, consistent with prior literature (Fig. 1a, Fig. 4b) (20). However, we show for the first time that heterodimeric and heterotrimeric ligand mixtures are possible, and indeed appear to be preferred SCN ligands in some mixed systems. In the complex urinary environment with multiple potential ligand species, enterobactin competition is a much more complex scenario than often played out *in vitro*. Native MS is demonstrated here as a powerful complement to traditional biophysical approaches to study small molecule ligand interactions with proteins, and further studies could apply these techniques to answer questions about *in vivo* ligand occupancy.

A causal, mechanistic link between diet-derived metabolites and antimicrobial activity suggests avenues for non-traditional antibiotic UTI control. Patients suffering from recurrent cystitis could benefit particularly from controlling urinary composition to limit bacterial colonization. Aryl metabolites such as pyrogallol, caffeic acid, and catechol derive from many plant-based polyphenolic precursors, often cited as products of coffee, tea, berry, and wine consumption (21, 51–53). Cranberry products have long been touted for UTI prevention, but recent literature reviews and carefully controlled studies often fail to find robust, significant benefits (6, 54, 55). The results presented here suggest that some metabolites present in cranberries, tea, and coffee,

for example, may indeed potentiate SCN's protective activity. However, because iron sequestration requires an alkaline pH and many urinary metabolites may require particular gut microbiome compositions (19, 40, 42, 56), the beneficial effects may be masked or inconsistent in existing human studies. Further understanding the effects of these manipulations on SCN's antimicrobial activity could inform future clinical interventions designed to reduce UTI susceptibility.

ACKNOWLEDGEMENTS

The authors thank Roland Strong for generously sharing siderocalin constructs. J.P.H. holds a Career Award for Medical Scientists from the Burroughs Wellcome Fund and acknowledges National Institute of Diabetes and Digestive and Kidney Diseases grants R01DK099534 and P50DK064540, the National Center for Advancing Translational Sciences UL1TR000448, and the Longer Life Foundation. Mass spectrometry was supported by United States Public Health Service grants P41-RR00954, P30-DK20579, and P30-DK56341. R.R.S.-C. acknowledges NIH training grant T32GM007067-37 and a Monsanto Excellence Fund Graduate Fellowship.

CHAPTER THREE: FIGURES

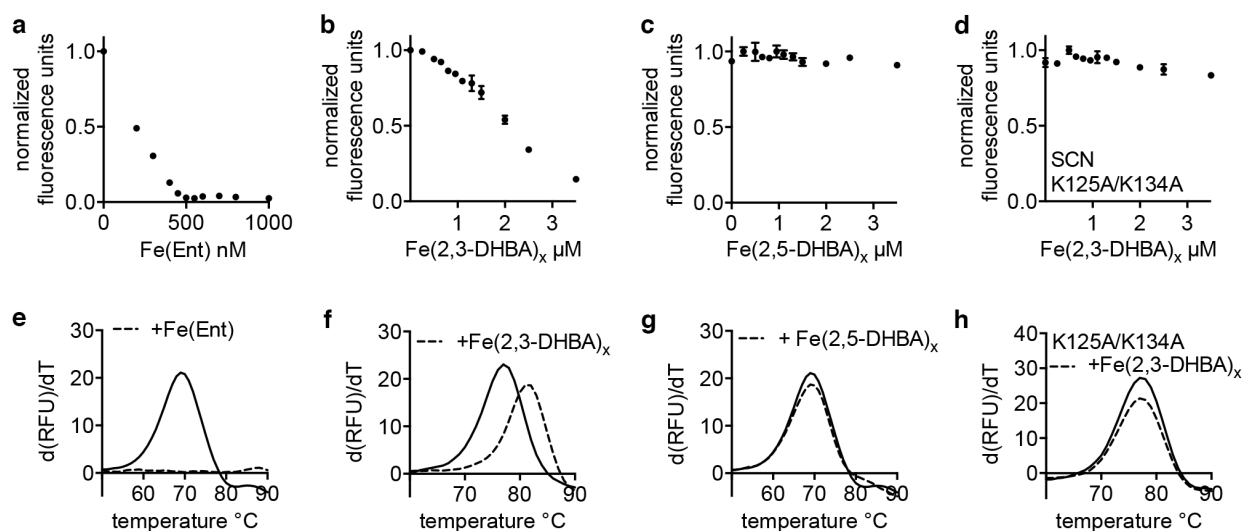


Figure 1. Differential scanning fluorimetry (DSF) detects SCN-ferric complexes. Known SCN ligands enterobactin (a) and 2,3-dihydroxybenzoic acid (2,3-DHBA) (b) quench SCN's (500 nM) intrinsic tryptophan fluorescence, as established. Titration with a benzoic acid that does not bind SCN (2,5-DHBA) does not exhibit quenching (c), and neither does the SCN calyx mutant, K125A/K134A (500 nM), which is unable to bind ferric complexes (d). DSF of these complexes validates this technique's ability to detect small molecule binding to SCN. SCN (3 μM) binding produced either a notable reduction in thermal melt signal, as observed with 30 μM ferric enterobactin (e), or an increased melting temperature (T_M), such as with 30 μM ferric 2,3-DHBA (f). Consistent with the quenching results, the DSF signal is unchanged in the presence of 30 μM ferric 2,5-DHBA (g), and similarly no change is seen when SCN K125A/K134A (3 μM) is melted in the presence of ferric 2,3-DHBA (30 μM) (h).

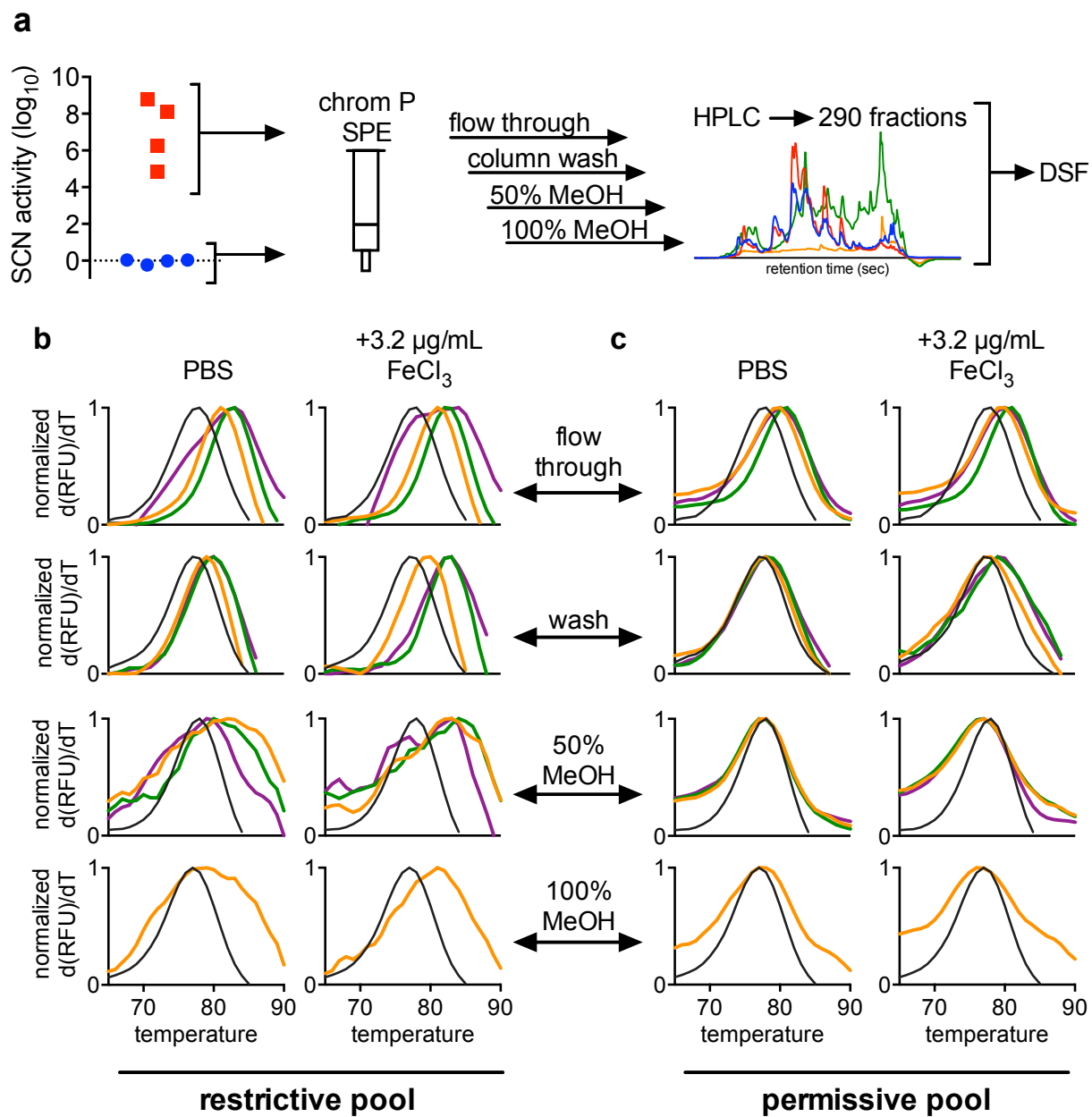


Figure 2. DSF screening reveals multiple iron-dependent SCN-binding fractions in human urine. (a) Urine fractionation scheme. Four restrictive (red squares) and four permissive (blue circles) urines were pooled and extracted before HPLC fractionation. To screen for SCN ligands, HPLC fractions (reconstituted to approximately 80-fold concentration over starting urine) were

screened both with and without iron by DSF in the presence of iron. Example melt curves from the 290 fractions are shown in **(b)** for restrictive and **(c)** for permissive. DSF identified several physiologic urine fractions, shown here, producing iron-dependent SCN binding profiles. Importantly, these effects were more pronounced in the fractions from restrictive specimens than from permissive, and showed iron-responsive changes in thermal stability.

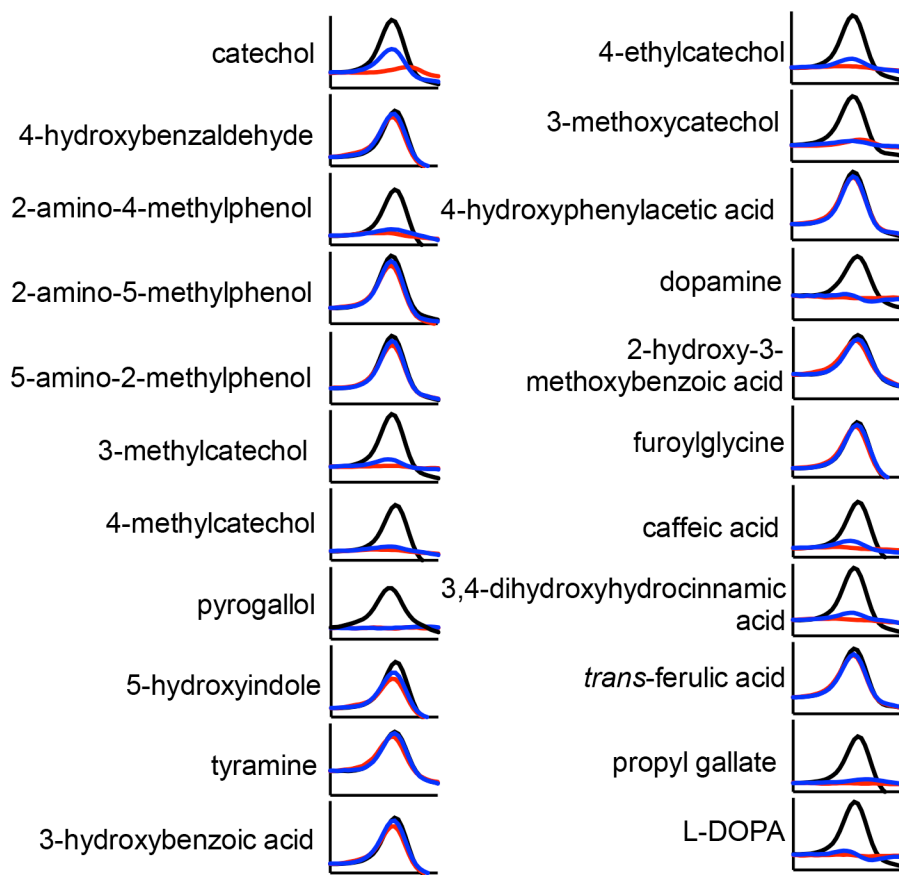


Figure 3. Urinary aryl alcohols perturb SCN thermal stability. Candidate metabolites and known SCN ligands were obtained commercially and tested for SCN binding in the presence and absence of iron. Compounds were mixed 3:1 with PBS (in blue) or FeCl₃ (in red) and added to SCN (3 μM) before measuring thermal stability by SYPRO Orange fluorescence. Plots are shown as the first derivative of the fluorescence signal (arbitrary units); black lines show SCN with buffer alone. Based on the behavior of known ligands (catechol, 3-methylcatechol) T_M shifts or signal ablation were considered positive results to be analyzed further. Of the 22 compounds tested, 10 had no impact on SCN's DSF signal; 12 showed increased thermal stability or decreased DSF signal, consistent with protein-ligand interactions. Notably, these effects were potentiated by iron with several candidates.

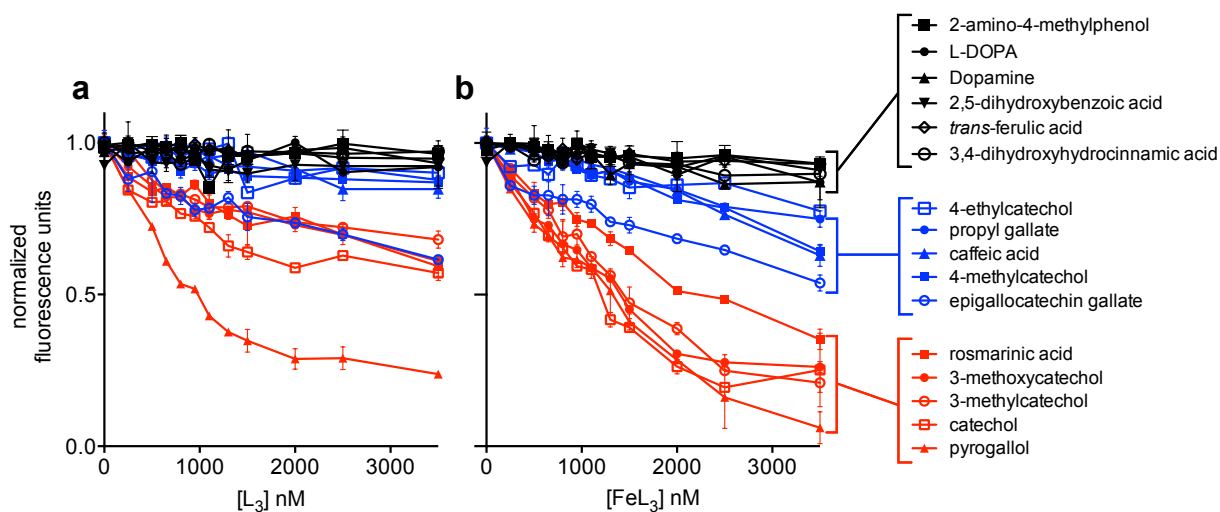


Figure 4. Direct measurement of SCN binding validates urinary ligands. SCN binding was directly observed using intrinsic tryptophan fluorescence quenching. DSF-positive candidates were added to SCN (500 nM) at a range of concentrations in the absence (**a**) or presence (**b**) of FeCl_3 at a 1:3 molar ratio to the compound. Candidate metabolites cluster into three binding groups: in black are metabolites that do not bind SCN even at large molar excess; in blue are intermediate ligands that bind moderately, and most only in the presence of added iron; in red are preferred ligands that show some binding in the absence of supplemental iron, and show the highest binding and nearly complete quenching when present in excess as ferric complexes.

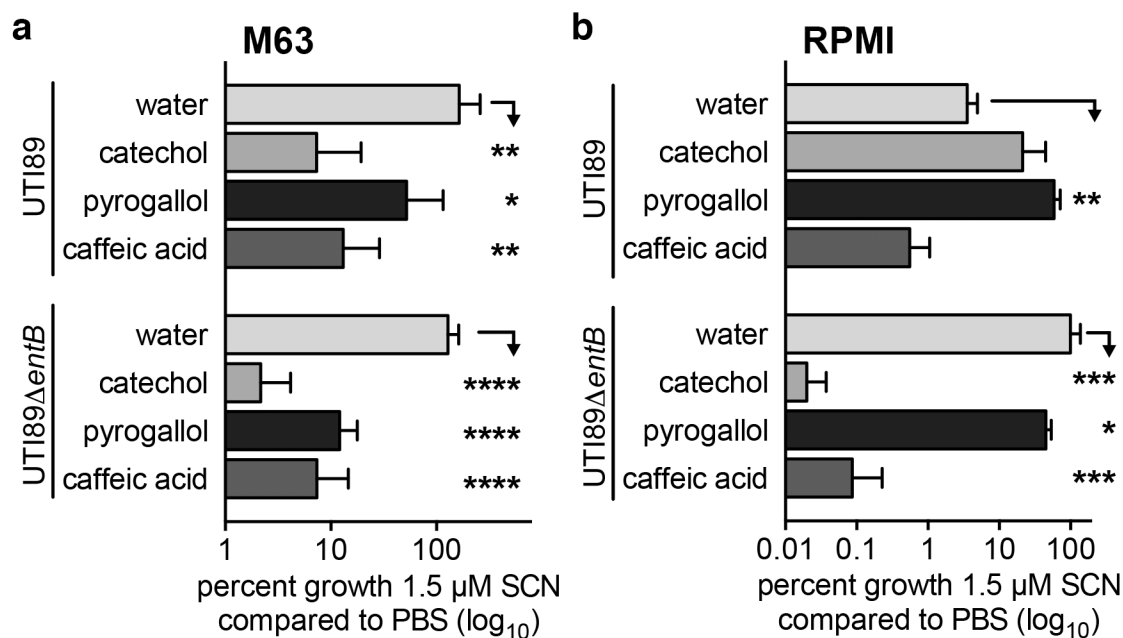


Figure 5. Candidate ligands potentiate SCN’s antimicrobial activity in defined growth media. (a) In M63 minimal media, supplementation with SCN ligands catechol, pyrogallol, or caffeic acid (5 μM) limits UPEC growth when combined with 1.5 μM SCN. Treatment with 1.5 μM SCN alone (SCN + water) does not limit UPEC growth in M63. Growth restriction is most dramatic in the enterobactin-deficient mutant, *UTI89ΔentB*. (b) In the iron-poor growth media RPMI, which is more chemically rich than M63, wild-type *UTI89* is inhibited by SCN treatment alone, likely due to enterobactin sequestration as previously published. Additional ligands have mixed effects, slightly promoting or restricting growth. In contrast to wild-type *UTI89*, enterobactin-deficient *UTI89ΔentB* is significantly inhibited by combined SCN and ligand treatment. Notably, this strain is not inhibited by SCN alone (water condition), demonstrating

that enterobactin sequestration is not part of the antimicrobial mechanism in this strain. Cultures were grown at 37°C for 20 hours and plated for cfu enumeration; bars indicate the mean \pm SD of at least three independent cultures. * $p < 0.05$; ** $p < 0.01$; *** $p < 0.001$; **** $p < 0.0001$; one-way ANOVA compared to water addition control.

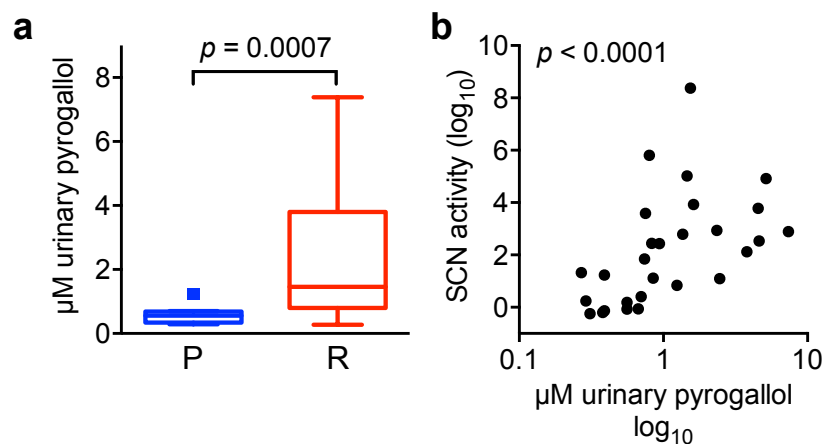


Figure 6. Pyrogallol concentrations are significantly correlated with SCN's activity. Molar concentrations of pyrogallol were measured in whole urine following urease treatment. Urines were spiked with the exometabolite 4-fluorosalicylic acid (4FSA) and peak area ratios were compared to standard curves prepared with pure standard and 4FSA. We compared permissive (P, blue boxes) and restrictive (R, red boxes) urines; pyrogallol was found to be significantly ($p = 0.0007$, Mann Whitney test) elevated in restrictive samples (a), and was also significantly ($p < 0.0001$, Spearman correlation) correlated with increasing SCN activity (b).

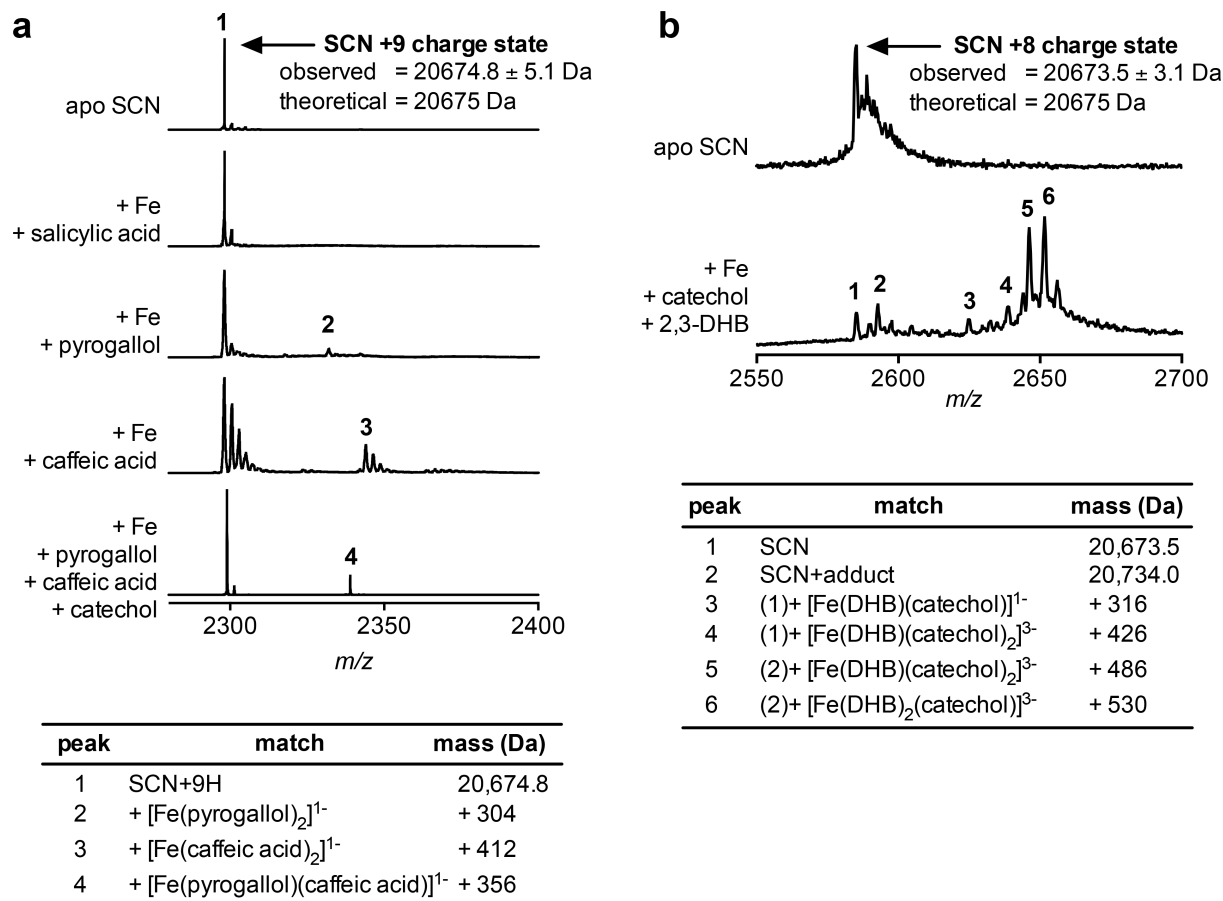
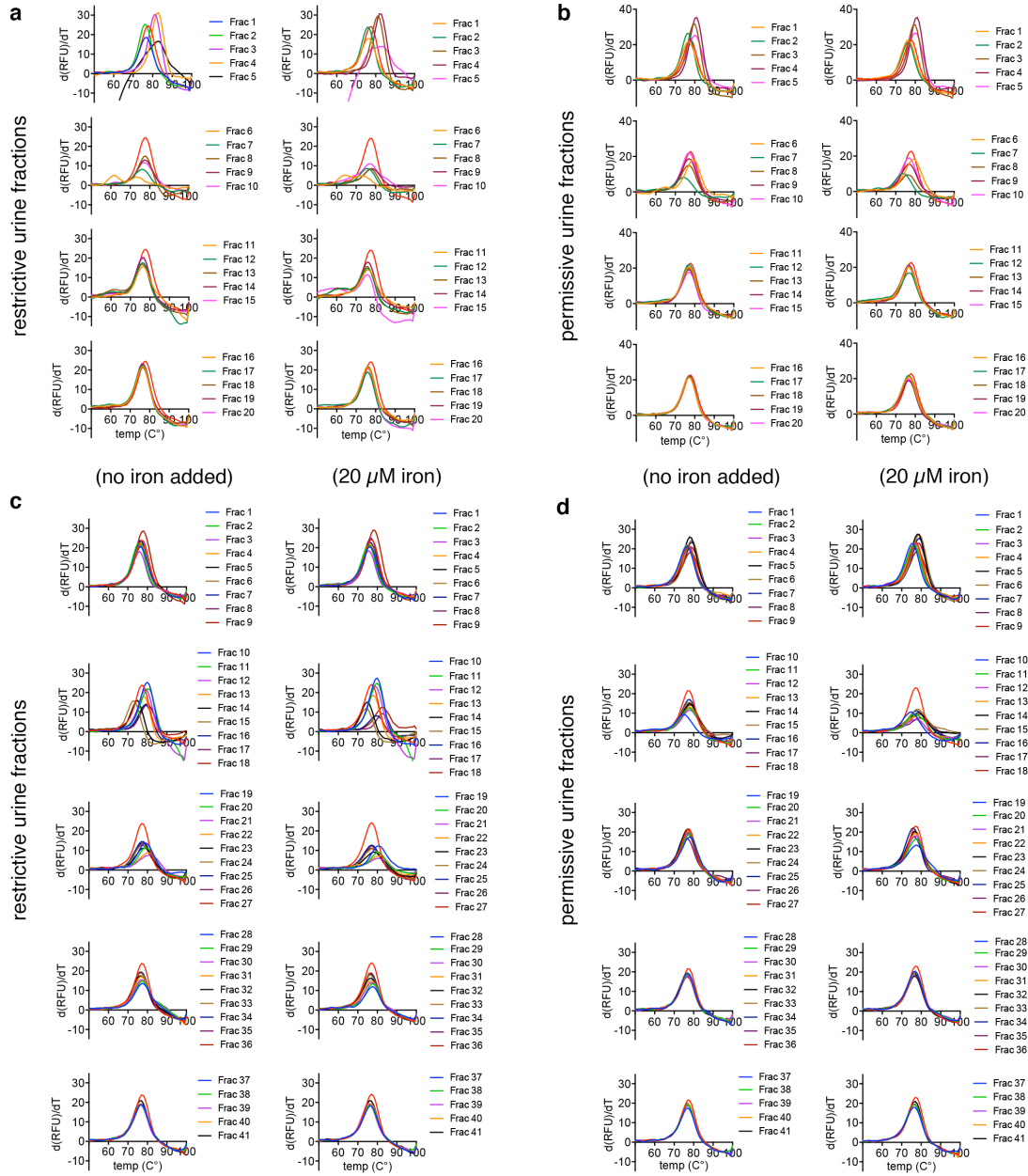
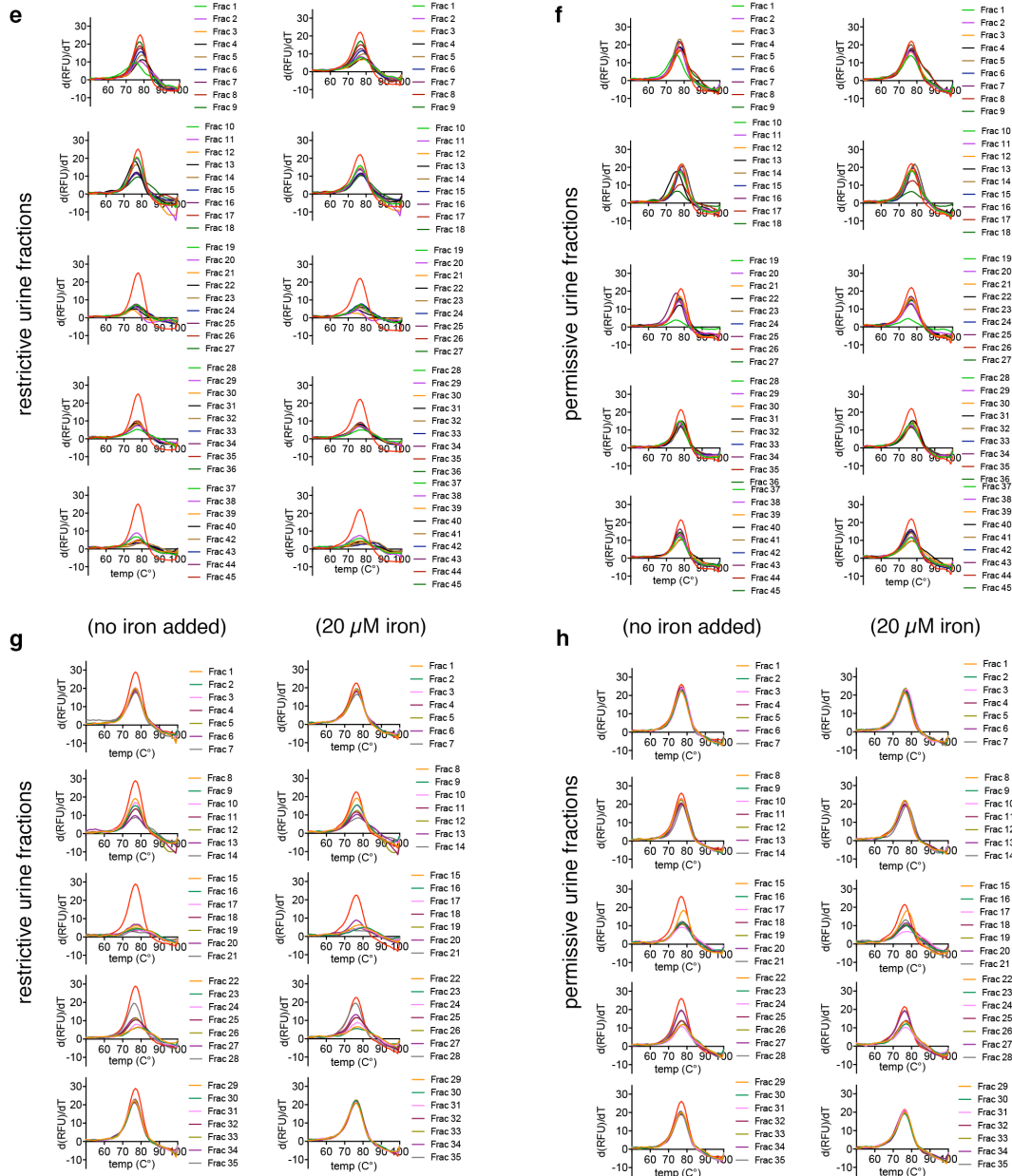


Figure 7. SCN binds heterogeneous ligand complexes. (a) Native FTICR mass spectrometry detects the +9 charge state of SCN with an observed mass of 20674.8 ± 5.1 Da (20675 Da calculated from sequence). Mixing SCN with the urinary ligand pyrogallol or with caffeic acid yields new peaks that correspond to the mass of a 2:1 ligand:iron complex (peaks 2 and 3), while a non-binding control, salicylic acid, does not result in new peaks. Incubating SCN with a mixture of three urinary ligands produces a distinct peak at a mass corresponding to a [Fe(pyrogallol)(caffeic acid)]¹⁻ complex (peak 4). (b) Native MS detects SCN's +8 charge state using nano-spray ESI coupled QTOF. The theoretical protein mass closely matches the mass

observed at 20673.5 ± 3.1 Da (top plot). A +60 secondary peak was also consistently detected. When mixed with Fe(III) and the ligands catechol and 2,3-dihydroxybenzoic acid (60 μ M, bottom plot), several mixed ligands species are detected as noted (peaks 3-6), the two most prominent of which (peaks 5 and 6) feature three non-identical ligands chelated to an iron atom. These results confirm that SCN does indeed bind heterogeneous complexes and suggests that these complexes may be preferentially bound over homogeneous complexes.

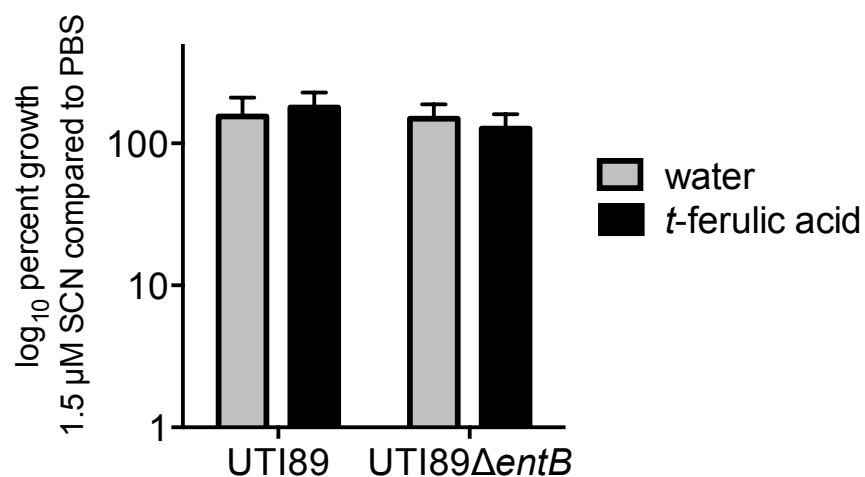
CHAPTER THREE: SUPPLEMENTARY FIGURES



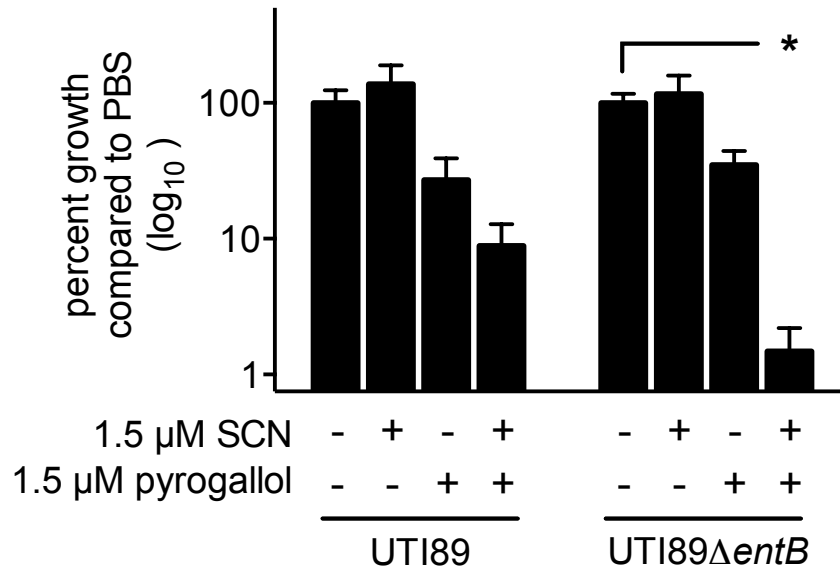


Supplementary Figure 1. DSF screen identifies fractions with SCN-binding profiles. HPLC fractions from four solid-phase elutions were individually tested for SCN binding by DSF. Fractions were reconstituted in water and mixed with 3 μM SCN in PBS with or without an additional 20 μM iron as indicated. Plots are divided into subgroups of sequential fractions for

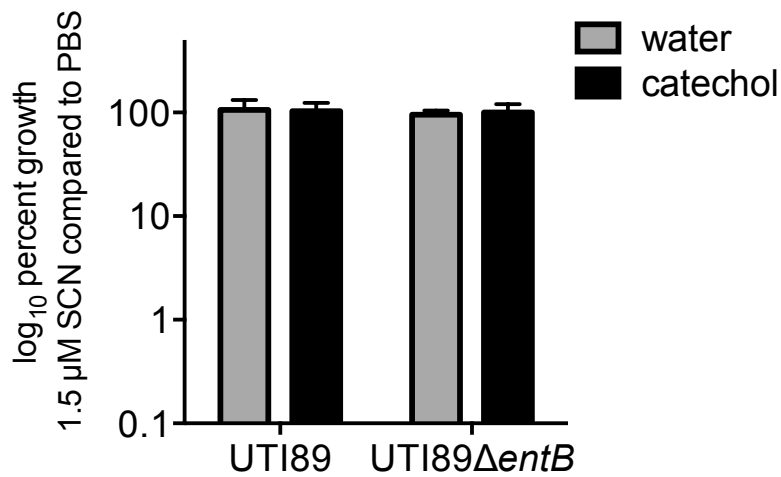
visibility. Pooled restrictive (left column of panel) or permissive (right column of panel) urines (four urines each) were fractionated over Chrom P SPE and collected as the flow-through (**a,b**), water wash (**c,d**), 50% methanol elution (**e,f**), and 100% methanol elution (**g,h**). DSF was performed as described in the methods; plots are shown as the first derivative of the fluorescence signal. In each plot, SCN protein alone is shown as a red line for comparison.



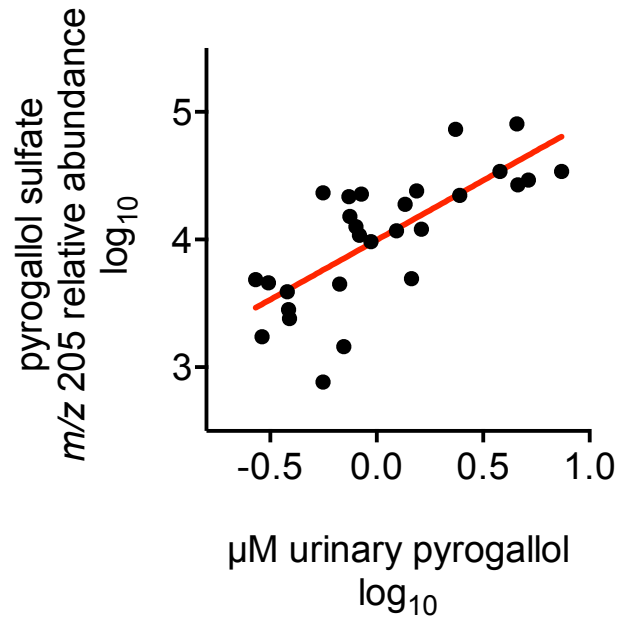
Supplementary Figure 2. A urinary metabolite that does not bind SCN also does not potentiate its antimicrobial activity in defined M63 media. UTI89 and its enterobactin-deficient mutant were grown for 20 hours with or without 5 μM t-ferulic acid, a candidate identified in the restrictive fractions but shown not to bind SCN by DSF and fluorescence quenching. Compared to PBS control, 1.5 μM SCN does not restrict bacterial growth in the presence of this metabolite. Bars represent three independent cultures, shown as mean ± S.D.



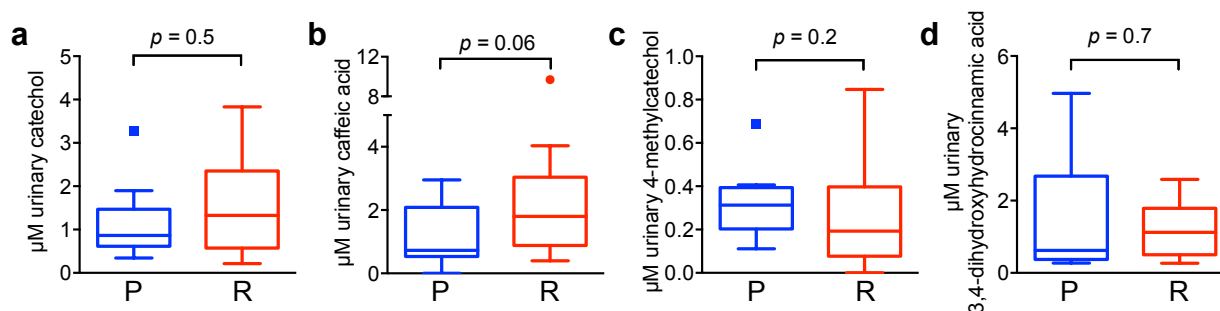
Supplementary Figure 3. Equimolar pyrogallol synergizes with SCN to restrict uropathogen growth. In M63 minimal media, 1.5 μM pyrogallol in combination with 1.5 μM SCN limits wild-type UTI89 and UTIΔentB growth compared to control PBS treatment. Media was inoculated with 10³ cfu/mL of the indicated strain and grown for 20 hours before plating for viable cfu. Bars represent the mean ± SD of three independent cultures. * $p < 0.05$, one-way ANOVA with multiple comparisons.



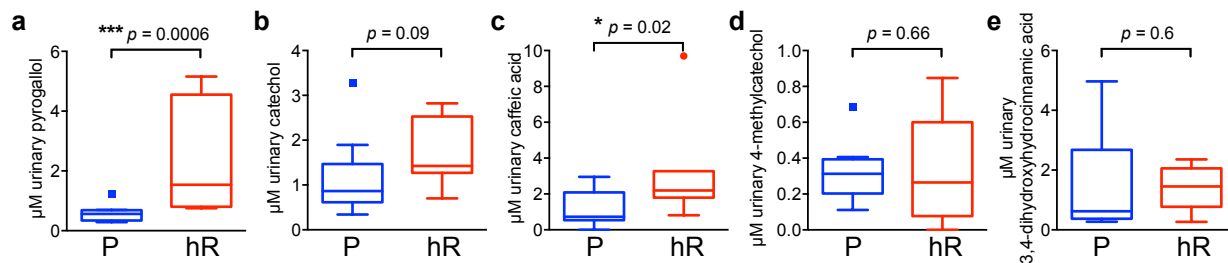
Supplementary Figure 4. Rich media (LB) does not support SCN activity, with or without supplemented catechol. UTI89 wild type and *entB* mutant were grown in rich LB media for 20 hours with 1.5 μM SCN or equivalent volume PBS (grey bars). Media was then supplemented with 5 μM catechol and re-tested for SCN activity (black bars). In contrast to the minimal media tested, LB does not support SCN's antimicrobial activity, even when supplemented with relevant catechol concentrations. Bars represent three independent cultures, shown as mean ± S.D.



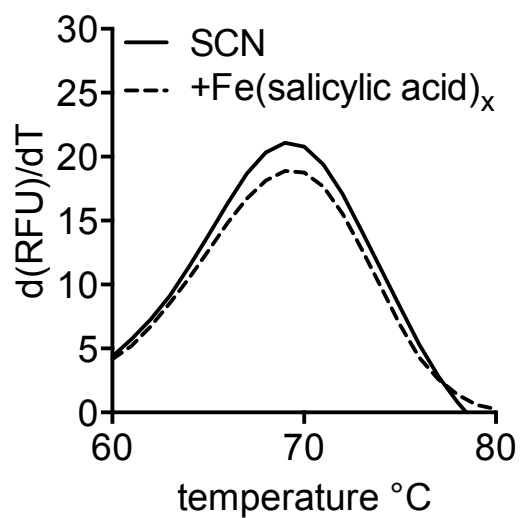
Supplementary Figure 5. Free urinary pyrogallol concentration is correlated with urinary sulfated pyrogallol. Elevated molar concentrations of pyrogallol are significantly correlated with relative abundance measured previously for sulfated pyrogallol. Data points represent data from a single donor urine specimen. $p < 0.0001$, Pearson correlation; Linear regression of log-transformed values (red line) yields $r = 0.74$ and slope = 0.9337.



Supplemental Figure 6. Urinary ligand quantification. Urinary concentrations of several free aryl alcohols were determined by GC-MS in a set of 28 healthy donor urines. Urines were spiked with 4FSA, urease treated, and derivatized for GC-MS. Ligand concentrations were determined from peak areas using standard curves developed with 4FSA for each ligand. Peak height was used for 4-methylcatechol (**c**) because of poor baseline resolution between closely neighboring peaks. Here, caffeic acid (**b**) approaches statistical significance ($p = 0.06$), while other ligands catechol (**a**), 4-methylcatechol (**c**), and 3,4-dihydroxyhydrocinnamic acid (**d**) do not appear to significantly distinguish these phenotypes in this urine set. Sets were compared for significance by the Mann Whitney test.



Supplementary Figure 7. Highly restrictive urines have improved correlation with urinary ligand concentrations. Samples with SCN activity greater than log 3 were previously identified as particularly associated with aryl metabolome signatures. We compared SCN ligand concentrations by GC-MS in highly restrictive (hR, red boxes) vs. permissive urines (P, blue boxes). Here, pyrogallol (a), catechol (b), and caffeic acid (c) more significantly distinguish highly restrictive from permissive urines, consistent with a higher aryl ligand association in these urines. (d) 4-methylcatechol and 3,4-dihydroxyhydrocinnamic acid (e) are less consistently associated with restrictive or permissive urines.



Supplementary Figure 8. Salicylic acid does not affect SCN melting in DSF. SCN was mixed with iron and salicylic acid and melted as described above. Fluorescence signal of the SYPRO dye was monitored on the HEX channel, and is plotted as the first derivative with respect to temperature.

CHAPTER THREE: TABLES

Table 1. Characteristics and parameters of pooled restrictive and permissive urines.

parameter	restrictive (mean \pm SD)	permissive (mean \pm SD)	<i>p</i> -value
age	36 \pm 9.35	34 \pm 6.73	0.7402
pH	6.87 \pm 0.24	5.74 \pm 0.61	0.0136
specific gravity	1.016 \pm 0.014	1.008 \pm 0.003	0.3033
SCN activity ^a	7.00 \pm 1.79	-0.05 \pm 0.13	0.0002

^a SCN activity is described in reference 19.

Supplementary Table 1. GC-MS metabolomics identifies candidate ligands enriched in DSF-positive fractions.

metabolite GC-MS identification	retention time	restrictive vs. permissive (approx. peak height ratio)	standard obtained
a-hydroxyphenylacetic acid	11.1	2.3	-
pyrogallol	11.9	16	yes
4-hydroxyphenylacetic acid	13.1	1.5	yes
3-hydroxyphenylacetic acid	12.7	1.3	-
3-hydroxybenzoic acid	13	1.5	yes
furoylglycine	13.4	7.7	yes
dihydroxy benzyl alcohol	13.7	R only	-
3-methoxy-4-hydroxybenzoic acid	14.5	8.9	-
3-(3-hydroxyphenyl)-3-hydroxypropanoic acid	15.5	33.1	-
3,4-dihydroxyhydrocinnamic acid	16.4	14.7	yes
caffeic acid	18.9	R only	yes
4-hydroxyhippuric acid	19.1	2.4	-
<i>t</i> -ferulic acid	17.7	11	yes
propyl gallate	17.2	16.7	yes
indole-3-acetic acid	16.6	20.3	-
methylcatechol	10	1.0	yes
5-hydroxyindole	13.3	P only	yes
4-hydroxybenzaldehyde	9.92	R only	yes

CHAPTER THREE: REFERENCES

1. Foxman, B. (2010) The epidemiology of urinary tract infection. *Nat. Rev. Urol.* **7**, 653–660
2. Hooton, T. M. (2012) Uncomplicated Urinary Tract Infection. *N. Engl. J. Med.* **366**, 1028–1037
3. Gupta, K., Hooton, T. M., and Stamm, W. E. (2001) Increasing antimicrobial resistance and the management of uncomplicated community-acquired urinary tract infections. *Ann. Intern. Med.* **135**, 41–50
4. Chen, S. L., Wu, M., Henderson, J. P., Hooton, T. M., Hibbing, M. E., Hultgren, S. J., and Gordon, J. I. (2013) Genomic diversity and fitness of *E. coli* strains recovered from the intestinal and urinary tracts of women with recurrent urinary tract infection. *Sci. Transl. Med.* **5**, 184ra60
5. Scholes, D., Hooton, T. M., Roberts, P. L., Stapleton, A. E., Gupta, K., and Stamm, W. E. (2000) Risk factors for recurrent urinary tract infection in young women. *J. Infect. Dis.* **182**, 1177–1182
6. Foxman, B., and Buxton, M. (2013) Alternative approaches to conventional treatment of acute uncomplicated urinary tract infection in women. *Curr. Infect. Dis. Rep.* **15**, 124–129
7. Hood, M. I., and Skaar, E. P. (2012) Nutritional immunity: transition metals at the pathogen-host interface. *Nat. Rev. Microbiol.* **10**, 525–537
8. Cassat, J. E., and Skaar, E. P. (2013) Iron in Infection and Immunity. *Cell Host Microbe.* **13**, 509–519
9. Cherayil, B. J. (2011) The role of iron in the immune response to bacterial infection. *Immunol. Res.* **50**, 1–9

10. Chen, S. L., Hung, C. S., Xu, J., Reigstad, C. S., Magrini, V., Sabo, A., Blasiar, D., Bieri, T., Meyer, R. R., and Ozersky, P. (2006) Identification of genes subject to positive selection in uropathogenic strains of *Escherichia coli*: a comparative genomics approach. *Proc. Natl. Acad. Sci.* **103**, 5977–5982
11. Reigstad, C. S., Hultgren, S. J., and Gordon, J. I. (2007) Functional genomic studies of uropathogenic *Escherichia coli* and host urothelial cells when intracellular bacterial communities are assembled. *J. Biol. Chem.* **282**, 21259–21267
12. Henderson, J. P., Crowley, J. R., Pinkner, J. S., Walker, J. N., Tsukayama, P., Stamm, W. E., Hooton, T. M., and Hultgren, S. J. (2009) Quantitative metabolomics reveals an epigenetic blueprint for iron acquisition in uropathogenic *Escherichia coli*. *PLoS Pathog.* **5**, e1000305
13. Chaturvedi, K. S., Hung, C. S., Crowley, J. R., Stapleton, A. E., and Henderson, J. P. (2012) The siderophore yersiniabactin binds copper to protect pathogens during infection. *Nat. Chem. Biol.* **8**, 731–736
14. Miethke, M., and Marahiel, M. A. (2007) Siderophore-based iron acquisition and pathogen control. *Microbiol. Mol. Biol. Rev.* **71**, 413–451
15. Paragas, N., Kulkarni, R., Werth, M., Schmidt-Ott, K. M., Forster, C., Deng, R., Zhang, Q., Singer, E., Klose, A. D., Shen, T. H., Francis, K. P., Ray, S., Vijayakumar, S., Seward, S., Bovino, M. E., Xu, K., Takabe, Y., Amaral, F. E., Mohan, S., Wax, R., Corbin, K., Sanna-Cherchi, S., Mori, K., Johnson, L., Nickolas, T., D’Agati, V., Lin, C.-S., Qiu, A., Al-Awqati, Q., Ratner, A. J., and Barasch, J. (2014) α -Intercalated cells defend the urinary system from bacterial infection. *J. Clin. Invest.* **124**, 2963–2976

16. Brumbaugh, A. R., Smith, S. N., Subashchandrabose, S., Himpsl, S. D., Hazen, T. H., Rasko, D. A., and Mobley, H. L. T. (2015) Blocking yersiniabactin import attenuates extraintestinal pathogenic *Escherichia coli* in cystitis and pyelonephritis and represents a novel target to prevent urinary tract infection. *Infect. Immun.* **83**, 1443–1450
17. Goetz, D. H., Holmes, M. A., Borregaard, N., Bluhm, M. E., Raymond, K. N., and Strong, R. K. (2002) The neutrophil lipocalin NGAL is a bacteriostatic agent that interferes with siderophore-mediated iron acquisition. *Mol. Cell.* **10**, 1033–1043
18. Kjeldsen, L., Bainton, D. F., Sengeløv, H., and Borregaard, N. (1994) Identification of neutrophil gelatinase-associated lipocalin as a novel matrix protein of specific granules in human neutrophils. *Blood.* **83**, 799–807
19. Shields-Cutler, R. R., Crowley, J. R., Hung, C. S., Stapleton, A. E., Aldrich, C. C., Marschall, J., and Henderson, J. P. (2015) Human Urinary Composition Controls Siderocalin's Antibacterial Activity. *J. Biol. Chem.* 10.1074/jbc.M115.645812
20. Bao, G., Clifton, M., Hoette, T. M., Mori, K., Deng, S.-X., Qiu, A., Viltard, M., Williams, D., Paragas, N., Leete, T., Kulkarni, R., Li, X., Lee, B., Kalandadze, A., Ratner, A. J., Pizarro, J. C., Schmidt-Ott, K. M., Landry, D. W., Raymond, K. N., Strong, R. K., and Barasch, J. (2010) Iron traffics in circulation bound to a siderocalin (Ngal)-catechol complex. *Nat. Chem. Biol.* **6**, 602–609
21. Van Duynhoven, J., Vaughan, E. E., Jacobs, D. M., Kemperman, R. A., van Velzen, E. J. J., Gross, G., Roger, L. C., Possemiers, S., Smilde, A. K., Doré, J., Westerhuis, J. A., and Van de Wiele, T. (2011) Metabolic fate of polyphenols in the human superorganism. *Proc. Natl. Acad. Sci. U. S. A.* **108 Suppl 1**, 4531–4538

22. Bachman, M. A., Oyler, J. E., Burns, S. H., Caza, M., Lépine, F., Dozois, C. M., and Weiser, J. N. (2011) *Klebsiella pneumoniae* yersiniabactin promotes respiratory tract infection through evasion of lipocalin 2. *Infect. Immun.* **79**, 3309–3316
23. Niesen, F. H., Berglund, H., and Vedadi, M. (2007) The use of differential scanning fluorimetry to detect ligand interactions that promote protein stability. *Nat. Protoc.* **2**, 2212–2221
24. Correnti, C., Richardson, V., Sia, A. K., Bandaranayake, A. D., Ruiz, M., Suryo Rahmanto, Y., Kovačević, Ž., Clifton, M. C., Holmes, M. A., Kaiser, B. K., Barasch, J., Raymond, K. N., Richardson, D. R., and Strong, R. K. (2012) Siderocalin/Lcn2/NGAL/24p3 does not drive apoptosis through gentisic acid mediated iron withdrawal in hematopoietic cell lines. *PloS One.* **7**, e43696
25. Chen, Z., Zheng, S., Li, L., and Jiang, H. (2014) Metabolism of flavonoids in human: a comprehensive review. *Curr. Drug Metab.* **15**, 48–61
26. Miller, R. J., Jackson, K. G., Dadd, T., Nicol, B., Dick, J. L., Mayes, A. E., Brown, A. L., and Minihane, A. M. (2012) A preliminary investigation of the impact of catechol-O-methyltransferase genotype on the absorption and metabolism of green tea catechins. *Eur. J. Nutr.* **51**, 47–55
27. Lv, H., Hung, C. S., Chaturvedi, K. S., Hooton, T. M., and Henderson, J. P. (2011) Development of an integrated metabolomic profiling approach for infectious diseases research. *Analyst.* **136**, 4752–4763

28. Andjelković, M., Van Camp, J., De Meulenaer, B., Depaemelaere, G., Socaciu, C., Verloo, M., and Verhe, R. (2006) Iron-chelation properties of phenolic acids bearing catechol and galloyl groups. *Food Chem.* **98**, 23–31
29. Gómez-Casado, C., Roth-Walter, F., Jensen-Jarolim, E., Díaz-Perales, A., and Pacios, L. F. (2013) Modeling iron-catecholates binding to NGAL protein. *J. Mol. Graph. Model.* **45C**, 111–121
30. Abergel, R. J., Moore, E. G., Strong, R. K., and Raymond, K. N. (2006) Microbial evasion of the immune system: structural modifications of enterobactin impair siderocalin recognition. *J. Am. Chem. Soc.* **128**, 10998–10999
31. Bachman, M. A., Lenio, S., Schmidt, L., Oyler, J. E., and Weiser, J. N. (2012) Interaction of lipocalin 2, transferrin, and siderophores determines the replicative niche of *Klebsiella pneumoniae* during pneumonia. *mBio*. 10.1128/mBio.00224-11
32. Holmes, M. A., Paulsene, W., Jide, X., Ratledge, C., and Strong, R. K. (2005) Siderocalin (Lcn 2) also binds carboxymycobactins, potentially defending against mycobacterial infections through iron sequestration. *Structure*. **13**, 29–41
33. Allred, B. E., Correnti, C., Clifton, M. C., Strong, R. K., and Raymond, K. N. (2013) Siderocalin Outwits the Coordination Chemistry of Vibriobactin, a Siderophore of *Vibrio cholerae*. *ACS Chem. Biol.* 10.1021/cb4002552
34. Hoette, T. M., Clifton, M. C., Zawadzka, A. M., Holmes, M. A., Strong, R. K., and Raymond, K. N. (2011) Immune interference in *Mycobacterium tuberculosis* intracellular iron acquisition through siderocalin recognition of carboxymycobactins. *ACS Chem. Biol.* **6**, 1327–1331

35. Doneanu, C. E., Strong, R. K., and Howald, W. N. (2004) Characterization of a noncovalent lipocalin complex by liquid chromatography/electrospray ionization mass spectrometry. *J. Biomol. Tech. JBT*. **15**, 208–212
36. Heck, A. J. R. (2008) Native mass spectrometry: a bridge between interactomics and structural biology. *Nat. Methods*. **5**, 927–933
37. Cui, W., Rohrs, H. W., and Gross, M. L. (2011) Top-down mass spectrometry: recent developments, applications and perspectives. *The Analyst*. **136**, 3854–3864
38. Ruotolo, B. T., and Robinson, C. V. (2006) Aspects of native proteins are retained in vacuum. *Curr. Opin. Chem. Biol.* **10**, 402–408
39. Raymond, K. N., Dertz, E. A., and Kim, S. S. (2003) Enterobactin: an archetype for microbial iron transport. *Proc. Natl. Acad. Sci. U. S. A.* **100**, 3584–3588
40. Lee, W.-J., and Hase, K. (2014) Gut microbiota-generated metabolites in animal health and disease. *Nat. Chem. Biol.* **10**, 416–424
41. Dorrestein, P. C., Mazmanian, S. K., and Knight, R. (2014) Finding the Missing Links among Metabolites, Microbes, and the Host. *Immunity*. **40**, 824–832
42. Lopez, C. A., Kingsbury, D. D., Velazquez, E. M., and Bäumler, A. J. (2014) Collateral Damage: Microbiota-Derived Metabolites and Immune Function in the Antibiotic Era. *Cell Host Microbe*. **16**, 156–163
43. Li, C., and Chan, Y. R. (2011) Lipocalin 2 regulation and its complex role in inflammation and cancer. *Cytokine*. **56**, 435–441
44. Zhao, H., Konishi, A., Fujita, Y., Yagi, M., Ohata, K., Aoshi, T., Itagaki, S., Sato, S., Narita, H., Abdelgelil, N. H., Inoue, M., Culleton, R., Kaneko, O., Nakagawa, A., Horii, T.,

- Akira, S., Ishii, K. J., and Coban, C. (2012) Lipocalin 2 Bolsters Innate and Adaptive Immune Responses to Blood-Stage Malaria Infection by Reinforcing Host Iron Metabolism. *Cell Host Microbe*. **12**, 705–716
45. Yang, J., Goetz, D., Li, J. Y., Wang, W., Mori, K., Setlik, D., Du, T., Erdjument-Bromage, H., Tempst, P., Strong, R., and Barasch, J. (2002) An iron delivery pathway mediated by a lipocalin. *Mol. Cell*. **10**, 1045–1056
46. Paragas, N., Qiu, A., Hollmen, M., Nickolas, T. L., Devarajan, P., and Barasch, J. (2012) NGAL-Siderocalin in kidney disease. *Biochim. Biophys. Acta*. **1823**, 1451–1458
47. Friedl, A., Stoesz, S. P., Buckley, P., and Gould, M. N. (1999) Neutrophil gelatinase-associated lipocalin in normal and neoplastic human tissues. Cell type-specific pattern of expression. *Histochem. J*. **31**, 433–441
48. Schmidt-Ott, K. M., Mori, K., Kalandadze, A., Li, J.-Y., Paragas, N., Nicholas, T., Devarajan, P., and Barasch, J. (2006) Neutrophil gelatinase-associated lipocalin-mediated iron traffic in kidney epithelia. *Curr. Opin. Nephrol. Hypertens*. **15**, 442–449
49. Martineau, A. R., Newton, S. M., Wilkinson, K. A., Kampmann, B., Hall, B. M., Nawroly, N., Packe, G. E., Davidson, R. N., Griffiths, C. J., and Wilkinson, R. J. (2007) Neutrophil-mediated innate immune resistance to mycobacteria. *J. Clin. Invest*. **117**, 1988–1994
50. Abergel, R. J., Warner, J. A., Shuh, D. K., and Raymond, K. N. (2006) Enterobactin Protonation and Iron Release: Structural Characterization of the Salicylate Coordination Shift in Ferric Enterobactin1. *J. Am. Chem. Soc*. **128**, 8920–8931
51. Stalmach, A., Mullen, W., Barron, D., Uchida, K., Yokota, T., Cavin, C., Steiling, H., Williamson, G., and Crozier, A. (2009) Metabolite profiling of hydroxycinnamate

- derivatives in plasma and urine after the ingestion of coffee by humans: identification of biomarkers of coffee consumption. *Drug Metab. Dispos. Biol. Fate Chem.* **37**, 1749–1758
52. Pérez-Jiménez, J., Hubert, J., Hooper, L., Cassidy, A., Manach, C., Williamson, G., and Scalbert, A. (2010) Urinary Metabolites as Biomarkers of Polyphenol Intake in Humans: A Systematic Review. *Am. J. Clin. Nutr.* **92**, 801–809
53. Gonthier, M.-P., Cheynier, V., Donovan, J. L., Manach, C., Morand, C., Mila, I., Lapierre, C., Rémésy, C., and Scalbert, A. (2003) Microbial Aromatic Acid Metabolites Formed in the Gut Account for a Major Fraction of the Polyphenols Excreted in Urine of Rats Fed Red Wine Polyphenols. *J. Nutr.* **133**, 461–467
54. Barbosa-Cesnik, C., Brown, M. B., Buxton, M., Zhang, L., DeBusscher, J., and Foxman, B. (2011) Cranberry juice fails to prevent recurrent urinary tract infection: results from a randomized placebo-controlled trial. *Clin. Infect. Dis. Off. Publ. Infect. Dis. Soc. Am.* **52**, 23–30
55. Vasileiou, I., Katsargyris, A., Theocharis, S., and Giaginis, C. (2013) Current clinical status on the preventive effects of cranberry consumption against urinary tract infections. *Nutr. Res. N. Y. N.* **33**, 595–607
56. Gonthier, M.-P., Verny, M.-A., Besson, C., Rémésy, C., and Scalbert, A. (2003) Chlorogenic Acid Bioavailability Largely Depends on Its Metabolism by the Gut Microflora in Rats. *J. Nutr.* **133**, 1853–1859

CHAPTER FOUR

Conclusions, Implications, and Prospects

4.1 Summary of the Thesis

This thesis describes how *Escherichia coli* urinary tract colonization is influenced by urine composition. During urinary tract infection (UTI), uropathogens and host cells modify urine and urine-exposed bladder surfaces with metal binding siderophores and the soluble siderophore-binding protein siderocalin (SCN), respectively (1–3). We investigated these agents' effects on uropathogenic *E. coli* (UPEC) growth in individual urine specimens from a healthy reference population. In a subgroup of individuals, we observed enterobactin expression to be a key factor permitting UPEC growth in SCN-supplemented human urine. Because SCN neutralizes enterobactin in non-urinary experimental systems, this result speaks to a distinctive role for urine-specific components. To determine the mechanism behind these individual differences, we compared individual specimens using microbiological and biochemical techniques. This multifaceted approach resolved a metabolomic signature associated with SCN antimicrobial activity, highlighting aryl alcohols and catecholates in the context of relatively alkaline urine pH. We further demonstrated that these catecholate urinary metabolites (Fig. 1a,b) participate in iron sequestration by acting as ferric cofactors of SCN (Fig. 1c). Biophysical screens on human specimens identified urine fractions enriched in certain catecholate ligands that were correlated with increased antimicrobial SCN activity. We then used quantitative mass spectrometry to determine the identity and concentrations of key metabolites responsible for the observed antimicrobial activity, and demonstrated that these cofactors could promote SCN activity when added to an iron-limited defined media condition.

These results support a model in which the urinary metabolome is able to control urinary tract colonization by pathogens, as summarized in Figure 2. Diet-derived factors (Fig. 2a) include metabolites (Fig. 2b) that can chelate iron in the urine (Fig. 2c). During UTI, SCN is elevated in the urine (Fig. 2b) and sequesters iron in ferric complexes with catecholate urinary ligands (Fig. 2d). These interactions prevent iron acquisition by UPEC, which require the siderophore enterobactin to efficiently obtain iron and grow (Fig. 2e). SCN's activity can also therefore be potentiated using drugs that block enterobactin biosynthesis, such as 2,3-DHB-AMS (Fig. 2e) (1). The human metabolome may thus represent an unappreciated contributor to UTI susceptibility and pathogen evolution. Overall, this work suggests dietary and physiologic determinants of UTI susceptibility in human populations.

4.2 Therapeutic Implications and Prospects

Since adult females experience UTI at much greater frequency than males (4), we hypothesized that perhaps female urine would be more permissive for UPEC growth (1). Categorically, a slight majority of female urines were permissive (65%) while male urines were equally distributed between permissive and restrictive, though this difference was not statistically significant. To test whether the degree of inhibition was correlated with sex, we compared the SCN activity of male restrictive vs. female restrictive urines (1). Male urine was indeed more restrictive than female ($p = 0.0405$, Fig. 3), though due to the small sample numbers (12 male, 9 female), this warrants evaluation on a larger data set. This trend is consistent with UTI's adult female predilection, and if validated more broadly, poses interesting and unexplored hypotheses about basic susceptibility differences. While the female anatomy is generally blamed for women's increased UTI

frequency (4, 5), sex-linked patterns in urinary composition would be a useful, but currently unappreciated factor for providers and patients alike: while anatomy is biologically rigid and intractable, urinary chemistry manipulations, as this thesis has suggested, are readily achievable and could represent a promising paradigmatic focus for future UTI control.

The aryl alcohol metabolites identified by these studies are known byproducts of human and commensal metabolism, derived largely from dietary plant sources such as berries, tea, and coffee (6–10). This raises an interesting question about the efficacy of cranberry products in popular use for preventing UTI. The literature on cranberries and UTI is vast, and although some studies show small protective effects, a recent meta-analysis concluded there was little to no evidence that cranberry products prevent community-acquired UTI (11). A recent double blind and placebo-controlled study in the USA showed no reduction in recurrent UTI in the cranberry patient group (12), while in a separate study, cranberry capsules significantly reduced the rate of UTI following elective gynecologic surgery (13).

This thesis, however, suggests alternative interpretations and directions for these studies. First, our results show that individual variability dominates antimicrobial responses in the urine; because of this, conclusions across an uncontrolled cohort will be inherently challenging. Second, while metabolites derived from cranberry consumption may be relevant and capable of restricting iron, as suggested by *in vitro* studies (14, 15), consuming effective quantities of cranberry juice also may lower the urinary pH. We have shown that acidic pH prevents cofactor-

mediated iron sequestration by SCN (1). Pairing cranberry, or other phenolic-rich dietary supplements, with urinary alkalinizing agents may enhance their protective effect.

Third, these cranberry products, much like antibiotics, may also be selecting for particular pathogens, as discussed below. Barbosa-Cesnick *et al.* tracked the bacterial species causing the index and recurrent UTI cases in their cohort, and although cranberry products did not reduce the frequency of recurrent UTI, the pathogen profile was slightly altered, in regard to the frequency of Enterobacteriaceae (12). Work in this thesis suggests that enterobactin is uniquely suited to acquiring iron in urines with a *restrictive* composition (1). If the etiologic species presented by the authors are divided into enterobactin-producers and non-producers (Table 1), a Fisher's exact test concludes that recurrent infections in the cranberry cohort are significantly associated with enterobactin producers vs. non-producers ($p = 0.02$); this association was not present at enrollment ($p = 0.45$). This correlation is consistent with the results of this thesis, and further argues for targeting enterobactin biosynthesis as part of an individualized UTI prophylactic regimen.

While many of the metabolites identified in this thesis may begin as plant-derived compounds, the process by which they are catabolized before being excreted in the urine could very well play an important role in UTI control. Microorganisms in the human intestine may extensively metabolize polyphenolic precursors, and studies in germ-free mice have shown significantly reduced aryl sulfate complexity in the absence of a conventional gut microbiome (7, 16, 17). One might therefore reasonably hypothesize that dietary control alone will not produce uniform

results in a heterogeneous cohort. Known variations in the activity and expression of metabolite-modifying enzymes such as human liver sulfotransferases and catechol-O-methyltransferases could also impact aryl metabolite conjugation and speciation in the urine (18–21). Although causal evidence linking specific microbes or specific genetic traits with urinary metabolites is sparse, microbiome and human genome studies indicate that such connections in human metabolism may one day be feasible (7, 16, 22–24). Extending these discoveries to the clinic could manifest as an individualized therapy involving particular diet and microbial manipulations as necessary to support a restrictive urinary environment. Metabolomic correlations, such as those presented in this thesis, also provide an example of how relatively rapid mass spectrometry analyses could identify patients who could benefit from this therapy, and may guide efforts to sustain unfavorable (i.e. restrictive) growth conditions in individuals prone to recurrent UTI. Understanding the restrictive mechanism in humans more completely will further aid our ability to predict susceptibility and outcomes in UTI, and provide a biochemical roadmap to support potential clinically relevant interventions based on controlling urinary composition.

4.3 Perspectives on *E. coli* Iron Acquisition in Human Urine

The data presented in this thesis also present a curious and unique role for the conserved siderophore enterobactin in resisting SCN inhibition during urinary growth. The previous dogma surrounding SCN and enterobactin was that the former made the latter essentially useless to the pathogen, thus motivating pathogen evolution towards additional “stealth” siderophores (25–27). Our model does not exclude this arrangement in other infection contexts, including other urinary

tract niches. Rather, we present additional evidence that multiple siderophores are useful to pathogens because they provide tailored, distinct advantages to the diverse microenvironments encountered during infection (3, 28, 29). Our data suggest that in restrictive individuals, enterobactin biosynthesis is critical for the pathogen to acquire urinary iron in the presence of SCN (1). This provides a possible explanation for the ubiquitous expression of enterobactin observed to date in *E. coli* and *K. pneumoniae* UTI isolates (2, 30) (and unpublished data). Ongoing work is exploring the role of enterobactin and its biosynthetic precursors in UPEC pathogenesis, with a focus on *in vivo* relevance. We hypothesize that enterobactin is critical because of its superior iron affinity relative to other siderophores—particularly at elevated pH—and because its chemical likeness to the aryl metabolites may enable it to more effectively compete with the SCN cofactors for iron coordination and eventual release (31–33). It is also possible that at some point during bacterial growth, enterobactin production outmatches local SCN concentrations and thus iron sequestration by SCN no longer offers a stoichiometrically meaningful antimicrobial response.

Our findings provide support and context to existing models of the early innate immune response to *E. coli* cystitis. During early experimental murine cystitis, both host SCN and *E. coli* enterobactin biosynthetic genes are upregulated within the bladder epithelium (34–37). In this thesis we showed that SCN levels in the human urinary tract were elevated in a stereotypical uncomplicated *E. coli* cystitis population (1). The baseline urinary metabolomic profiles determined here would be present during early UTI pathogenesis. These results suggest that SCN can act against UPEC in the bladder before ascension to the kidney parenchyma or blood, which

may trigger additional responses from renal alpha intercalated cells (36). If human alpha intercalated cells acidify urine in response to bacterial products as described in mice, current results indicate that this would diminish SCN's antibacterial activity (1). Acidification could correspond to a strategic shift away from SCN to control bacterial growth or to introduce additional innate defense factors that render SCN more active at lower pH. It is also possible that acidification may be part of a preemptive response to limit the systemic acidosis associated with Gram-negative sepsis. Further observational or interventional studies may be able to reconcile these events.

Associating individual factors with disease susceptibility or therapeutic options is of considerable interest. Precision medicine has provided immeasurable benefits to the fields of cancer treatment and diagnosis (38–42), and as antibiotic options for bacterial infections become increasingly limited, patient stratification and virulence-targeted, patient-matched therapies are of ever-increasing importance (4, 43–45). UTI is the second most common reason for antibiotic prescription, and would particularly benefit from new therapies and reduced antibiotic failure rates (5). This thesis highlights the only iron acquisition pathway present in all known UPEC and urinary *Klebsiella* isolates, the siderophore enterobactin, as a virulence target that synergizes with host immunity (1). A drug similar to 2,3-DHB-AMS, which abrogates enterobactin production and potentiates SCN activity in urine (1, 46), is now attractive for controlling recurrent UTI without the extensive collateral damage to the patient's commensal microbiota typical of traditional antibiotics (47–49). Our results further suggest that dietary manipulations

and urinary alkalization may be well-tolerated, non-pharmaceutical approaches to creating a urinary environment unfavorable to bacterial colonization.

4.4 Methodology Developments and Applications

Finally, the methodologies developed in this thesis are useful and applicable in research fields well beyond UTI and bacterial pathogenesis. Our growth assay makes use of human biological specimens and allows chemical manipulations that are difficult in humans, without resorting to animal models. The viable cfu endpoint is also critical, in that it is several orders of magnitude more sensitive than optical density readings, and allows the assay to begin with a small inoculum. This likely better represents a host's encounter with a given pathogen than a super-physiological experimental bolus, as is often required to observe a phenotype in experimental murine models. These assays also enabled us to focus on differences between individuals using human specimens. Most previous studies of urinary growth were performed on pooled urine specimens or a single sample (30, 36). Investigating the natural factors that make a human host more or less susceptible to infection precludes the experimental bias of inserting non-physiologic changes such as host species, genetic, or chemical manipulations. Instead, we identified key players native to human specimens.

Human sample exploration also permitted us to develop a multi-step biophysical screen for urinary SCN ligands. Unlike previous studies (32), this approach uses human urine that is chemically fractionated to improve sensitivity and downstream mass spectrometry. This method

could be optimized for other samples such as serum, saliva, or cerebrospinal fluid to identify protein-ligand interactions, or for more robust and sensitive small molecule chemical analyses.

Mass spectrometry's role in biomedical inquiry has grown recently as metadata and multi-omics approaches become more tractable and common (50, 51). Our urinary metabolomic approach (1, 52) capitalizes on both untargeted and targeted mass spectrometry, using the former to highlight patterns that are validated by quantitative targeted analyses. By identifying chemical patterns, such as the aryl sulfates in this thesis, one is able to bootstrap protocols that amplify an instrument's analytical power (53). Those wary of conclusions drawn from untargeted, multivariate dataset can then validate results on the same platform and also by orthogonal techniques. As large datasets become more common, these reductionist validation strategies will become more critical when drawing inferences from spectral studies.

Lastly, this thesis presents a novel approach to understanding degenerate small molecule ligand binding. We hypothesized that as a non-symmetric tripartite binding site, the SCN calyx could bind mixtures of urinary ligands with varying levels of preference. This hypothesis is difficult to test by X-ray crystallography and NMR, as signals in these techniques are population averages and cannot adequately resolve heterogeneous ligand occupancy. By using non-denaturing, or native, mass spectrometry to detect the mass of non-covalent complexes (54, 55), we were able to resolve heterogeneous ferric-ligand mixtures bound to SCN, since the ligand mixtures possess unique total masses. This demonstrates for the first time that human urinary ligands can occupy the SCN calyx in an assortment of permutations. Our results suggest that these combinations

may even be the preferred ligands in a mixed environment. This discovery underlines the importance of investigating biological processes in a relevant context; our results suggest that the idiosyncratic ligand combinations possible *in vivo* are vast and biologically relevant, and highly variable between individuals. Appreciating such subtle biochemical differences that could affect human health will be necessary to fully understand and effectively address the full spectrum of human disease.

4.5 Closing Remarks

The findings in this thesis show the importance of the host biochemical context in understanding particular host-pathogen interactions. We show that urinary chemical composition varies significantly between individuals, and this has dramatic and causal effects on an important antimicrobial protein's activity (1). Compositional differences are also shown to affect the pathogen's metabolic needs, requiring the siderophore enterobactin for efficient iron acquisition in this context. These findings describe a novel relationship between the antimicrobial protein siderocalin and bacterial siderophores, distinct from that described in other infection models, further arguing for chemically distinct siderophores' environment-specific and niche-adapted roles (3, 28, 29, 56, 57). These individual differences led us to identify characteristic metabolites (Fig. 1) that control SCN's activity and can prevent uropathogen growth. Together, this thesis presents a new paradigm for pathogen iron acquisition in urine (Fig. 2), and strongly supports therapeutic urinary composition manipulation as a personalized, non-antibiotic alternative to controlling UTI incidence in susceptible populations. As concerns mount about an impending post-antibiotic era (58), developing truly novel antimicrobial therapies is an unequivocal public

health imperative. This thesis indicates that analyzing human specimens and observing how individuals respond to particular infections may illuminate new directions for the treatment of numerous infectious diseases.

CHAPTER FOUR: FIGURES

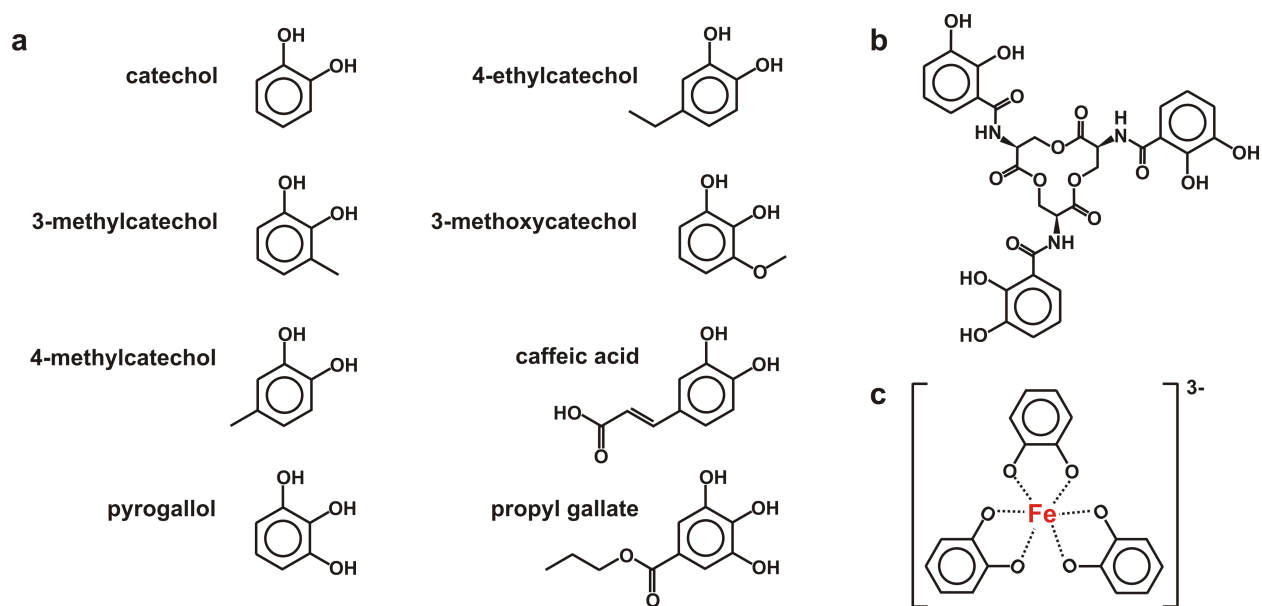


Figure 1. Aryl alcohols make up the set of SCN ligands that contribute to its antimicrobial activity in urine. (a) Highlighted urinary metabolites that bind SCN as ferric cofactors. These ligands share obvious structural similarity with each other, and with the bacterial siderophore enterobactin **(b)**. When deprotonated, the catecholate moiety is capable of coordinating an Fe(III) ion **(c)**; the resulting triscatecholate complex's negative charge, delocalized over the aromatic complex, helps make these aryl cofactors highly stable occupants of the positively charged SCN calyx.

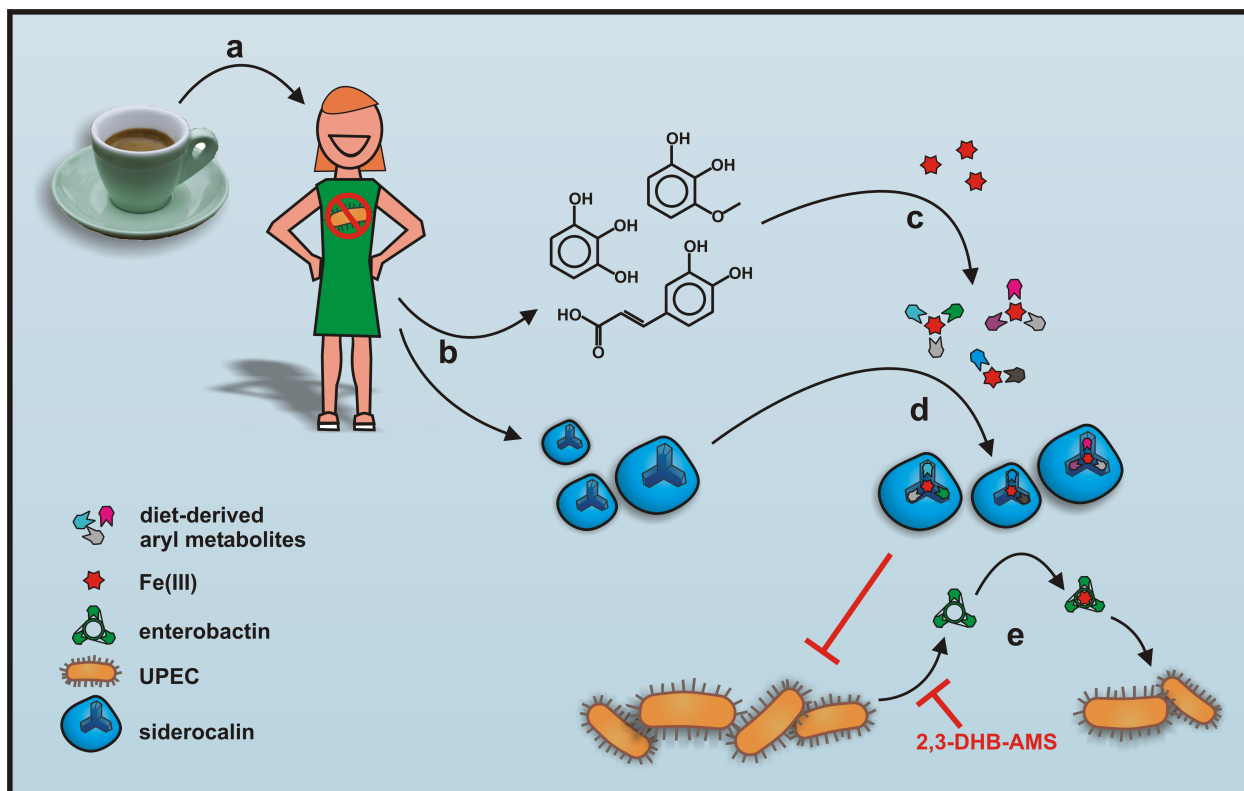


Figure 2. Diet-derived urinary metabolites promote SCN iron sequestration and antimicrobial activity. The data presented in this thesis supports a model in which consuming certain plant-based foods and beverages (a) establishes an aryl alcohol-enriched urinary metabolome (b) that is likely the product of host and microbiome metabolic processes. In the urine, certain catecholate metabolites are able to participate in iron chelation (c). When UPEC enter the bladder, upregulated SCN helps further drive pH-dependent ferric complex formation with aryl cofactors (d), aiding the immune response in restricting pathogen iron access. Our data suggests that in this infection context, the UPEC siderophore enterobactin is necessary to efficiently acquire iron (e). This demonstrates that drugs targeting enterobactin pathways (like 2,3-DHB-AMS) may be promising therapeutic leads, and may synergize with diet and pH manipulations.

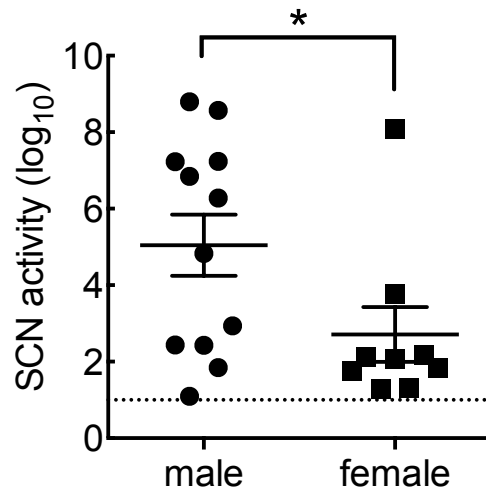


Figure 3. Among restrictive urine specimens, males exhibit higher SCN activity levels than females. SCN antimicrobial activity was measured as previously described in individual donor urine specimens. Those termed restrictive (SCN activity > 1; n = 21) were compared by the donors' reported sex. Here, males showed a significant tendency toward higher levels of SCN activity. * $p = 0.0405$, Mann-Whitney test.

CHAPTER FOUR: TABLES

Table 1. Cranberry products may select for enterobactin-producing uropathogens in patients experiencing recurrent UTI (adapted from reference 12).

	first infection ^a		first recurrence ^a	
	Ent+ strains ^b	Ent- strains	Ent+ strains	Ent- strains
cranberry	130	36	28	3
placebo	135	46	15	9

^a First infection, $p = 0.45$; first recurrence, $p = 0.02$; Fisher's exact test.

^b Enterobactin positive vs. negative based on bacterial species identified from patient urine specimens. All *E. coli* and *K. pneumoniae* isolates were assumed to produce enterobactin, consistent with published studies and the author's unpublished observations.

CHAPTER FOUR: REFERENCES

1. Shields-Cutler, R. R., Crowley, J. R., Hung, C. S., Stapleton, A. E., Aldrich, C. C., Marschall, J., and Henderson, J. P. (2015) Human Urinary Composition Controls Siderocalin's Antibacterial Activity. *J. Biol. Chem.* 10.1074/jbc.M115.645812
2. Henderson, J. P., Crowley, J. R., Pinkner, J. S., Walker, J. N., Tsukayama, P., Stamm, W. E., Hooton, T. M., and Hultgren, S. J. (2009) Quantitative metabolomics reveals an epigenetic blueprint for iron acquisition in uropathogenic *Escherichia coli*. *PLoS Pathog.* **5**, e1000305
3. Chaturvedi, K. S., Hung, C. S., Crowley, J. R., Stapleton, A. E., and Henderson, J. P. (2012) The siderophore yersiniabactin binds copper to protect pathogens during infection. *Nat. Chem. Biol.* **8**, 731–736
4. Hooton, T. M. (2012) Uncomplicated Urinary Tract Infection. *N. Engl. J. Med.* **366**, 1028–1037
5. Foxman, B. (2010) The epidemiology of urinary tract infection. *Nat. Rev. Urol.* **7**, 653–660
6. Lang, R., Mueller, C., and Hofmann, T. (2006) Development of a stable isotope dilution analysis with liquid chromatography-tandem mass spectrometry detection for the quantitative analysis of di- and trihydroxybenzenes in foods and model systems. *J. Agric. Food Chem.* **54**, 5755–5762
7. Van Duynhoven, J., Vaughan, E. E., Jacobs, D. M., Kemperman, R. A., van Velzen, E. J. J., Gross, G., Roger, L. C., Possemiers, S., Smilde, A. K., Doré, J., Westerhuis, J. A., and

- Van de Wiele, T. (2011) Metabolic fate of polyphenols in the human superorganism. *Proc. Natl. Acad. Sci. U. S. A.* **108 Suppl 1**, 4531–4538
8. Pérez-Jiménez, J., Hubert, J., Hooper, L., Cassidy, A., Manach, C., Williamson, G., and Scalbert, A. (2010) Urinary Metabolites as Biomarkers of Polyphenol Intake in Humans: A Systematic Review. *Am. J. Clin. Nutr.* **92**, 801–809
 9. Gonthier, M.-P., Cheynier, V., Donovan, J. L., Manach, C., Morand, C., Mila, I., Lapierre, C., Rémésy, C., and Scalbert, A. (2003) Microbial Aromatic Acid Metabolites Formed in the Gut Account for a Major Fraction of the Polyphenols Excreted in Urine of Rats Fed Red Wine Polyphenols. *J. Nutr.* **133**, 461–467
 10. Manach, C., Williamson, G., Morand, C., Scalbert, A., and Rémésy, C. (2005) Bioavailability and bioefficacy of polyphenols in humans. I. Review of 97 bioavailability studies. *Am. J. Clin. Nutr.* **81**, 230S–242S
 11. Vasileiou, I., Katsargyris, A., Theocharis, S., and Giaginis, C. (2013) Current clinical status on the preventive effects of cranberry consumption against urinary tract infections. *Nutr. Res. N. Y. N.* **33**, 595–607
 12. Barbosa-Cesnik, C., Brown, M. B., Buxton, M., Zhang, L., DeBusscher, J., and Foxman, B. (2011) Cranberry juice fails to prevent recurrent urinary tract infection: results from a randomized placebo-controlled trial. *Clin. Infect. Dis. Off. Publ. Infect. Dis. Soc. Am.* **52**, 23–30
 13. Foxman, B., Cronenwett, A. E. W., Spino, C., Berger, M. B., and Morgan, D. M. (2015) Cranberry juice capsules and urinary tract infection after surgery: results of a randomized trial. *Am. J. Obstet. Gynecol.* 10.1016/j.ajog.2015.04.003

14. Hidalgo, G., Ponton, A., Fatisson, J., O'May, C., Asadishad, B., Schinner, T., and Tufenkji, N. (2011) Induction of a state of iron limitation in uropathogenic *Escherichia coli* CFT073 by cranberry-derived proanthocyanidins as revealed by microarray analysis. *Appl. Environ. Microbiol.* **77**, 1532–1535
15. Lin, B., Johnson, B. J., Rubin, R. A., Malanoski, A. P., and Ligler, F. S. (2011) Iron chelation by cranberry juice and its impact on *Escherichia coli* growth. *BioFactors Oxf. Engl.* **37**, 121–130
16. Wikoff, W. R., Anfora, A. T., Liu, J., Schultz, P. G., Lesley, S. A., Peters, E. C., and Siuzdak, G. (2009) Metabolomics analysis reveals large effects of gut microflora on mammalian blood metabolites. *Proc. Natl. Acad. Sci.* **106**, 3698–3703
17. Clayton, T. A., Baker, D., Lindon, J. C., Everett, J. R., and Nicholson, J. K. (2009) Pharmacometabonomic identification of a significant host-microbiome metabolic interaction affecting human drug metabolism. *Proc. Natl. Acad. Sci. U. S. A.* **106**, 14728–14733
18. Riches, Z., Stanley, E. L., Bloomer, J. C., and Coughtrie, M. W. H. (2009) Quantitative evaluation of the expression and activity of five major sulfotransferases (SULTs) in human tissues: the SULT “pie.” *Drug Metab. Dispos. Biol. Fate Chem.* **37**, 2255–2261
19. Falany, C. N. (1997) Enzymology of human cytosolic sulfotransferases. *FASEB J.* **11**, 206–216
20. Nishimuta, H., Ohtani, H., Tsujimoto, M., Ogura, K., Hiratsuka, A., and Sawada, Y. (2007) Inhibitory effects of various beverages on human recombinant sulfotransferase isoforms SULT1A1 and SULT1A3. *Biopharm. Drug Dispos.* **28**, 491–500

21. Happonen, P., Voutilainen, S., Tuomainen, T.-P., and Salonen, J. T. (2006) Catechol-O-Methyltransferase Gene Polymorphism Modifies the Effect of Coffee Intake on Incidence of Acute Coronary Events. *PLoS ONE*. **1**, e117
22. Kemperman, R. A., Bolca, S., Roger, L. C., and Vaughan, E. E. (2010) Novel Approaches for Analysing Gut Microbes and Dietary Polyphenols: Challenges and Opportunities. *Microbiology*. **156**, 3224–3231
23. Inoue-Choi, M., Yuan, J.-M., Yang, C. S., Berg, D. J. V. D., Lee, M.-J., Gao, Y.-T., and Yu, M. C. (2010) Genetic association between the COMT genotype and urinary levels of tea polyphenols and their metabolites among daily green tea drinkers. *Int. J. Mol. Epidemiol. Genet.* **1**, 114
24. Wikoff, W. R., Nagle, M. A., Kouznetsova, V. L., Tsigelny, I. F., and Nigam, S. K. (2011) Untargeted metabolomics identifies enterobiome metabolites and putative uremic toxins as substrates of organic anion transporter 1 (Oat1). *J. Proteome Res.* **10**, 2842–2851
25. Raymond, K. N., Dertz, E. A., and Kim, S. S. (2003) Enterobactin: an archetype for microbial iron transport. *Proc. Natl. Acad. Sci. U. S. A.* **100**, 3584–3588
26. Abergel, R. J., Moore, E. G., Strong, R. K., and Raymond, K. N. (2006) Microbial evasion of the immune system: structural modifications of enterobactin impair siderocalin recognition. *J. Am. Chem. Soc.* **128**, 10998–10999
27. Sia, A. K., Allred, B. E., and Raymond, K. N. (2013) Siderocalins: Siderophore binding proteins evolved for primary pathogen host defense. *Curr. Opin. Chem. Biol.* **17**, 150–157

28. Bachman, M. A., Lenio, S., Schmidt, L., Oyler, J. E., and Weiser, J. N. (2012) Interaction of lipocalin 2, transferrin, and siderophores determines the replicative niche of *Klebsiella pneumoniae* during pneumonia. *mBio*. 10.1128/mBio.00224-11
29. Holden, V. I., and Bachman, M. A. (2015) Diverging roles of bacterial siderophores during infection. *Met. Integr. Biometal Sci.* 10.1039/c4mt00333k
30. Bachman, M. A., Oyler, J. E., Burns, S. H., Caza, M., Lépine, F., Dozois, C. M., and Weiser, J. N. (2011) *Klebsiella pneumoniae* yersiniabactin promotes respiratory tract infection through evasion of lipocalin 2. *Infect. Immun.* **79**, 3309–3316
31. Abergel, R. J., Warner, J. A., Shuh, D. K., and Raymond, K. N. (2006) Enterobactin Protonation and Iron Release: Structural Characterization of the Salicylate Coordination Shift in Ferric Enterobactin1. *J. Am. Chem. Soc.* **128**, 8920–8931
32. Bao, G., Clifton, M., Hoette, T. M., Mori, K., Deng, S.-X., Qiu, A., Viltard, M., Williams, D., Paragas, N., Leete, T., Kulkarni, R., Li, X., Lee, B., Kalandadze, A., Ratner, A. J., Pizarro, J. C., Schmidt-Ott, K. M., Landry, D. W., Raymond, K. N., Strong, R. K., and Barasch, J. (2010) Iron traffics in circulation bound to a siderocalin (Ngal)-catechol complex. *Nat. Chem. Biol.* **6**, 602–609
33. Miethke, M., and Marahiel, M. A. (2007) Siderophore-based iron acquisition and pathogen control. *Microbiol. Mol. Biol. Rev.* **71**, 413–451
34. Chen, S. L., Hung, C. S., Xu, J., Reigstad, C. S., Magrini, V., Sabo, A., Blasiar, D., Bieri, T., Meyer, R. R., and Ozersky, P. (2006) Identification of genes subject to positive selection in uropathogenic strains of *Escherichia coli*: a comparative genomics approach. *Proc. Natl. Acad. Sci.* **103**, 5977–5982

35. Reigstad, C. S., Hultgren, S. J., and Gordon, J. I. (2007) Functional genomic studies of uropathogenic *Escherichia coli* and host urothelial cells when intracellular bacterial communities are assembled. *J. Biol. Chem.* **282**, 21259–21267
36. Paragas, N., Kulkarni, R., Werth, M., Schmidt-Ott, K. M., Forster, C., Deng, R., Zhang, Q., Singer, E., Klose, A. D., Shen, T. H., Francis, K. P., Ray, S., Vijayakumar, S., Seward, S., Bovino, M. E., Xu, K., Takabe, Y., Amaral, F. E., Mohan, S., Wax, R., Corbin, K., Sanna-Cherchi, S., Mori, K., Johnson, L., Nickolas, T., D'Agati, V., Lin, C.-S., Qiu, A., Al-Awqati, Q., Ratner, A. J., and Barasch, J. (2014) α -Intercalated cells defend the urinary system from bacterial infection. *J. Clin. Invest.* **124**, 2963–2976
37. Snyder, J. A., Haugen, B. J., Buckles, E. L., Lockatell, C. V., Johnson, D. E., Donnenberg, M. S., Welch, R. A., and Mobley, H. L. T. (2004) Transcriptome of uropathogenic *Escherichia coli* during urinary tract infection. *Infect. Immun.* **72**, 6373–6381
38. Church, G. M. (2015) Precision Chemistry for Precision Medicine. *ACS Cent. Sci.* **1**, 11–13
39. Everett, J. R. (2015) Pharmacometabonomics in humans: a new tool for personalized medicine. *Pharmacogenomics*. 10.2217/pgs.15.20
40. Collins, F. S., and Varmus, H. (2015) A new initiative on precision medicine. *N. Engl. J. Med.* **372**, 793–795
41. Mirnezami, R., Nicholson, J., and Darzi, A. (2012) Preparing for precision medicine. *N. Engl. J. Med.* **366**, 489–491
42. Simonds, N. I., Khoury, M. J., Schully, S. D., Armstrong, K., Cohn, W. F., Fenstermacher, D. A., Ginsburg, G. S., Goddard, K. A. B., Knaus, W. A., Lyman, G. H., Ramsey, S. D.,

- Xu, J., and Freedman, A. N. (2013) Comparative Effectiveness Research in Cancer Genomics and Precision Medicine: Current Landscape and Future Prospects. *J. Natl. Cancer Inst.* **105**, 929–936
43. Cegelski, L., Marshall, G. R., Eldridge, G. R., and Hultgren, S. J. (2008) The biology and future prospects of antivirulence therapies. *Nat. Rev. Microbiol.* **6**, 17–27
44. Foxman, B., and Buxton, M. (2013) Alternative approaches to conventional treatment of acute uncomplicated urinary tract infection in women. *Curr. Infect. Dis. Rep.* **15**, 124–129
45. Lewis, K. (2012) Antibiotics: Recover the lost art of drug discovery. *Nature.* **485**, 439–440
46. Sikora, A. L., Wilson, D. J., Aldrich, C. C., and Blanchard, J. S. (2010) Kinetic and inhibition studies of dihydroxybenzoate-AMP ligase from *Escherichia coli*. *Biochemistry (Mosc.)*. **49**, 3648–3657
47. Lozupone, C. A., Stombaugh, J. I., Gordon, J. I., Jansson, J. K., and Knight, R. (2012) Diversity, stability and resilience of the human gut microbiota. *Nature.* **489**, 220–230
48. Dethlefsen, L., Huse, S., Sogin, M. L., and Relman, D. A. (2008) The Pervasive Effects of an Antibiotic on the Human Gut Microbiota, as Revealed by Deep 16S rRNA Sequencing. *PLoS Biol.* **6**, e280
49. Jernberg, C., Löfmark, S., Edlund, C., and Jansson, J. K. (2010) Long-term impacts of antibiotic exposure on the human intestinal microbiota. *Microbiology.* **156**, 3216–3223
50. Langley, R. J., Tsalik, E. L., Velkinburgh, J. C. van, Glickman, S. W., Rice, B. J., Wang, C., Chen, B., Carin, L., Suarez, A., Mohny, R. P., Freeman, D. H., Wang, M., You, J., Wulff, J., Thompson, J. W., Moseley, M. A., Reisinger, S., Edmonds, B. T., Grinnell, B.,

- Nelson, D. R., Dinwiddie, D. L., Miller, N. A., Saunders, C. J., Soden, S. S., Rogers, A. J., Gazourian, L., Fredenburgh, L. E., Massaro, A. F., Baron, R. M., Choi, A. M. K., Corey, G. R., Ginsburg, G. S., Cairns, C. B., Otero, R. M., Fowler, V. G., Rivers, E. P., Woods, C. W., and Kingsmore, S. F. (2013) An Integrated Clinico-Metabolomic Model Improves Prediction of Death in Sepsis. *Sci. Transl. Med.* **5**, 195ra95–195ra95
51. Vinayavekhin, N., Homan, E. A., and Saghatelian, A. (2010) Exploring Disease through Metabolomics. *ACS Chem. Biol.* **5**, 91–103
52. Lv, H., Hung, C. S., Chaturvedi, K. S., Hooton, T. M., and Henderson, J. P. (2011) Development of an integrated metabolomic profiling approach for infectious diseases research. *Analyst.* **136**, 4752–4763
53. Yi, L., Dratter, J., Wang, C., Tunge, J. A., and Desaire, H. (2006) Identification of sulfation sites of metabolites and prediction of the compounds' biological effects. *Anal. Bioanal. Chem.* **386**, 666–674
54. Heck, A. J. R. (2008) Native mass spectrometry: a bridge between interactomics and structural biology. *Nat. Methods.* **5**, 927–933
55. Cui, W., Rohrs, H. W., and Gross, M. L. (2011) Top-down mass spectrometry: recent developments, applications and perspectives. *The Analyst.* **136**, 3854–3864
56. Chaturvedi, K. S., Hung, C. S., Giblin, D. E., Urushidani, S., Austin, A. M., Dinauer, M. C., and Henderson, J. P. (2014) Cupric yersiniabactin is a virulence-associated superoxide dismutase mimic. *ACS Chem. Biol.* **9**, 551–561

57. Luo, M., Lin, H., Fischbach, M. A., Liu, D. R., Walsh, C. T., and Groves, J. T. (2006) Enzymatic Tailoring of Enterobactin Alters Membrane Partitioning and Iron Acquisition. *ACS Chem. Biol.* **1**, 29–32
58. World Health Organization (2014) *Antimicrobial Resistance: Global Report on Surveillance*, World Health Organization

APPENDIX

**Detection and expression studies on uropathogenic
Escherichia coli siderophores.**

BACKGROUND

Uropathogenic *Escherichia coli* (UPEC), the most common pathogen associated with urinary tract infections (UTIs) (1), synthesizes and secretes small molecular weight chelators called siderophores to acquire essential iron during infection (2–4). Since host innate immune factors extensively sequester available iron, siderophore expression is widely considered a critical virulence adaptation for UPEC and many other human pathogens (4–7). Evidence supporting this conclusion includes siderophore mutants' attenuated virulence in animal models, identification of biosynthesis genes under positive selection, and transcriptomic datasets showing significantly upregulated siderophore gene expression during murine infection, during growth in normal human urine *ex vivo*, and in RNA isolated from cystitis patients' urine (8–12). Specifically measuring complete siderophore production in these environments, however, requires sensitive analytical techniques even under ideal, controlled conditions. As a result, bona fide siderophore production during UTI is poorly understood.

Bacterial pathogens often possess the biosynthetic machinery to make multiple siderophores. These seemingly redundant efforts are thought to provide particular advantages in specific host contexts, and to bind metals for both nutrient acquisition and defense against host-driven toxic assaults (3, 13–15). All known UPEC isolates produce the catecholate siderophore enterobactin, and strains may also possess the pathways for salmochelin, yersiniabactin, and aerobactin (2). Because genetic assays like PCR are rapid, straightforward, and widely available, a UPEC strain's siderophore arsenal is generally assessed by the presence of one gene in each pathway (16). However, this assignment can be misleading: genotype positivity does not equivocally

predict siderophore production. A notable example is the well-studied pyelonephritis isolate CFT073, which has the common yersiniabactin marker gene *fyuA* but does not produce yersiniabactin when grown in iron-limiting media (2). To identify these discrepancies, siderophore products must be measured. Without these data, comparisons among strains and explanations for virulence may be incomplete and misrepresented.

Addressing these shortcomings requires optimization in analytical siderophore detection. Here, we describe improvements in methods for detecting the siderophores enterobactin, salmochelin, and aerobactin by liquid chromatography-mass spectrometry (LC-MS). For enterobactin and aerobactin, we present an improved MRM scheme for detecting each siderophore with greater sensitivity and specificity. These methods are then applied to demonstrate their utility in human clinical sample analysis, detecting chemical modifications, and developing true siderophore production profiles for clinical isolates. Together, these data exhibit the potential gains in knowledge from sensitive siderophore detection, and provide tools to more accurately understand host-pathogen interactions during human UTI.

EXPERIMENTAL PROCEDURES

Bacterial strains. For method development, we used the well-characterized clinical isolates UTI89 and CFT073. Cultures were grown from a single colony in LB for 4-6 hours before diluting 1:1000 into M63 minimal media and incubating at 37°C overnight. After centrifuging for 10 min at 7,700 rpm, supernatants were either filtered through 0.2 µm syringe filters, or extracted on DEAE solid phase extraction (SPE) as previously described (2).

For aerobactin screening, *iucD*-positive clinical isolates were obtained from a previous study of *E. coli* bacteriuria at Barnes Jewish Hospital in St. Louis, Missouri that is described elsewhere (17). Strains were genotyped by dot-blot hybridization at the Molecular and Clinical Epidemiology Laboratory at the School of Public Health, University of Michigan, Ann Arbor. All studies were approved by institutional review boards at Washington University School of Medicine and the University of Michigan.

Human urine specimens. Human urines specimens were collected from patients presenting to an outpatient clinic with uncomplicated *E. coli* cystitis at the University of Washington, Seattle, WA, as described elsewhere (18). Here, frozen urine specimens were thawed on ice, centrifuged, then 100 µL internal standard was added to 900 µL urine. After 0.2 µM filtration, samples were diluted 1:1 with water and promptly analyzed by LC-MS-MRM. For controls, healthy urine specimens were obtained from volunteers at Washington University School of Medicine and prepared identically. All participants provided informed consent and studies were approved by

institutional review boards at the University of Washington and Washington University School of Medicine.

Enterobactin halogenation. To test enterobactin oxidation, we used a purified components system to monitor enterobactin halogenation by LC-MS. Enterobactin was purified by HPLC from UTI89 Δ *iroA/ybtS* as described previously (18). Reagent NaOCl (Sigma) was checked for hypochlorite concentration by UV spectroscopy at $\epsilon_{292} = 350 \text{ M}^{-1}\text{cm}^{-1}$ (19). Enterobactin (500 μM) was mixed with various molar ratios of NaOCl (from 5 μM to 5mM) as indicated and incubated at 37°C for 1 hour. Reactions were analyzed by LC-MS in negative ion full scan (EMS) mode and peaks were compared to calculated masses for chlorinated enterobactin products.

Liquid chromatography-mass spectrometry. LC-MS studies were performed on a Shimadzu Prominence LC-20 XR UFLC-coupled AB Sciex QTRAP 4000 hybrid triple-quadrupole/linear ion trap instrument. Chromatography was achieved on an Ascentis Express phenyl-hexyl column (100 x 2.1 mm, 2.7 μm ; Supelco, Sigma) over a gradient of 0.1% formic acid (Fluka, Sigma) to 90% acetonitrile (EMD Millipore) + 0.1% formic acid. Full-scan experiments used the enhanced MS (EMS) mode, scanning from m/z 100 to 1400 at scan speed of 1000 Da/s. The IonSpray voltage was 4,500 V in positive mode and -4,500 V in negative mode. Curtain gas and source temperature were 10 units and 500°C, respectively. The declustering potential was set to 110 or -110 V, and collision energy was set to 5 or -5 V. Tandem MS experiments were carried out in enhanced product ion (EPI) mode using collision-activated dissociation (CAD). The declustering

potential, entrance potential, and collision exit cell potential were set to 110, 10, and 12 V, respectively (-110, -10, and -12 V for negative mode). For siderophore detection and quantification experiments, multiple reaction monitoring (MRM) methods were used to monitor transitions as detailed in Table 1. Spectra were visually evaluated and peak areas were measured with Analyst version 1.5.1 (AB Sciex).

Table 1. MRM transitions for siderophore ions in positive and negative mode.

analyte	Q1	Q3	collision energy (V)
positive mode			
linear enterobactin	688	447, 224	35
¹³ C linear enterobactin	718	467, 234	35
cyclic enterobactin	670	447, 224	35
¹³ C cyclic enterobactin	700	467, 234	35
aerobactin	565	547	35
¹³ C aerobactin	587	569	35
negative mode			
linear enterobactin	686	445, 222	-40
¹³ C linear enterobactin	716	465, 232	-40
cyclic enterobactin	668	445, 222	-40
¹³ C cyclic enterobactin	698	465, 232	-40
aerobactin	563	527, 483, 297	-25, -35, -39
¹³ C aerobactin	585	504, 381, 310	-35, -40, -39

RESULTS AND DISCUSSION

Enterobactin and salmochelin have improved signal in negative ion ESI.

Siderophore detection has largely relied on LC-MS approaches because of the siderophores' relatively large masses and the advantage of analyzing aqueous samples with minimal preparation by reverse phase chromatography-coupled instruments. For practical and technical reasons, previously published methods have used positive mode electrospray ionization (+ESI) (2, 3, 20, 21). However, preliminary work was unable to detect enterobactin or salmochelin in urine, and detection in supernatants often required chemical extraction to concentrate samples prior to analysis (unpublished observations and personal communications; Robin Shields-Cutler, Chia Hung, Jeffrey Henderson). Since technologic advances have improved sensitivity issues for which negative mode had suffered (22), and the multiple hydroxyl groups on the highly conjugated enterobactin structure would provide ample sites for deprotonation, we hypothesized that negative mode could detect enterobactin and salmochelin with greater sensitivity than positive mode.

Using an AB Sciex hybrid triple-quadrupole/linear ion trap mass spectrometer, we compared catecholate siderophore detection by positive and negative mode. Figure 1 shows the improved EMS signal for linear (Fig. 1a) and cyclic enterobactin (Fig. 1b), and salmochelin MGE (monoglucosylated enterobactin; Fig. 1c). In positive MS/MS, enterobactin and salmochelin fragmented into detectable ions for a linearized dimer and 2,3-dihydroxybenzoyl-serine monomer (2). These fragments were also produced in negative mode (data not shown), and therefore can be used in MRM methods for improved signal to noise. While enterobactin's signal

increase in full-scan -EMS appeared somewhat modest in magnitude (Fig. 1a), the difference became more prominent during MS/MS methods, in particular when analyzing siderophores in urine. In this context, negative mode MRM was far superior at detecting ^{13}C -labeled cyclic enterobactin standard (Fig. 2). These results show that negative mode ESI-LC-MS is a sensitive approach for detecting catecholate siderophores, and may be preferable for MS/MS-based studies in complex fluids.

Detecting enterobactin oxidation products by negative mode LC-MS.

During infection, host neutrophils use NADPH oxidase and myeloperoxidase (MPO) to produce hypochlorous acid (HOCl), which targets a variety of biomolecules and plays an important role in phagocytes' ability to kill pathogens (23, 24). Enterobactin, with its catecholate rings, is a plausible target for halogenation by HOCl. Since neutrophils and other phagocytes are part of the inflammatory response during UTI (25, 26), we tested whether negative mode LC-MS could detect enterobactin oxidation products *in vitro*. Purified linear enterobactin was mixed with NaOCl and incubated for 1 hour at 37°C. When mixed with a 10-fold excess of NaOCl, native enterobactin (m/z 686) signal decreased, and this treatment revealed a new peak at m/z 720, and a small peak at m/z 754-758 (Fig. 3a); these peaks match the expected masses for Cl-ent and Cl₂-ent. Treating enterobactin with increasing doses of oxidant showed a dose-dependent formation of the m/z 720 peak (Fig. 3b). Finally, the set of peaks at m/z 720-722 displayed the expected isotope distribution of a singly-chlorinated enterobactin species (Fig. 3c).

These results show that enterobactin is a potential oxidation target of neutrophils and other phagocytes during infection, and that negative ion, LC-MS is capable of detecting these products. Chlorination most likely occurs on the catechol ring in the activated C5 position, though this has not been confirmed here. Interestingly, this position is the same location that glucose is added by IroB in the salmochelin pathway. Lin and colleagues showed that a synthetic enterobactin brominated at the C5 position prevented glucosylation by IroB *in vitro* (27). While further studies are necessary to explore enterobactin oxidation *in vivo*, this may represent a serendipitous host defense. It is also unclear what effect halogenation has on enterobactin's iron affinity, its recognition by bacterial receptors like FepA, or its sequestration by the innate immune protein siderocalin. Manipulating these interactions through oxidative modifications could have significant consequences on pathogenesis in the inflamed bladder, and are worthy of further biochemical study.

Enterobactin is produced and detectable during human UTI.

To date in the literature, yersiniabactin is the only siderophore shown to be present during human UTI (3). Since the negative mode enterobactin MRM showed initial promise in urine specimens, we wanted to know whether we could detect enterobactin in clinical UTI urine specimens. Recent analyses on RNA preserved from human UTI specimens showed significantly upregulated enterobactin pathway gene expression (9, 10), but it was unclear whether the enterobactin product would be stable and abundant to enable detection in frozen urine supernatants. Using the negative mode MRM as described above with ¹³C-labeled internal standard, we indeed detected linear and cyclic enterobactin in cystitis patient urine (Fig. 4a). Of

the 15 specimens analyzed, 12 had detectable levels of cyclic and/or linear enterobactin (Fig. 4b). These samples were processed without additional concentration, so it is possible that with chemical extraction, enterobactin might be detectable in the other three specimens as well.

This finding shows, for the first time, direct evidence that enterobactin is produced at detectable levels in urine during human UTI. Further studies using calibrated standards could quantify the enterobactin present. Enterobactin has recently been highlighted as a key UPEC factor allowing urinary growth in the presence of SCN (18). If enterobactin concentrations greatly exceed those of SCN in urine, that could provide one explanation for this siderophore's importance during UTI. Since this siderophore is the only UPEC siderophore produced by all known UPEC isolates (2, 4) (unpublished data), detection across a range of clinical samples shows that this product is indeed synthesized and could play an important role in iron acquisition during human disease.

Optimized aerobactin detection by LC-MS.

Aerobactin is a linear siderophore synthesized from citrate and lysine, and has been correlated with virulent and often invasive Gram-negative infections (28–30). Typical siderophore preparations in our lab have used anion exchange on iron-treated minimal media supernatants, but aerobactin signal was often very low compared to yersiniabactin or enterobactin. Indeed, internal standards often contained too little or barely enough ¹³C-aerobactin signal for peak area comparisons by this method (unpublished observations). We tested aerobactin detection from the pyelonephritis strain CFT073, using filtered supernatants without prior anion exchange, and

found that this approach, combined with negative mode LC-MS-MRM, yielded superior sensitivity (Fig. 5a).

However, higher aerobactin signal brought to our attention a problem: samples without ^{13}C aerobactin had measurable MRM signal at the ^{13}C -labeled aerobactin transition (Fig. 5b). This co-fragmenting peak could confound quantitative isotope ratios by artificially inflating the ^{13}C -aerobactin peak area. Because the difference in mass to the isotope-labeled version is 22 Da, we hypothesized this represented a persistent sodium adduct that was not dissociated during MS/MS. Using negative mode EPI, we then fragmented ^{12}C and ^{13}C aerobactin under higher collision energies to identify unique transitions without overlapping masses (Fig 5c). From this, we identified several transitions for negative mode LC-MS-MRM that offer sensitive and now specific detection of ^{12}C - or ^{13}C -aerobactin in bacterial supernatants. While the transition m/z 563 > 527 offers the greatest sensitivity for ^{12}C -aerobactin (Fig. 5d), for the most consistent comparison to internal standard, the transition pairs m/z 563 > 297 and m/z 585 > 310 for ^{12}C and ^{13}C aerobactin, respectively, represent the same molecular fragmentation. As a demonstration, when unlabeled and ^{13}C -labeled CFT073 supernatants are mixed 1:1, these two transitions yield identical signals on LC-MS-MRM (Fig 5d).

Aerobactin expression patterns revealed by LC-MS.

To study aerobactin expression by UTI clinical isolates, we prepared minimal media supernatants from 70 isolates that had previously tested positive for the aerobactin biosynthesis gene *iucD* (17). Initial siderophore screens were carried out using the prior MRM method in

positive mode (Fig. 6a). These screens also showed that enterobactin was produced by 70/70 strains (100%) and yersiniabactin by 60/70 (86%). However, because of positive mode's limitations, aerobactin was poorly detected in a large subset of samples. We therefore used the improved negative mode MRM described above to re-evaluate these strains.

Negative mode MRM provides sensitive detection with low background, which aided aerobactin quantification in these repeated *iucD*⁺ strains. Here, expression data naturally groups strains into three categories of moderate, low, and no aerobactin production—as defined by the positive control CFT073 and the negative control CFT073 Δ *iucD* (Fig. 6b). Interestingly, these data reveal a subset of *iucD*⁺ isolates which produce no aerobactin under iron limiting conditions. Of the 70 *iucD*⁺ strains assessed, 15 (21%) produced no detectable aerobactin by negative or positive mode MRM. These strains may represent siderophore “cheaters,” strains that possess the machinery to use certain siderophores without expending the energy required for *de novo* synthesis. The large proportion of discordant strains also cautions against using genotype data to draw conclusions about siderophore expression (16).

In summary, these methodology pursuits have established new standard protocols for sensitive siderophore detection in the laboratory. As demonstrated here, they are suitable for applications ranging from biological product discovery to clinical sample investigation. Further work could aim to improve sample preparation or chromatography and continue to reduce the limits of detection. Together, they allow a greater understanding of the molecular mechanisms that determine pathogen iron acquisition during UTI.

ACKNOWLEDGEMENTS

Connelly Miller contributed significantly to the aerobactin studies, especially in sample preparation and analysis for the sizable clinical isolate screen. We would also like to thank Jonas Marschall and Chia Hung for collecting and organizing the clinical isolates in these studies. Jan Crowley provided technical advice for mass spectrometry methods.

APPENDIX: FIGURES

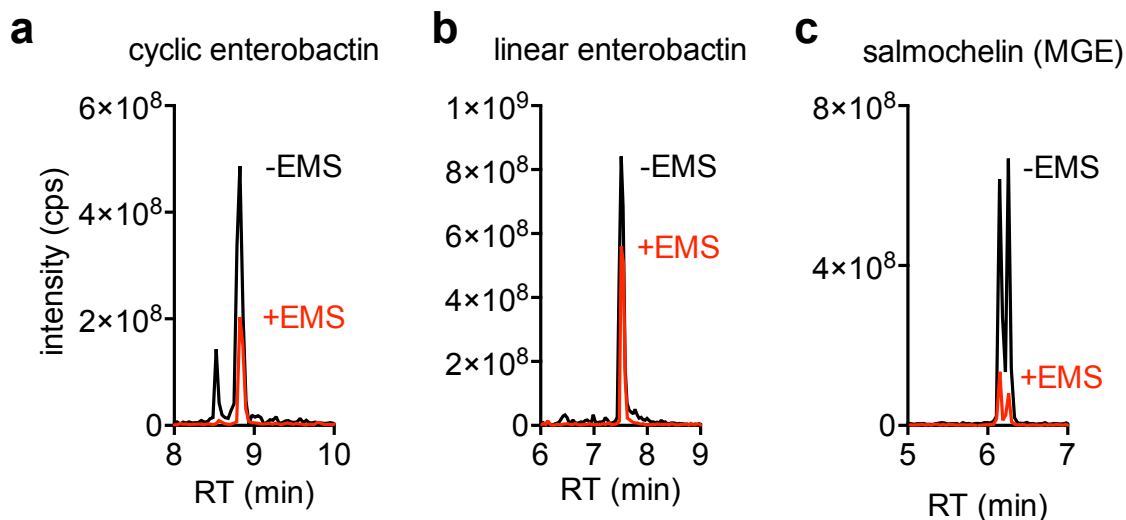


Figure 1. Negative mode LC-MS shows improved catechol siderophore signal. LC-MS was carried out in Positive and negative ion full-scan EMS with identical HPLC parameters. Shown are extracted ion chromatograms at the expected negative (-EMS) and positive (+EMS) ion masses for cyclic enterobactin (a), linear enterobactin (b), and the monoglucosylated salmochelin (c). The two salmochelin peaks result from different glucose locations along the linearized molecule (data not shown). Siderophores were HPLC purified from supernatants of UTI89 grown overnight in M63 minimal media.

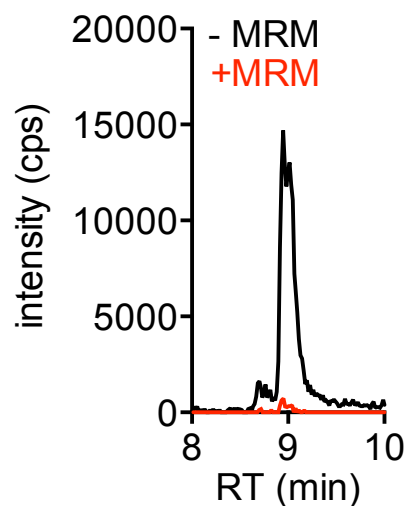


Figure 2. Negative mode LC-MS-MRM detects cyclic enterobactin standards in urine. Filtered human urine from a single donor was spiked with ^{13}C -labeled internal standard, diluted 1:1 with water, and analyzed by LC-MS-MRM in positive (red) and negative (black) mode. The MS/MS transitions monitored the same enterobactin fragmentation pattern, but negative mode yielded superior detection compared to positive mode.

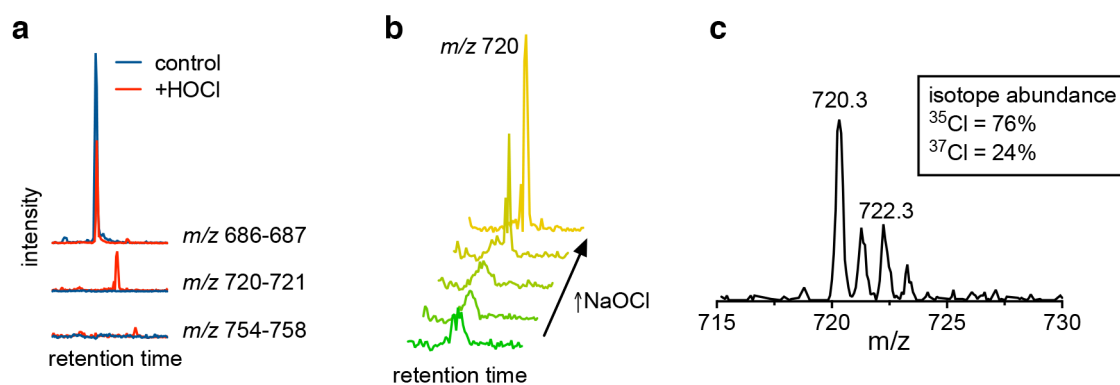


Figure 3. Enterobactin is sensitive to halogenation *in vitro*. (a) Purified linear enterobactin (500 μM) was mixed with water (blue) or 5 mM NaOCl (red) and incubated for 1 hour at 37°C. Traces are extracted ion chromatograms from negative mode EMS for the expected m/z ranges indicated: top, linear enterobactin; middle, monochloro-enterobactin; bottom, dichloro-enterobactin. (b) Enterobactin (500 μM) was mixed with increasing concentrations (from bottom, 0, 5, 50, 500, 5000 mM) of NaOCl and incubated and detected as before. (c) Mass spectrum of the suspected monochloro-enterobactin species is consistent with chlorine's natural isotope abundance.

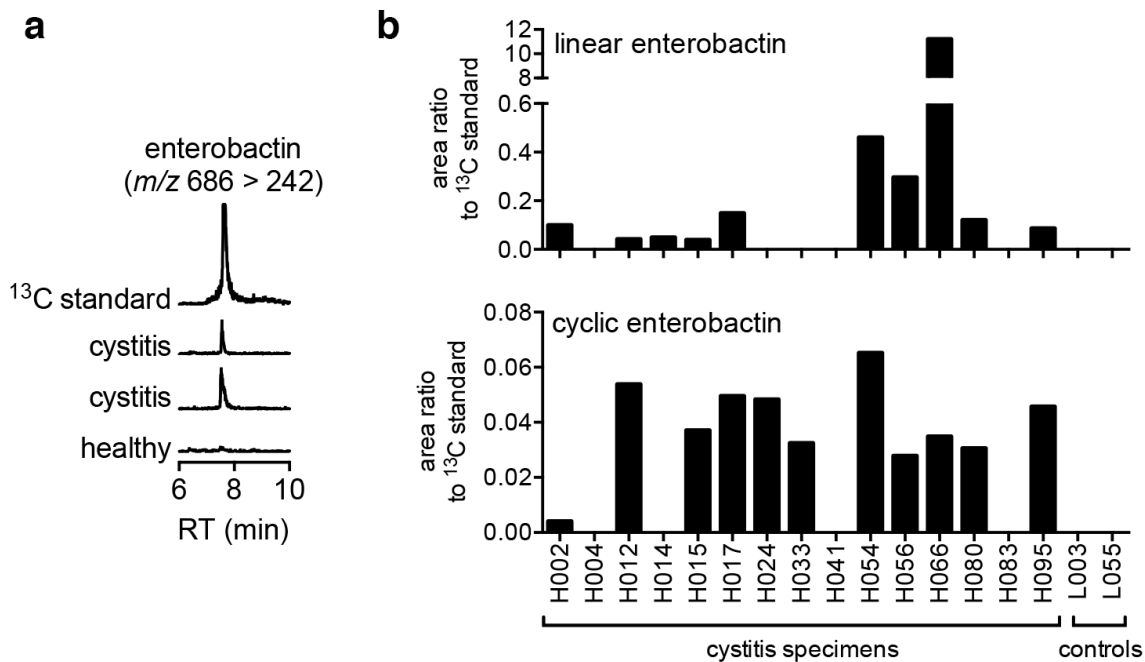


Figure 4. Enterobactin is produced by UPEC during human UTI. Human uncomplicated *E. coli* cystitis samples were spiked 1:10 with ^{13}C -labeled internal standard, then filtered and diluted 1:1 with water before analyzing by negative mode LC-MS-MRM. **(a)** Linear enterobactin MRM traces from two representative cystitis urines compared to a healthy control urine and ^{13}C standard. **(b)** Urines from 15 cystitis patients were analyzed as in **(a)** for linear and cyclic enterobactin. Bars represent the peak area ratio relative to internal standard. *Controls* are urines from healthy individuals, prepared and analyzed identically.

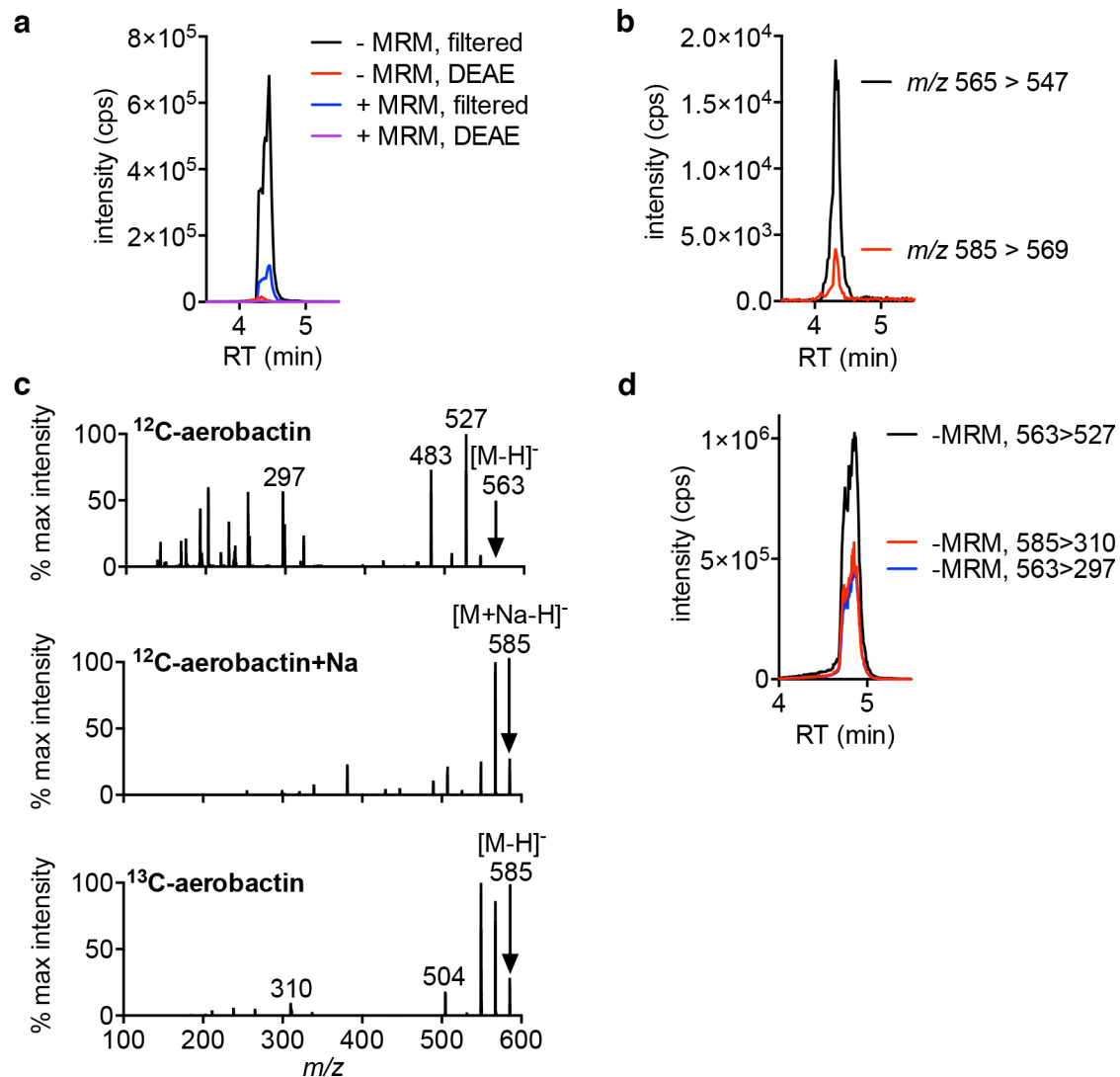


Figure 5. Improved aerobactin detection sensitivity and specificity in negative ion MRM.

(a) UPEC strain CFT073 was grown overnight in M63 minimal media, centrifuged, and either extracted with solid phase anion exchange (DEAE) or 0.2 μM filtered. Samples were then run in negative and positive mode LC-MS-MRM monitoring apo-aerobactin (564 Da). (b) Representative plot from positive mode MRM showing the aerobactin $[M+H]^+$ at m/z 565 > 547 and a species at m/z 585 > 569, the expected mass transition for ^{13}C -aerobactin. Similar results

were obtained in negative mode (data not shown). While no ^{13}C -labeled product was added to the sample, this mass is consistent with the $[\text{M}+\text{Na}+\text{H}]^+$ adduct species. (c) Tandem MS (negative EPI mode) shows that the m/z 585 species in (b) is indeed not ^{13}C -aerobactin. These fragmentation patterns also reveal unique transitions for avoiding species cross-contamination in MRM. After accounting for ^{13}C mass, the transitions m/z 563>297 and 585>310 were determined to represent the same molecular fragmentation. Consistent with this assignment, negative mode MRM peaks from a 1:1 mixture of unlabeled and ^{13}C -labeled supernatants are nearly identical for these two transitions (d). Monitoring m/z 563>527, however, yields the greatest sensitivity and largest ^{12}C -aerobactin peak.

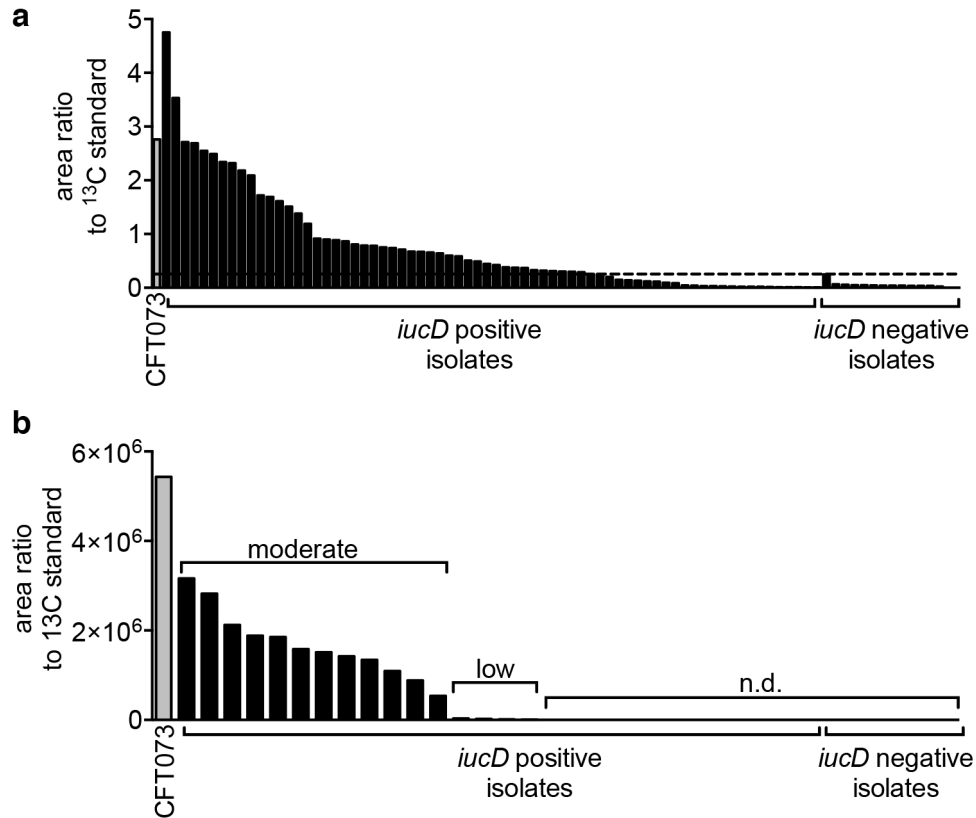


Figure 6. Aerobactin expression varies among *iucD*⁺ clinical isolates. (a) Aerobactin area ratios from positive MRM siderophore screen. Supernatants from clinical isolates grown overnight in M63 minimal media were extracted using DEAE SPE and analyzed directly by LC-MS-MRM. Peak areas were normalized to cfu and ^{13}C internal standard peak area. A horizontal dotted line indicates the level of background signal as defined by *iucD* negative samples after normalization to internal standard. (b) Isolates with low or undetectable aerobactin expression in (a) were reanalyzed using negative mode MRM on filtered supernatants. This method reveals several low-expressers and a population of *iucD*⁺ isolates that do not produce aerobactin (n.d., not detected) in low-iron media.

APPENDIX: REFERENCES

1. Foxman, B. (2010) The epidemiology of urinary tract infection. *Nat. Rev. Urol.* **7**, 653–660
2. Henderson, J. P., Crowley, J. R., Pinkner, J. S., Walker, J. N., Tsukayama, P., Stamm, W. E., Hooton, T. M., and Hultgren, S. J. (2009) Quantitative metabolomics reveals an epigenetic blueprint for iron acquisition in uropathogenic *Escherichia coli*. *PLoS Pathog.* **5**, e1000305
3. Chaturvedi, K. S., Hung, C. S., Crowley, J. R., Stapleton, A. E., and Henderson, J. P. (2012) The siderophore yersiniabactin binds copper to protect pathogens during infection. *Nat. Chem. Biol.* **8**, 731–736
4. Miethke, M., and Marahiel, M. A. (2007) Siderophore-based iron acquisition and pathogen control. *Microbiol. Mol. Biol. Rev.* **71**, 413–451
5. Cassat, J. E., and Skaar, E. P. (2013) Iron in Infection and Immunity. *Cell Host Microbe.* **13**, 509–519
6. Cherayil, B. J. (2011) The role of iron in the immune response to bacterial infection. *Immunol. Res.* **50**, 1–9
7. Hood, M. I., and Skaar, E. P. (2012) Nutritional immunity: transition metals at the pathogen-host interface. *Nat. Rev. Microbiol.* **10**, 525–537
8. Chen, S. L., Hung, C. S., Xu, J., Reigstad, C. S., Magrini, V., Sabo, A., Blasiar, D., Bieri, T., Meyer, R. R., and Ozersky, P. (2006) Identification of genes subject to positive selection in uropathogenic strains of *Escherichia coli*: a comparative genomics approach. *Proc. Natl. Acad. Sci.* **103**, 5977–5982

9. Reigstad, C. S., Hultgren, S. J., and Gordon, J. I. (2007) Functional genomic studies of uropathogenic *Escherichia coli* and host urothelial cells when intracellular bacterial communities are assembled. *J. Biol. Chem.* **282**, 21259–21267
10. Brumbaugh, A. R., Smith, S. N., Subashchandrabose, S., Himpsl, S. D., Hazen, T. H., Rasko, D. A., and Mobley, H. L. T. (2015) Blocking yersiniabactin import attenuates extraintestinal pathogenic *Escherichia coli* in cystitis and pyelonephritis and represents a novel target to prevent urinary tract infection. *Infect. Immun.* **83**, 1443–1450
11. Snyder, J. A., Haugen, B. J., Buckles, E. L., Lockatell, C. V., Johnson, D. E., Donnenberg, M. S., Welch, R. A., and Mobley, H. L. T. (2004) Transcriptome of uropathogenic *Escherichia coli* during urinary tract infection. *Infect. Immun.* **72**, 6373–6381
12. Garcia, E. C., Brumbaugh, A. R., and Mobley, H. L. T. (2011) Redundancy and specificity of *Escherichia coli* iron acquisition systems during urinary tract infection. *Infect. Immun.* **79**, 1225–1235
13. Holden, V. I., and Bachman, M. A. (2015) Diverging roles of bacterial siderophores during infection. *Met. Integr. Biometal Sci.* 10.1039/c4mt00333k
14. Bachman, M. A., Lenio, S., Schmidt, L., Oyler, J. E., and Weiser, J. N. (2012) Interaction of lipocalin 2, transferrin, and siderophores determines the replicative niche of *Klebsiella pneumoniae* during pneumonia. *mBio.* 10.1128/mBio.00224-11
15. Chaturvedi, K. S., Hung, C. S., Giblin, D. E., Urushidani, S., Austin, A. M., Dinauer, M. C., and Henderson, J. P. (2014) Cupric yersiniabactin is a virulence-associated superoxide dismutase mimic. *ACS Chem. Biol.* **9**, 551–561

16. Steigedal, M., Marstad, A., Haug, M., Damås, J. K., Strong, R. K., Roberts, P. L., Himpl, S. D., Stapleton, A., Hooton, T. M., Mobley, H. L. T., Hawn, T. R., and Flo, T. H. (2014) Lipocalin 2 imparts selective pressure on bacterial growth in the bladder and is elevated in women with urinary tract infection. *J. Immunol. Baltim. Md 1950.* **193**, 6081–6089
17. Marschall, J., Zhang, L., Foxman, B., Warren, D. K., Henderson, J. P., and CDC Prevention Epicenters Program (2012) Both host and pathogen factors predispose to Escherichia coli urinary-source bacteremia in hospitalized patients. *Clin. Infect. Dis.* **54**, 1692–1698
18. Shields-Cutler, R. R., Crowley, J. R., Hung, C. S., Stapleton, A. E., Aldrich, C. C., Marschall, J., and Henderson, J. P. (2015) Human Urinary Composition Controls Siderocalin's Antibacterial Activity. *J. Biol. Chem.* 10.1074/jbc.M115.645812
19. Morris, J. C. (1966) The Acid Ionization Constant of HOCl from 5 to 35°. *J. Phys. Chem.* **70**, 3798–3805
20. Caza, M., Garénaux, A., Lépine, F., and Dozois, C. M. (2015) Catecholate siderophore esterases Fes, IroD and IroE are required for salmochelins secretion following utilisation, but only IroD contributes to virulence of extra-intestinal pathogenic Escherichia coli. *Mol. Microbiol.* 10.1111/mmi.13059
21. Caza, M., Lépine, F., Milot, S., and Dozois, C. M. (2008) Specific Roles of the iroBCDEN Genes in Virulence of an Avian Pathogenic Escherichia coli O78 Strain and in Production of Salmochelins. *Infect. Immun.* **76**, 3539–3549
22. Yamashita, M., and Fenn, J. B. (1984) Negative ion production with the electrospray ion source. *J. Phys. Chem.* **88**, 4671–4675

23. Gaut, J. P., Yeh, G. C., Tran, H. D., Byun, J., Henderson, J. P., Richter, G. M., Brennan, M. L., Lusic, A. J., Belaouaj, A., Hotchkiss, R. S., and Heinecke, J. W. (2001) Neutrophils employ the myeloperoxidase system to generate antimicrobial brominating and chlorinating oxidants during sepsis. *Proc. Natl. Acad. Sci. U. S. A.* **98**, 11961–11966
24. Amulic, B., Cazalet, C., Hayes, G. L., Metzler, K. D., and Zychlinsky, A. (2012) Neutrophil Function: From Mechanisms to Disease. *Annu. Rev. Immunol.* **30**, 459–489
25. Hannan, T. J., Totsika, M., Mansfield, K. J., Moore, K. H., Schembri, M. A., and Hultgren, S. J. (2012) Host-pathogen checkpoints and population bottlenecks in persistent and intracellular uropathogenic *Escherichia coli* bladder infection. *FEMS Microbiol. Rev.* **36**, 616–648
26. Hannan, T. J., Mysorekar, I. U., Hung, C. S., Isaacson-Schmid, M. L., and Hultgren, S. J. (2010) Early Severe Inflammatory Responses to Uropathogenic *E. coli* Predispose to Chronic and Recurrent Urinary Tract Infection. *PLoS Pathog.* **6**, e1001042
27. Lin, H., Fischbach, M. A., Gatto, G. J., Liu, D. R., and Walsh, C. T. (2006) Bromoenterobactins as potent inhibitors of a pathogen-associated, siderophore-modifying C-glycosyltransferase. *J. Am. Chem. Soc.* **128**, 9324–9325
28. Torres, A. G., Redford, P., Welch, R. A., and Payne, S. M. (2001) TonB-dependent systems of uropathogenic *Escherichia coli*: aerobactin and heme transport and TonB are required for virulence in the mouse. *Infect. Immun.* **69**, 6179–6185
29. Russo, T. A., Olson, R., MacDonald, U., Metzger, D., Maltese, L. M., Drake, E. J., and Gulick, A. M. (2014) Aerobactin Mediates Virulence and Accounts for Increased

Siderophore Production under Iron-Limiting Conditions by Hypervirulent

(Hypermucoviscous) *Klebsiella pneumoniae*. *Infect. Immun.* **82**, 2356–2367

30. Russo, T. A., Olson, R., MacDonald, U., Beanan, J., and Davidson, B. A. (2015)

Aerobactin, but not yersiniabactin, salmochelin and enterobactin, enables the

growth/survival of hypervirulent (hypermucoviscous) *Klebsiella pneumoniae* ex vivo and in

vivo. *Infect. Immun.* 10.1128/IAI.00430-15

ROBIN REID SHIELDS-CUTLER

Curriculum Vitae

Education

Washington University School of Medicine (WUSM); St. Louis, MO

Ph.D. expected August 2015

Division of Biology and Biomedical Sciences

Molecular Microbiology and Microbial Pathogenesis

Qualifying Exam: Pass with Distinction, December 2012

Grinnell College; Grinnell, IA

B.A. with Honors, Biological Chemistry, May 2008

Research Experience

- 2011 - 2015 “Iron acquisition in urine by pathogenic *E. coli*”
Laboratory of Dr. Jeffrey Henderson, Division of Infectious Diseases,
Washington University School of Medicine, St. Louis, MO
- 2008 - 2010 “Engineering ferritin as a novel MR contrast agent”
Postbaccalaureate Intramural Research Training Award
Laboratory of Dr. Henry Levin, NIH/NICHD, Bethesda, MD
- Spring 2008 “Investigating biofilm mutants of *Psychrobacter arcticus*”
Laboratory of Dr. Shannon Hinsa-Leasure, Grinnell College, Grinnell, IA
- 2007 “Class comparison of *Haemophilus ducreyi*”
Laboratory of Dr. Tricia Humphreys, Grinnell College, Grinnell, IA
- Summer 2006 “Novel inhibitors of HIV-1 Reverse Transcriptase”
NSF Research Experience for Undergraduates in Biology/Biochemistry
Laboratory of Dr. Donald H. Burke, University of Missouri-Columbia

Teaching and Leadership Experience

- 2015 Lecturer, Bio4933 “Molecular Biology at the Cutting Edge,” WUSTL
 “*Mass spectrometry: A powerful tool in biological inquiry*”
- 2014 - present Associate Member, WU-CIRTL Program for Future STEM Faculty
- 2014 - 2015 Laboratory mentor and supervisor for undergraduate research fellow
- 2012 - 2014 Microbiology Program Steering Committee Representative, WUSM
 Elected by peers to function as student liaison to committee
- 2012 Teaching Assistant: BIO4820 - Biochemistry II, WUSTL
- 2011 - 2014 Volunteer Educator: Young Scientist Program, WUSM
- 2007 - 2008 Mentor: Introduction to Biological Chemistry, Grinnell College

2007 Tutor: Molecules, Cells, and Organisms, Grinnell College
2006 - 2008 Biochemistry Student Educational Policy Committee, Grinnell College
2006 - 2008 Student Curriculum Committee, Grinnell College
2006 Mentor: Molecules, Cells, and Organisms, Grinnell College
2006, 2008 Mentor: Introduction to Biological Inquiry, Grinnell College

Teaching Workshop Participation

Washington University Teaching Center

Fostering Active Student Engagement in the Classroom
STEM Pedagogies: Incorporating active learning
STEM Pedagogies: Intro to the Scholarship of Teaching and Learning
STEM Pedagogies: Inquiry-based laboratory teaching: philosophy and implementation
STEM Pedagogies: Inclusive teaching in STEM
STEM Pedagogies: Applying cognitive science to improve learning

Honors and Awards

2015 Ceil M. DeGutis Prize in Chemical Biology or Medicinal Chemistry
For significant contributions to the fields of Chemical Biology or Medicinal Chemistry
2012 - 2015 WUSM - Monsanto Excellence Fund Graduate Fellowship
2010 - 2012 NIH Cell and Molecular Biology Training Grant 5T32GM007067-36
2008 Grinnell College Biological Chemistry Alumni Award
2005 - 2008 Florence Smith-Sifferd Science Scholarship, Grinnell College
2004 - 2008 Trustee Honor Scholarship, Grinnell College
2004 - 2008 Tozer Foundation, Inc. Scholarship
2004 - 2006 Dean's List, Grinnell College

Professional Memberships

2012 - 2015 American Society for Microbiology

Publications

Robin R. Shields-Cutler, Connelly Miller, Jan R. Crowley, and Jeffrey P. Henderson. The innate immune protein siderocalin binds urinary metabolites to deprive bacteria of iron. (Manuscript in preparation.)

Robin R. Shields-Cutler, Jan R. Crowley, Chia S. Hung, Ann E. Stapleton, Courtney C. Aldrich, Jonas Marschall, and Jeffrey P. Henderson. Human urinary composition controls siderocalin's antibacterial activity. (2015) *Journal of Biological Chemistry*. doi:10.1074/jbc.M115.645812

Selected as JBC Paper of the Week
Cover art selected for accompanying print issue

Emily E. Ricotta, Nan Wang, Robin Cutler, Jeffrey G. Lawrence, and Tricia L. Humphreys. Rapid Divergence of Two Classes of *Haemophilus ducreyi*. *Journal of Bacteriology* **193** (12), 2941-2947 (2011).

Invited Seminars

2014 Women's Health Research Seminar Series, WUSM, Dept. of OB/GYN

Posters and Abstracts

Robin R. Shields-Cutler, Jan R. Crowley, Connelly Miller, Chia S. Hung, Jonas Marschall, and Jeffrey P. Henderson. Human urinary composition controls siderocalin's antibacterial activity. Gordon Research Conferences; Cell Biology of Metals. Mount Snow, VT, July 26, 2015.

Robin R. Shields-Cutler, Jan R. Crowley, Chia S. Hung, Jonas Marschall, and Jeffrey P. Henderson. Uropathogenic *Escherichia coli* Growth Phenotypes Derived from Human Urinary Metabolomic Differences. American Society for Microbiology; General Meeting, Boston, MA, May 18, 2014.

Robin R. Shields-Cutler, Jan R. Crowley, Chia S. Hung, Jonas Marschall, and Jeffrey P. Henderson. Urine Metabolomes Reveal Individual Variation in Uropathogenic *E.coli* Growth Requirements. Monsanto Science Fellows Microbiome Symposium, Chesterfield, MO; January 2014.

Robin R. Cutler, Jan R. Crowley, Chia S. Hung, Jonas Marschall, and Jeffrey P. Henderson. Lipocalin 2 synergizes with individual metabolomes to restrict uropathogen growth. Midwest Microbial Pathogenesis Conference, The Ohio State University, Columbus, OH; August 2013.

Robin R. Cutler, Tricia L. Humphreys. Three-Part Class Comparison of *Haemophilus ducreyi*: Two Clonal Populations at the Level of Genome, Cell Structure, and Gene. Pew Biological Sciences and Psychology Undergraduate Research Symposium, Washington University, St. Louis, MO; November 2007.

Robin R. Cutler, Ferrill Rose, Daniel Held, Donald H. Burke. HIV-1 Reverse Transcriptase Inhibition by Multiple RNA Aptamers. Howard Hughes Medical Institute Symposium for Undergraduate Research, Grinnell College, Grinnell, IA; February 2007.